

**OREGON HEALTH & SCIENCE UNIVERSITY
SCHOOL OF MEDICINE – GRADUATE STUDIES**

**THE HYALURONIDASE CELL MIGRATION INDUCING AND HYALURONAN
BINDING PROTEIN IS ELEVATED DURING INFLAMMATORY
DEMYELINATION AND INHIBITS REMYELINATION**

By

Alec J. Peters

A DISSERTATION

Presented to the Department of Cell, Developmental, and Cancer Biology
and the Oregon Health & Science University
School of Medicine
in partial fulfillment of
the requirements for the degree of

Doctor of Philosophy

December 2023

TABLE OF CONTENTS

LIST OF FIGURES	ii
LIST OF ABBREVIATIONS	iv
ACKNOWLEDGEMENTS	vii
ABSTRACT	viii
CHAPTER 1: INTRODUCTION	1
Hyaluronic acid acts as both a structural element of the extracellular matrix and a signaling molecule regulating multiple cellular processes ..	2
HA synthesis is tightly regulated in the nervous system	12
Regulation of HA catabolism in the nervous system	16
Multiple HA receptors respond to HA in the developing, mature, and diseases nervous system	20
Summary	27
Rationale and hypotheses	30
CHAPTER 2: THE CEMIP HYALURONIDASE IS ELEVATED DURING INFLAMMATORY DEMYELINATION AND PRODUCES BIOACTIVE HYALURONIC ACID FRAGMENTS THAT DELAY REMYELINATION	33
Introduction	33
Materials and methods	35
Results	46
Discussion	61
CHAPTER 3: DISTINCT CHEMICAL STRUCTURES INHIBIT THE CEMIP HYALURONIDASE AND PROMOTE OLIGODEDROCYTE PROGENITOR CELL MATURATION	67
Introduction	67
Materials and methods	70
Results	76
Discussion	85
CHAPTER 4: CONCLUSIONS	89
APPENDIX: ADDITIONAL STUDIES PERFORMED	99
REFERENCES	108

LIST OF FIGURES

Figure 1: General model for hyaluronan metabolism and signaling in the nervous system, and how it changes during neural activity and disease.

Figure 2: qPCR results of RNA from lumbar spinal cords of mice with experimental autoimmune encephalomyelitis, assaying changes in neuroinflammatory genes, hyaluronic acid synthases, and hyaluronidases.

Figure 3: *In situ* hybridization and immunofluorescence results showing that elevated CEMIP levels occur at areas of demyelination and reduced HA levels in mice, and this is consistent in human multiple sclerosis.

Figure 4: *In situ* hybridization paired with immunofluorescent results (both for CEMIP) showing co-localization of transcript and protein signal.

Figure 5: qPCR results in cultured oligodendrocyte progenitor cells demonstrating that CEMIP expression decreases as cells differentiate into oligodendrocytes, as well as Immunofluorescent experiments showing that CEMIP expression co-localized with markers for oligodendrocyte progenitor and not astrocytes or microglia.

Figure 6: qPCR results showing CEMIP transcript increases with markers of oligodendrocyte lineage cells paired with immunofluorescent images showing CEMIP expression colocalized with a oligodendrocyte progenitor marker in the adult mouse median eminence.

Figure 7: *In vitro* oligodendrocyte differentiation assay showing that CEMIP overexpression delays differentiation rates in the presence and absence of high molecular weight hyaluronan.

Figure 8: Gel and nanopore assay results demonstrating that CEMIP hyaluronidase activity produces bioactive hyaluronic acid sizes that delay cultured oligodendrocyte differentiation rates.

Figure 9: Results demonstrating that hyaluronan fragments produced by CEMIP activity delay functional remyelination rates when compared to high molecular weight hyaluronic acid.

Figure 10: Names and structures of naturally derived compounds that block hyaluronidase activity.

Figure 11: Names and structures of chemically synthesized compounds that block hyaluronidase activity.

Figure 12: Results demonstrating sulfuretin, BIC-1A, and BIC-4A block CEMIP hyaluronidase activity with differing potencies in two different cell types.

Figure 13: Viability assay of selected compounds in 293T cells and cultured oligodendrocyte progenitors.

Figure 14: Proliferation assay results showing selected compounds do not alter cell proliferation.

Figure 15: Oligodendrocyte assay results demonstrating that selected compounds restore cultured oligodendrocyte differentiation rates in the presence of high molecular weight hyaluronic acid.

Figure 16: Summary figure showing findings from the dissertation, and potential mechanisms of remyelination delay induced by HA fragments generated by CEMIP activity.

Figure 17: qPCR assay results demonstrating *CEMIP* transcript levels generally decrease with age in the mouse brain, while hyaluronic acid synthase genes generally don't change or decrease as well.

LIST OF ABBREVIATIONS

HA	Hyaluronic acid, hyaluronan
ECM	Extracellular matrix
HMW	High molecular weight
CNS	Central nervous system
PNN	Perineuronal net
NSC	Neural stem cell
PNS	Peripheral nervous system
SVZ	Subventricular zone
SGZ	Subgranular zone
MS	Multiple sclerosis
OPC	Oligodendrocyte progenitor cell
OL	Oligodendrocyte
BBB	Blood-brain barrier
CD	Cluster of differentiation
RHAMM/HMMR	Receptor for hyaluronan mediated motility/ hyaluronan mediated motility receptor
LYVE1	Lymphatic vessel endothelial hyaluronan receptor 1
TLR	Toll-like receptor
HAPLN1	Hyaluronan and proteoglycan link protein 1
Bral	Brain link protein
Ial	Inter-alpha-inter

HC	Heavy chain
TSG-6	Tumor necrosis factor-stimulated gene 6
HAS	Hyaluronic acid synthase
TRPV1	Transient receptor potential cation channel subfamily V member 1
CSPG	Chondroitin sulfate proteoglycan
HYAL	Hyaluronidase
GPI	Glycosylphosphatidylinositol
CEMIP	Cell migration inducing and hyaluronan binding protein
TMEM2	Transmembrane Protein 2
NHE1	Sodium/hydrogen antiporter 1
TNF α	Tumor necrosis factor alpha
IFN γ	Interferon gamma
DNA	Deoxyribo nucleic acid
RNA	Ribonucleic acid
cDNA	Complimentary DNA
qPCR	Quantitative polymerase chain reaction
DMEM	Dulbecco's modified eagle medium
NAC	5-N-acetyl cysteine
PBS	Phosphate buffer saline
FBS	Fetal bovine serum
PDGF-AA	Platlet-derived growth factor AA

BrdU	Bromodeoxyuridine
EAE	Experimental Autoimmune Encephalomyelitis
dpi	Days post inoculation
CDI	Cumulative disease index
aCSF	Artificial cerebrospinal fluid
CAP	Compound action potential
PDGFR α	Platlet-derived growth factor receptor alpha
MBP	Myelin basic protein
Iba1	Ionized calcium-binding adapter molecule 1
GFAP	Glial fibrillary acidic protein
VE-cadherin	Vascular endothelial cadherin
HABP	Hyaluronic acid binding protein
DAPI	4,6-diamidino-2-phenylindole
AF	AlexaFluor

I dedicate this dissertation to my wife and best friend Yunhan Duan. Words cannot express my love for you, so you will need to wait and see how I show it over our years together.

ACKNOWLEDGMENTS

I would like to acknowledge my mentor, Dr. Lawrence S. Sherman, for his unwavering support of my efforts in his laboratory. His support and guidance allowed me to thrive even through a global pandemic.

I would also like to thank Dr. Philip Copenhaver, my committee chair and program director, for his support of my academic progress. Your advice and efforts at crucial times were greatly appreciated.

My other committee members, Dr. Stephen Back and Dr. Anthony Barnes, also provided valuable insights in experimental design and analysis throughout the years.

Thank you as well to Dr. Ben Emery for his support as my final dissertation committee member.

Many thanks to the members and of the Sherman lab for their assistance with advice and technical support during experiments: Dr. Steven Matsumoto, Dr. Weiping Su, Dr. Fatima Banine, and Kanon Yasuhara.

Thank you to Lola Bichler and Louise Sacha, the departmental coordinators that kept me on track with deadlines and gave me invaluable assistance during funding applications.

Abstract: Central nervous system demyelination occurs in numerous conditions, including multiple sclerosis (MS). Remyelination in acute lesions involves the recruitment and maturation of oligodendrocyte progenitor cells (OPCs). However, remyelination fails in chronic lesions in part due to the failure of OPCs to mature into myelinating oligodendrocytes (OLs). Digestion products of the glycosaminoglycan hyaluronan (HA), generated by hyaluronidase activity within demyelinating lesions, are among the signals that block OPC maturation and remyelination. However, the identity and source of this hyaluronidase activity is unknown. I screened demyelinating tissues during different times of disease progression from mice with experimental autoimmune encephalomyelitis (EAE), a model of MS. I found that the Cell Migration Inducing and hyaluronan binding Protein (CEMIP) is elevated in inflammatory demyelinating lesions during peak demyelinating disease and when neuroinflammatory mediators, including tumor necrosis factor- α (TNF α), are at their highest levels. I also found elevated CEMIP expression in demyelinated lesions from MS patients. *Cemip* is expressed by OPCs, and TNF α induces increased *Cemip* expression in OPCs. Both increased *Cemip* expression and HA fragments generated by CEMIP block OPC maturation into OLs. Furthermore, CEMIP-derived HA fragments prevent functional remyelination *in vivo*. Altogether, these data indicate that CEMIP blocks remyelination by generating bioactive HA fragment that inhibit OPC maturation. CEMIP is therefore a potential target for therapies aimed at promoting remyelination.

I also have screened a group of chemically synthesized and naturally derived small molecule inhibitors and found three compounds that effectively blocked CEMIP activity in two different cell types. These compounds also accelerated OPC differentiation in the presence of high molecular weight HA. These findings have begun to identify potential therapeutic agents to accelerate functional remyelination in demyelinating diseases.

CHAPTER 1: INTRODUCTION

Adapted from: Peters A, Sherman LS. Diverse Roles for Hyaluronan and Hyaluronan Receptors in the Developing and Adult Nervous System. Int J Mol Sci. 2020 Aug 20;21(17):5988. doi:10.3390/ijms21175988. PMID: 32825309; PMCID: PMC7504301.

Hyaluronic acid (HA), or hyaluronan, is a linear unsulfated glycosaminoglycan composed of repeating units of D-glucuronic acid and N-acetyl-D-glucosamine that can be thousands of residues in length and megadaltons in size^{1,2}. HA is a major component of the extracellular matrix (ECM) in many tissues, including the central nervous system (CNS)³⁻⁵. HA has a diverse set of mechanical functions in tissues, such as providing elasticity in skin and acting as a lubricant between articulating bones in joints⁵. However, this relatively simple glycosaminoglycan also acts as a complex extracellular signal that can regulate a diverse set of cell processes based on its size, associated proteins, and interactions with receptors.

Hyaluronan has been found to regulate cellular activities in development, homeostasis, and disease states in a variety of tissues, including the nervous system, where it has been implicated in regulating neuronal and glial cell differentiation, the activity of neurons, and nervous system repair in neurodegenerative diseases and following CNS injuries. These functions depend on tightly regulated changes in HA synthesis and catabolism. This introduction

focuses on recent findings supporting distinct roles for HA in each of these processes, and I examine evidence that HA acts as a dynamic signaling molecule that can influence diverse activities in the developing and mature mammalian brain.

Hyaluronic acid acts as both a structural element of the extracellular matrix and a signaling molecule regulating multiple cellular processes

High molecular weight HA has function in the nervous system that are distinct from HA fragments

Native extracellular HA can be large (megadaltons in size) and is often termed high molecular weight (HMW) HA. Through hyaluronidase activity or reactions with reactive oxygen species, HMW HA can be broken down into fragments of varying sizes^{5, 6}. HMW HA and fragments of different sizes can influence a variety of biological processes through interactions with receptors such as cluster of differentiation 44 (CD44), the receptor for hyaluronan-mediated motility (RHAMM, otherwise known as hyaluronan-mediated motility receptor or HMMR), and lymphatic vessel endothelial hyaluronan receptor 1 (LYVE1). HA can also activate toll-like receptors (TLRs) 2 and 4, although it is currently unclear if this occurs through direct HA binding^{2, 7}.

Different sizes of HA can have distinct biological activities. HMW HA is known to reduce inflammation in a variety of tissues, while fragments of different sizes either promote or inhibit inflammatory processes^{6, 8}. HMW HA also reduces

proliferation of multiple neural cell types⁹⁻¹³, and both HMW HA and HA fragments can regulate cell differentiation in the CNS¹²⁻¹⁵. Additionally, HA signaling can change based on its association with other ECM components, as well as covalent modifications. HA-associated proteins and protein complexes, such as the proteoglycans aggrecan, brevican, and neurocan, and link proteins, such as brain link protein-1 (Bral1), Bral2, and hyaluronan and proteoglycan link protein 1 (HAPLN1), associate with HA in the nervous system ECM¹⁶⁻¹⁹. These large HA-protein complexes help to regulate nervous system functions, including cell adhesion, migration, and neurite outgrowth. HA is also found in the proteoglycans that form the specialized ECM around neurons called perineuronal nets (PNN)²⁰⁻³⁰. Covalent modifications to HA, such as the addition of the inter- α -trypsin inhibitor (I α I) heavy chain (HC) catalyzed by tumor necrosis factor stimulated gene 6 (TSG-6), also changes the signaling properties of HA and can modulate neuroinflammation, HA crosslinking, and interactions between HA and receptors³¹⁻³⁶.

HA is required for nervous system development

HA is found in the CNS at the earliest stages of development, as the neural plate folds into the neural tube. The amounts of HA peak in the embryonic nervous system, then decline in adulthood^{37, 38}, although the absolute amounts of HA in any area of the CNS or PNS have yet to be quantified at any stage of life. The treatment of embryos with a hyaluronidase to digest HMW HA led to delays

in neurulation, linking HA to some of the earliest morphogenic processes during neurodevelopment³⁹.

After neurulation, the lowest concentration of HA is found in the ventricular zone, where neural stem cells (NSCs) undergo self-renewal¹³. HA receptors including *Cd44* and *Rhamm*, are also expressed in the ventricular zone, and RNA analyses of the developing CNS indicate that cell–ECM interactions through these and other ECM receptors may be crucial for the proliferative capacity of NSCs⁴⁰⁻⁴². A higher concentration of HA is found in the intermediate zone, where stem cells differentiate into neuroblasts¹³, though it is unclear if the higher HA concentrations induce differentiation or act in a different capacity, such as providing a permissive environment for the migration of cells that have already begun to differentiate. During later stages of neurodevelopment, HA is required for proper neocortical folding⁴³. HA has also been shown to be involved in neurite extension and proper axon routing, such as that of retinal neuron axons in the optic pathway⁴⁴⁻⁴⁶, as well as cell migration in the developing cerebellum⁴⁷. More studies are required to fully understand how changes in HA and HA-mediated signaling contribute to CNS morphogenesis.

In addition to early CNS development, HA is required for early events in peripheral nervous system (PNS) development. HA is found around the neural tube, notochord, and neural crest after neurulation^{19, 48, 49}. Neural crest cells express HA synthases (HAS) 1 and 2, and this expression is downregulated

during migration⁵⁰. Neural crest cells also express *Cd44* and *Rhmm*^{40, 51}. HAS expression, notably *Has2*, as well as HA, is also found along neural crest migratory paths^{19, 52}. Knockdown of *Cd44* delays neural crest migration⁵¹, and silencing of *Has2* during neural crest migration induces migratory defects⁵³. All together, these findings indicate that HA has crucial roles in the initiation of neural crest cell emigration from the dorsal neural tube and in migration as these cells differentiate into neurons, Schwann cells and other peripheral nerve cell populations.

HA is required for mature nervous system function

HA is a nearly ubiquitous component of the extracellular matrix in the adult CNS, found in both gray and white matter. HA is found surrounding myelinated axons in white matter, while in a gray matter, it is found in a more diffuse distribution as part of the ECM and as a component of PNN surrounding neurons^{17, 54, 55}. HA concentrations vary by brain region, as shown by studies observing distinct HA staining patterns in the somatosensory and piriform cortices⁵⁶, as well as the cerebellum⁵⁷. HA has diverse structural and signaling functions in the nervous system, such as forming a scaffold for the development of PNNs in gray matter⁵⁸ while having a critical structural role in myelinated axons and axon fiber tracts in white matter^{54, 55, 59, 60}, as well as in myelinated axons of the PNS⁵⁹.

Adult neurogenic niches, including the subgranular zone (SGZ) of the hippocampal dentate gyrus and the subventricular zone (SVZ), harbor NSCs that undergo self-renewal, as well as asymmetric division to form new neurons and glial cells. HA is a major extracellular component in both of these niches^{12, 61}. HA has been linked to cell quiescence in many *in vitro* and *in vivo* studies in both NSCs and glia^{9-13, 62}. HA signaling through receptors such as CD44 and TLR2 help to regulate stem cell proliferation and differentiation^{12, 63}, and loss of *Cd44* leads to hippocampal dysfunction and spatial learning and memory deficits⁶⁴. These discoveries suggest an essential role for HA signaling in adult neurogenesis, as well as for behaviors that rely on incorporating new neurons into neural circuits throughout life. *In vitro* studies indicate that embryonic neural stem cells have hyaluronidase activity⁶⁵, suggesting that neural stem cells could possibly regulate neurogenesis through the modulation of HA concentration and fragment size in neurogenic niches. It is possible then that learning and memory lead to activity-dependent changes in HA synthesis and hyaluronidase activity that regulate the generation of new neurons and neuronal maturation.

HA and HA signaling has also been shown to be correlated with cell migration in the adult nervous system. HA is elevated in the rostral migratory stream, a specialized migratory route along which neuronal precursors that originated in the SVZ migrate to reach the olfactory bulb. Migrating immature neurons in the rostral migratory stream express *Rhamm*, indicating that HA-RHAMM interactions may be required for the proper migration of these cells⁶¹.

In vitro studies with 3D HA hydrogels have found that the stiffness of the ECM can influence properties of neural stem and progenitor cells. For example, by modulating HA concentrations to generate hydrogels that mimic elasticities of the developing and adult brain, it was found that an elasticity similar to that of the developing embryonic brain permitted neuronal progenitor migration and branching, while higher elasticities mimicking the adult brain did not⁶⁵. Furthermore, 3D hydrogels with higher HA concentrations had decreased stem cell proliferation and differentiation^{62, 65}.

The stiffness of the ECM might also affect proliferation, migration, and branching of one cell lineage over another⁶⁶ and can even direct stem cell differentiation into different lineages⁶⁷. It is possible that gradients of ECM can guide cell migration from areas of lower to higher stiffness⁶⁸. Although how HA influences ECM stiffness in CNS tissues is not fully elucidated, HA-binding proteins such as TSG-6 might play a role in modulating HA crosslinking and changes to the stiffness of the ECM. The size of the component HA can also directly influence ECM stiffness either directly or through modulating TSG-induced crosslinking of HA strands^{31, 69}. These findings suggest that changes in extracellular HA concentration during development can lead to cell responses by changing the mechanical properties of the ECM, as well as through interactions with HA receptors. Modifying the mechanical properties of the ECM by altering HA size

and concentration could also help regulate neurogenesis in adult neurogenic niches.

In addition to regulating the expansion and differentiation of neural stem cell populations, HA can also regulate receptor function in both CNS and PNS neurons. Direct interactions between HA and the transient receptor potential cation channel subfamily V member 1 (TrpV1; also known as the capsaicin receptor) expressed by dorsal root ganglion neurons decreased receptor activation and sensitization, leading to reduced responses to capsaicin and heat⁷⁰. Loss of HA through hyaluronidase administration to the footpad of rats increased pain sensitivity in a CD44-dependent manner⁷¹, suggesting that HA can also influence neuronal activity at sensory neuron endings. HA has also been found to modulate the activities of CNS neurons. For example, hyaluronidase administration reduced L-type voltage gated calcium channel activity in hippocampal neurons⁷², as well as increasing α -amino-3-hydroxy-5-methyl-4-isoxazolepropionic acid (AMPA) receptor trafficking⁷³. These findings raise the possibility that PNNs or similar structures may be dynamically regulated to alter neuronal activity.

The role of HA in PNNs has been reviewed previously⁷⁴, and so the role of PNNs, their development, and the function of HA in these structures will only be briefly reviewed here. HA is a critical component of most PNNs along with chondroitin sulfate proteoglycans (CSPGs) and link proteins. HA forms a scaffold onto which

these other ECM components can be organized on to form fully functional PNNs⁷⁵. While originally thought to be synthesized by glia or a combination of glia and developing neurons⁷⁶, other studies reported that developing neurons alone express HAS enzymes and synthesize PNNs^{58, 77}. However, glial cells and neurons may synthesize different components to form fully functional PNNs in different regions of the brain⁷⁸.

Cultured developing neurons slowly generate PNNs over the course of days^{58, 77}, mimicking the slow development and maturation of these structures in the developing CNS^{17, 54, 79-81}. In the developing CNS, PNNs form in a region-specific manner that correlates with functional maturation⁷⁹. PNNs mostly surround parvalbumin-expressing inhibitory neurons^{58, 82}, and it is thought that synthesis and maturation of PNNs leads to decreased synaptic plasticity⁸¹, possibly due to restricting lateral diffusion of receptors such as AMPA receptors to specific areas on neuronal cell bodies, including postsynaptic densities⁷³. This idea is reinforced through studies that show that the removal of PNNs through hyaluronidase treatment increased excitatory neuronal activity, as well as changing receptor subunit expression to those observed during critical periods^{81, 83}. Loss of PNNs through hyaluronidase treatment also increased the seizure-like activity of neurons *in vitro*⁸⁴ and increased the rates of seizures in animal models⁸⁵. Interestingly, the prefrontal cortex in schizophrenics displayed decreased PNNs⁸⁶. These observations suggest that developmental deficits in HA synthesis

leading to decreased PNN formation could lead to CNS disorders such as epilepsy and schizophrenia.

In addition to its effects on progenitor cells and neurons, HA can also influence the behaviors of glial cells. Astrocytes express HAS enzymes and synthesize HA^{61, 76, 87}. As with NSCs, extracellular HMW HA seems to be a quiescence signal for astrocytes both *in vitro*^{10, 65} and *in vivo*⁹, as well as for O2A progenitors that give rise to type II astrocytes¹¹. HA has been shown to regulate the migration and morphology of astrocytes through interactions with CD44 and RHAMM⁸⁸⁻⁹⁰. The proper trafficking and function of glutamate transporters in astrocytes also rely on HA⁹¹. During late embryonic and postnatal development, HA production by astrocytes might help to form the extracellular matrix as well as decrease proliferation of neighboring astrocytes and, in neurogenic niches, neural stem cells.

The few studies to investigate HA changes with aging have reported increases in HA content in older nervous systems^{12, 92-95}. The increased HA observed in aged brains is synthesized by different cell types, including astrocytes and cells of the microvasculature^{93, 94}. Both the cause of this excess HA synthesis and the effects of the increased HA remain unclear. Given that increased HA levels generally lead to cell quiescence, reduced cell proliferation is a likely outcome. In neurogenic niches such as the SGZ, increased HA content could be one of the causes of significantly decreased neurogenesis observed in older brains⁹⁶.

HA in injury and disease

Increases in both HMW HA and HA fragments have been found in a variety of CNS insults, including trauma, dementia, ischemia, and inflammatory demyelinating diseases such as multiple sclerosis (MS)⁹⁷⁻⁹⁹. During trauma and disease, HMW HA can regulate astrocyte proliferation and glial scar formation, as well as microglial activation^{9, 10, 100, 101}. Additionally, HMW HA impacts vascular endothelial cell barrier function¹⁰² and contributes to lymphocyte extravasation and the onset of experimental autoimmune encephalomyelitis (EAE)—a model of MS¹⁰³. HA fragments can influence angiogenesis^{104, 105}, neural stem cell proliferation⁶³, and differentiation of neural progenitor cells, such as oligodendrocyte progenitor cells (OPCs) under pathological conditions^{15, 106, 107}.

HA-binding proteins such as CSPGs are found in glial scars and help form a barrier that reduces the spread of inflammatory cells but also contribute to the impairment of axonal regeneration. Other binding proteins such as TSG-6 are upregulated in CNS insults such as injury and Alzheimer's disease^{34, 35, 108}. TSG-6 is involved in the induction of reactive astrocytes in a model of traumatic brain injury, but it also has been shown to inhibit microglial activation *in vitro*^{35, 36}. TSG-6 could exert its effects through the covalent modification of HA and the formation of HA-HC complexes, the crosslinking of HA, and regulating HA interactions with receptors such as CD44, all of which could change the signaling properties of HA in nervous system insults.

Interestingly, the effects of TSG-6 are dependent on the sizes of HA and the presence of Ial. For example, TSG-6 catalyzed binding of HC onto HA molecules is reversible in HMW HA, but HC is irreversibly bound to small HA fragments (4–12 oligosaccharide polymers)³³. Additionally, Ial inhibits HA crosslinking by TSG-6¹⁰⁹. These results suggest that the effects of TSG-6 on HA can be modulated in injury and disease through the breakdown of HMW HA and expression of Ial to generate different cell responses.

Whereas changes in HA size, structure, and binding proteins may be beneficial in the case of trauma to reduce the amount of neuronal damage due to inflammation, in other cases such as chronic diseases, changes in HA amount and size may be detrimental to regeneration. For instance, in white matter diseases such as MS and vanishing white matter disease, accumulation of HMW HA and HA fragments in plaques have been found to inhibit the maturation of OPCs and functional remyelination^{15, 106, 107, 110}.

HA synthesis is tightly regulated in the nervous system

Hyaluronic acid synthases and their distribution in the CNS

HA in mammalian cells is synthesized by three HA synthases (HAS1–3)—transmembrane enzymes localized to the plasma membrane of cells that extrude HA into the extracellular space during synthesis¹¹¹. HAS activity increases pericellular HA levels, and each of the three HAS enzymes have different kinetics

and synthesize different size ranges of HA¹¹¹. The expression patterns of each HAS protein are not identical throughout development, in the adult, and in old age. This observation suggests that HA of different size ranges synthesized by each of the different HAS proteins play distinct roles in the development and functioning of the nervous system through differential signaling of their respective products. Supporting this hypothesis are studies showing that silencing of different *Has* genes leads to opposite effects on cell motility *in vitro*¹¹².

There are some differences in HAS expression patterns in different species. In developing *Xenopus* embryos, *Has1* is expressed throughout the ectoderm, excluding the neural plate, while *Has2* is expressed in mesoderm, and *Has3* is restricted to a small number of structures such as the developing otic vesicles⁵⁰. In bovine embryos, whereas *Has2* and *Has3* are expressed throughout embryonic development, *Has1* is only expressed in early (2- and 4-cell) stages¹¹³. In mice, *Has1* is widely expressed in early development until about embryonic day 8.5, when its levels are markedly decreased⁵². *Has2* expression continues but is eventually restricted to specific structures, including the developing heart and in craniofacial development, while *Has3* expression appears at later times in structures such as developing teeth and hair follicles⁵². Human embryonic stem cell lines express *Has2* as they are induced to form blastocysts¹¹⁴, which influences their differentiation into extraembryonic cell types^{14, 114}. HAS proteins, therefore, play critical roles in early development that may be distinct in different species.

HAS regulation in the nervous system

HAS enzymes synthesize pericellular HA matrices *in vitro* that differ depending on which enzyme is expressed^{111, 115}. Cultured primary cortical neurons express all three *Has* genes, with *Has3* having the highest expression⁷⁷. HAS enzymes play an important role in PNN development by synthesizing the HA that serves as the backbone for PNN formation surrounding neurons. *Has3* co-expressed with other components of PNNs in human embryonic kidney cells leads to the synthesis of a compact extracellular matrix that is similar in structure to neuronal PNNs⁷⁵. It is possible that HAS enzymes are an integral part of the PNN and not simply synthesizing the HA backbone of PNNs, as there is evidence that HA can be tethered to the cell membrane by HAS enzymes and not just receptors such as CD44¹¹⁶. *Has1* and *Has2* are differentially expressed in neural crest cells, and the silencing of either enzyme delays neural crest migration⁵¹.

In the aging nervous system, accumulation of HA is correlated with increases in different HAS protein expression, based on location and cell type. HA accumulation in aged gray matter around astrocytes is linked to increased *Has1* expression⁹³, while HA accumulation around cortical microvasculature is associated with increased expression of *Has2*⁹⁴. These studies show that in developing, adult, and aging nervous systems, the three HAS enzymes have different spatiotemporal expression patterns and generally nonoverlapping functions.

Pharmacologic and genetic inhibition of HA synthesis impacts nervous system development and function

While a *Has2* global knockout is embryonic lethal, loss of either *Has1* or *Has3* leads to normal development with no obvious morphological changes¹¹⁷, further supporting the idea that HAS enzymes have distinct functions in neurodevelopment. However, there are some contexts in which the other HAS proteins can compensate for the lack of one. For example, only the loss of all three proteins abolishes glutamate transporter localization to the tips of astrocyte cell processes⁹¹. *Has3* knockout mice and mice lacking *Has2* in the nervous system (through a nestin-driven conditional knockout) lack HA in different brain regions. While *Has3* knockout mice have less HA in the hippocampus, *Has2* conditional knockout animals have reduced HA levels in the cortex and white matter, including the corpus callosum¹¹⁷. *Has2* also plays a role in the development of myelin sheaths, as knockout mice display a greater number of myelin sheath abnormalities, resulting in less compact myelin lamellae and decreased axon diameter⁶⁰.

Interestingly, inhibition of HAS activity through the administration of 4-methylumbelliferone, which inhibits hyaluronan synthesis by depletion of cellular UDP-glucuronic acid and, possibly, by the downregulation of *Has2* and *Has3* expression, delayed the onset and severity of EAE¹¹⁸. These findings suggest that increased hyaluronan synthesis can potentiate autoimmune neuroinflammatory events.

Regulation of HA catabolism in the nervous system

Multiple HA catabolizing proteins are expressed in the nervous system

Hyaluronidases and HA catabolizing proteins are dynamically regulated in the nervous system, and it is increasingly clear that fragments produced by hyaluronidase-driven catabolism of HMW HA have distinct signaling roles in the CNS. HA is catabolized by multiple hyaluronidases (i.e., HYAL1–3 and HYAL5/SPAM1/PH20), the products of which can vary in size¹¹⁹. HYAL1, 2, 3, and PH20 have sequence and structural homology and catabolize HMW HA using the same basic reaction mechanism, but each one has different subcellular locations and optimal conditions for activity¹¹⁹. Another related enzyme, HYAL4, does not have hyaluronidase activity and hydrolyzes chondroitin sulfate¹²⁰.

HYAL1 is located in lysosomes, while HYAL2 is glycosylphosphatidylinositol (GPI)-anchored to the plasma membrane^{121, 122}. It is thought that native high molecular weight HA present in the extracellular matrix is partially degraded first outside the cell, and smaller HA sizes are endocytosed and further degraded by HYAL1 in lysosomes. Early studies show that HA turnover and hyaluronidase activity is highest during development³⁸; however, it is not completely clear which hyaluronidases play a role in the developing and adult nervous systems.

Two more recently discovered proteins display hyaluronidase activity but are structurally distinct from the other hyaluronidases. These two proteins are CEMIP

(cell migration inducing and hyaluronan binding protein, also known as HYBID or KIAA1199) and transmembrane protein-2 (TMEM2). *Cemip* expression has been shown to lead to the degradation of extracellular HA in cultured cells¹²³; however, its expression in the developing nervous system was not previously elucidated. TMEM2 has also been shown to be involved in the digestion of extracellular HA¹²⁴, but its role as a hyaluronidase is currently debated, as another study has shown that the silencing of *Tmem2* increases the degradation of HA¹²⁵.

Hyaluronidases have diverse functions in the nervous system

There is a great deal that is still unknown about the role of hyaluronidases in the development of the nervous system, their functions in the adult nervous system, and how they change with aging. Hyaluronidase activity can influence cells through at least two mechanisms: the reduction in extracellular HMW HA and the production of HA fragments with signaling activity.

Hyal2 expression leads to the degradation of extracellular HA in a CD44 dependent manner¹²⁶, and HA binding to CD44 has been shown to recruit HYAL2 and a sodium/hydrogen antiporter-1 (NHE1) into a macromolecular complex that causes local acidification and HYAL2-dependent extracellular HA degradation¹²⁷. HYAL2 function has also been associated with cell motility¹¹². It is possible that migrating cells use a CD44/NHE1/HYAL2 complex for the localized degradation of extracellular HA in the direction of movement to allow cells to move through an environment that otherwise would not permit migration. On the other hand, other

studies have shown that *Hyal2* silencing does not abrogate the degradation of extracellular HA¹²³, indicating that at least under some conditions, HYAL2 is not necessary to degrade HA in the ECM. Furthermore, studies in early development have indicated a role for HYAL2 in blastocyst formation¹¹³, but observations that *Hyal2* null animals survive to a later stage in development indicate that HYAL2 is not completely necessary for early embryogenesis.

Mice lacking either *Hyal1* or *Hyal3* show no accumulation of HA in the nervous system, indicating that the roles of these hyaluronidases may not be as significant in the CNS and PNS as in other tissues^{128, 129}. *Hyal2* null mice have severely decreased lifespans due to cardiac defects caused by an accumulation of HA¹³⁰. These mice do exhibit HA accumulation in the CNS; however, the only CNS cells that were shown to express *Hyal2* were endothelial cells and cells of the choroid plexus¹³¹.

In contrast to studies of *Hyal* knockout animals, *Cemip* knockout mice show an accumulation of HA in the hippocampus as well as hippocampal dysfunction, resulting in spatial learning and memory defects^{132, 133}. These findings indicate that CEMIP is involved in the catabolism of extracellular HA in the CNS and suggest that HA plays an important role in hippocampal function. However, *Cemip* null animals live to adulthood with no other obvious abnormalities, again suggesting that it is not the only hyaluronidase active in neurodevelopment.

Hyaluronidases in CNS disease

Hyaluronidase expression and activity are increased following a number of insults to the CNS, including ischemia^{97, 99}. The activities of different hyaluronidases can produce HA fragments of different sizes and alter signaling activities that affect nervous system repair. OPCs express multiple hyaluronidases, including *Hyal1* and *Hyal2*¹⁰⁷. The expression of *Ph20* in OPCs and the CNS is disputed¹³⁴. HA fragments generated by increased HA-depolymerizing activity in injured CNS tissues can block the differentiation of OPCs into myelinating oligodendrocytes, thereby inhibiting functional remyelination in inflammatory demyelinating lesions^{15, 106, 107, 110}.

Blocking hyaluronidase activity using a small molecule inhibitor promoted OPC maturation and functional remyelination¹³⁵, though the identity of the hyaluronidase responsible for the catabolism of HA in the ECM and production of these inhibitory fragments is currently unknown. Other than PH20, TMEM2 has been shown to digest extracellular HA¹²⁴; however, its function as a hyaluronidase is currently debated. CEMIP is another candidate, given that the small molecule inhibitor that promotes functional remyelination also blocks HA degradation by CEMIP¹³⁵. The focus of this dissertation is to determine the hyaluronidase(s) involved in generating inhibitory HA fragments in CNS disease.

Multiple HA receptors respond to HA in the developing, mature, and diseases nervous system

CD44, RHAMM, TLR2, and TLR4 are expressed throughout the CNS and PNS

Receptors involved in HA signaling are highly regulated during neurodevelopment, aging, and disease. Among these receptors, CD44 is the most studied. CD44 is one of the main HA receptors in tissues¹³⁶. It is a single-pass transmembrane glycoprotein that transmits changes in extracellular HA to the cytoplasm to allow cell responses to alterations in content and abundance of HA^{2, 136}. CD44 binding to HA in cells is variable and can be regulated based on its expression, alternative splicing, and post-translational modifications. Although many alternative splice variants exist with different affinities for HA, one of the most prominent in the nervous system is the standard form CD44s, encoded by exons 1–5 and 16–20^{3, 137}. Other splice variants have been reported in certain types of neurons¹³⁷. The functions of CD44 variants in the nervous system, both developing and adult, have yet to be fully elucidated.

CD44s binding to HA is partly dependent on N-glycosylation and sialic acid modifications to the extracellular domain^{138, 139}. Loss of both N-glycosylation and bound sialic acid moieties increases the binding of HA to CD44, presumably through the selection of a protein folding conformation that has a greater HA affinity^{138, 139}. Additionally, membrane clustering of CD44 is in part determined by the size of interacting HA molecules, which can regulate downstream signaling and cell responses¹⁴⁰. HA signaling through CD44 plays multiple roles in the

developing and adult nervous system, influencing the proliferation, differentiation, migration, and morphology of many different cell types in diverse contexts.

RHAMM (or HMMR) also has multiple functions in both the developing and adult CNS. Originally found to function in cell migration, as the name suggests, more recent studies have ascribed a greater variety of functions for RHAMM.

Interestingly, RHAMM is found both on the cell surface and intracellularly^{114, 141, 142}, indicating that the cellular location of RHAMM may determine its function.

Surface expression of *Rhamm* could be involved in the regulation of cell migration and process extension through interaction with extracellular HA, while intracellular RHAMM could be involved in microtubule dynamics such as chromosomal segregation and mitosis, as well as maintenance of cell polarity.

The cellular location and subsequent function of RHAMM may be determined by expression of different isoforms via alternative splicing¹⁴².

While TLRs have been extensively studied as pattern receptors involved in innate immune responses to stimuli such as lipopolysaccharide, double stranded RNA, and other damage- and pathogen-associated molecular patterns, TLR2 and TLR4 also function in HA signaling involving HMW HA, as well as lower molecular weight HA fragments¹⁴³. Although it is unclear if HA binds directly to TLRs, TLR2 and TLR4 have been shown to be involved in various aspects of nervous system development, including cell proliferation and differentiation. HA

activation of TLRs may therefore be a critical part of the signaling involved in nervous system morphogenesis and function.

HA receptors in neurodevelopment and the adult nervous system

Cd44 is expressed by numerous nervous system cell types^{12, 41, 44, 46, 144-147}, and a variety of functions have been attributed to CD44-HA interactions in each of these cells. *Cd44* is expressed on neural progenitor cells in the developing CNS and is restricted to subsets of cells as development proceeds^{41, 144}, including adult NSCs¹². In adult NSCs, *Cd44* expression is associated with both self-renewal and differentiation into neurons. NSCs lacking *Cd44* have increased proliferation rates, as well as increased rates of differentiation into immature neurons that display maturation deficits¹², suggesting an essential role of HA signaling through CD44 in regulating adult neurogenesis. CD44- and HA-dependent regulation of adult neurogenesis may explain why *Cd44* null animals experience learning and memory defects⁶⁴. These findings are consistent with studies showing that CD44 has functions in other embryonic and adult stem/progenitor cell populations^{148, 149}.

In developing embryos, *Cd44* knockdown was found to delay migration of neural crest cells⁵¹, indicating a role of CD44 signaling in PNS development.

Additionally, CD44 was found to be involved in the recognition of axon routing cues. Expression of *Cd44* was found at the midline of the optic chiasm⁴⁴, and the inhibition of CD44 with neutralizing antibodies blocked the crossing of growing

retinal neuron axons through the optic chiasm during the development of the optic pathway⁴⁶. In other populations of neurons, CD44 has been shown to play a role in the establishment of dendrite morphology¹⁴⁵, as well as the formation of dendritic spines and functional synapses¹⁴⁶. Furthermore, antagonism of CD44 reduced long-term potentiation in hippocampal neurons¹⁴⁶, and CD44-HA interactions contribute to pain sensitivity⁷⁰, as well as anxiety-like behavior¹⁵⁰.

CD44-HA interactions contribute to lamellipodia outgrowth and increased cell migration^{112, 150-153}, indicating multiple functions of HA signaling in different cell types and contexts through cytoskeletal rearrangements. Through CD44, HA was found to promote migration in both astrocytes⁸⁸ and OPCs¹⁵⁴, as well as contributing to the establishment and maintenance of astrocyte morphology⁸⁹. The ECM might regulate cell migration through the direct binding of HA to CD44 or through changes in extracellular matrix stiffness brought about by increasing local concentrations of HA¹⁵⁵. *Rhamm* is expressed during embryonic development in a variety of species^{40, 114, 156}.

In developing blastocysts, *Rhamm* has been found to be expressed throughout the ectoderm, becoming restricted to the neural plate, and eventually to migratory and post migratory neural crest cells and the ventricular zone of the neural tube after neurulation⁴⁰. These observations suggest a role for RHAMM in regulating both stem cell proliferation and migration. In human embryonic stem cells, RHAMM was shown to function in mitosis as well as maintenance of

pluripotency¹¹⁴. These effects on stem cell proliferation and pluripotency were also observed in mouse embryonic stem cells, in which *Rhamm* silencing reduced cell proliferation and increased differentiation through upregulation of the MEK/ERK pathway¹⁴¹.

RHAMM plays an important role in nervous system development. It is required for proper radial intercalation of neuroepithelial cells and the formation of the neural tube¹⁵⁷. RHAMM-HA interactions also play an important role in neocortical folding⁴³. In the adult CNS, *Rhamm* has been found to be expressed by neural progenitor cells in HA-enriched neurogenic niches such as the SVZ, as well as by migrating neural progenitors in the rostral migratory stream⁶¹. *Rhamm* is also expressed by a subset of neurons in the hippocampus¹⁵⁸.

Interactions between HA and RHAMM have been found to regulate process extension and cell migration in both neurons and glial cells. Neurons express *Rhamm*, and blocking interactions between HA and RHAMM inhibit neuronal migration and neurite extension¹⁵⁹. There is also evidence that both astrocytes and microglia express *Rhamm*, and that HA-RHAMM interactions regulate migration in both glial cell types⁹⁰.

TLR2 and TLR4 both function in NSC proliferation and neurogenesis. *Tlr2* expression has been observed on cortical neuron progenitors in the SVZ, and in these cells, stimulation of TLR2 with an agonist decreased cell proliferation *in*

vitro. In developing brains, TLR2 activation increased ventricular size and decreased the size of proliferative zones⁶³. *Tlr4* expression was observed in neural progenitors in the retina, and the activation of TLR4 decreased cell proliferation and induced the differentiation of progenitors into neurons¹⁶⁰. Human NSCs express both *TLR2* and *TLR4*, which decrease upon differentiation¹⁶¹. TLR4 inhibition decreased human NSC proliferation, while its activation increased differentiation rates¹⁶¹.

Tlr2 and *Tlr4* are expressed in adult neurogenic niches, such as the hippocampus and SVZ, where TLR2 modulates adult NSC differentiation into different lineages (i.e., neurons or astrocytes), and TLR4 regulates stem cell proliferation¹⁶². These observations of *Tlr2* and *Tlr4* expression by both embryonic and neural stem cells, as well as their involvement with NSC proliferation and differentiation, suggest that both TLRs are involved in the modulation of stem cell proliferation and stem/progenitor cell differentiation throughout life, at least in part through interactions with HMW HA and HA fragments.

OPCs express multiple HA receptors, including *Cd44*, *Tlr2*, and *Tlr4*^{15, 41, 163}. Originally it was found that HMW HA blocked OPC differentiation into oligodendrocytes through interactions with TLR2¹⁵. Later studies showed that HMW HA may regulate OPC differentiation in a TLR2- and CD44-dependent manner, while HA fragments of specific size block (~106-310 kDa) OPC

maturation through TLR4^{15, 106, 107}. This result suggests a mechanism whereby HMW HA interactions with TLR2 and CD44 potentiate hyaluronidase activity, and the HA fragments produced from this activity go on to inhibit OPC differentiation. HA fragments interacting with OPCs suppress AKT activation through TLR4 and its adaptor TRIF, leading to the dissociation of transcription factors such as Olig2 from myelin gene promoters and their transcriptional repression, ultimately inhibiting OPC maturation to myelinating oligodendrocytes¹⁰⁶.

HA receptors in nervous system disease

Receptors for HA regulate multiple cell processes in a variety of nervous system diseases. *CD44* expression is elevated in multiple types of CNS insults, including ischemia⁹⁹, traumatic injury^{164, 165}, Alzheimer's disease (including multiple splice variants of *CD44*)¹⁶⁶, Parkinson's disease¹⁶⁷, and white matter diseases such as MS and animal models of MS^{97, 98, 168}. This increase in expression is primarily observed in astrocytes and microglia^{110, 147, 168}. Although *CD44* plays a role in inflammation and immune cell infiltration into the CNS during neuroinflammatory events such as EAE, there are conflicting results showing that *CD44* attenuation may either enhance¹⁶⁹ or inhibit^{103, 170, 171} EAE onset and progression. *CD44* also regulates OPC migration to sites of injury, and OPC differentiation arrest in demyelinated lesions^{106, 154}, indicating a multifaceted role of *CD44* in CNS inflammation and disease. RHAMM was also found to be upregulated after ischemic events^{61, 99}, although the consequences of this increased expression are not completely clear.

As mentioned above, CD44, TLR2, and TLR4 are implicated in the inhibition of OPC maturation in demyelinating lesions through interactions with HMW and HA fragments of certain sizes (175 to 300 kDa)^{15, 106}. TLR4 has also been shown to play an important role in nervous system inflammation after insults such as trauma and ischemia, based on observations that pharmacological inhibition of TLR4 improves outcomes after these events^{163, 172, 173}. Interestingly, HA tetrasaccharides can improve outcomes after spinal cord injury in a CD44 and TLR4 dependent manner¹⁷⁴, and also protect hippocampal neurons during ischemia through the inhibition of TLR2 signaling¹⁷⁵.

Summary

HA plays numerous roles in multiple cell types in the developing and adult nervous system (Figure 1). Although much work remains to be conducted to fully understand the different functions of HA in the CNS and PNS, it is clear that HA acts both by signaling through HA receptors and through its physical properties to influence the structural features of tissues to regulate neural stem/progenitor cell, neuronal, and glial cell behaviors. In particular, the balance of HA synthesis and catabolism must be regulated during nervous system development, providing cues that influence neural stem/progenitor cell expansion and differentiation, cell migration, and process extension of differentiating neurons and glia. In the mature nervous system, HAS and hyaluronidase gene expression appear to be influenced by neuronal activity, leading to the dynamic regulation of HA synthesis

and degradation to influence neuron function but also processes such as neurogenesis during learning and memory. In the mature nervous system, I propose that hyaluronic acid synthase and hyaluronidase gene expression is influenced by neuronal activity, leading to the dynamic regulation of HA synthesis and degradation to influence neuron function, but also processes such as neurogenesis during learning and memory. Finally, this dynamic regulation of HA is altered following nervous insults, initially leading to increased HA synthesis that may temper inflammatory responses that cause nervous system damage, but later resulting in the accumulation of HA fragments that feed back on progenitor cell populations to limit their repair capacity (e.g., limiting OPC maturation by blocking myelin gene expression). This framework provides numerous opportunities to explore signaling cascades that are influenced by changes in the HA-based ECM and to identify possible targets, such as TMEM2, HYAL2, or CEMIP, to promote nervous system repair following injury and in neurodegenerative diseases.

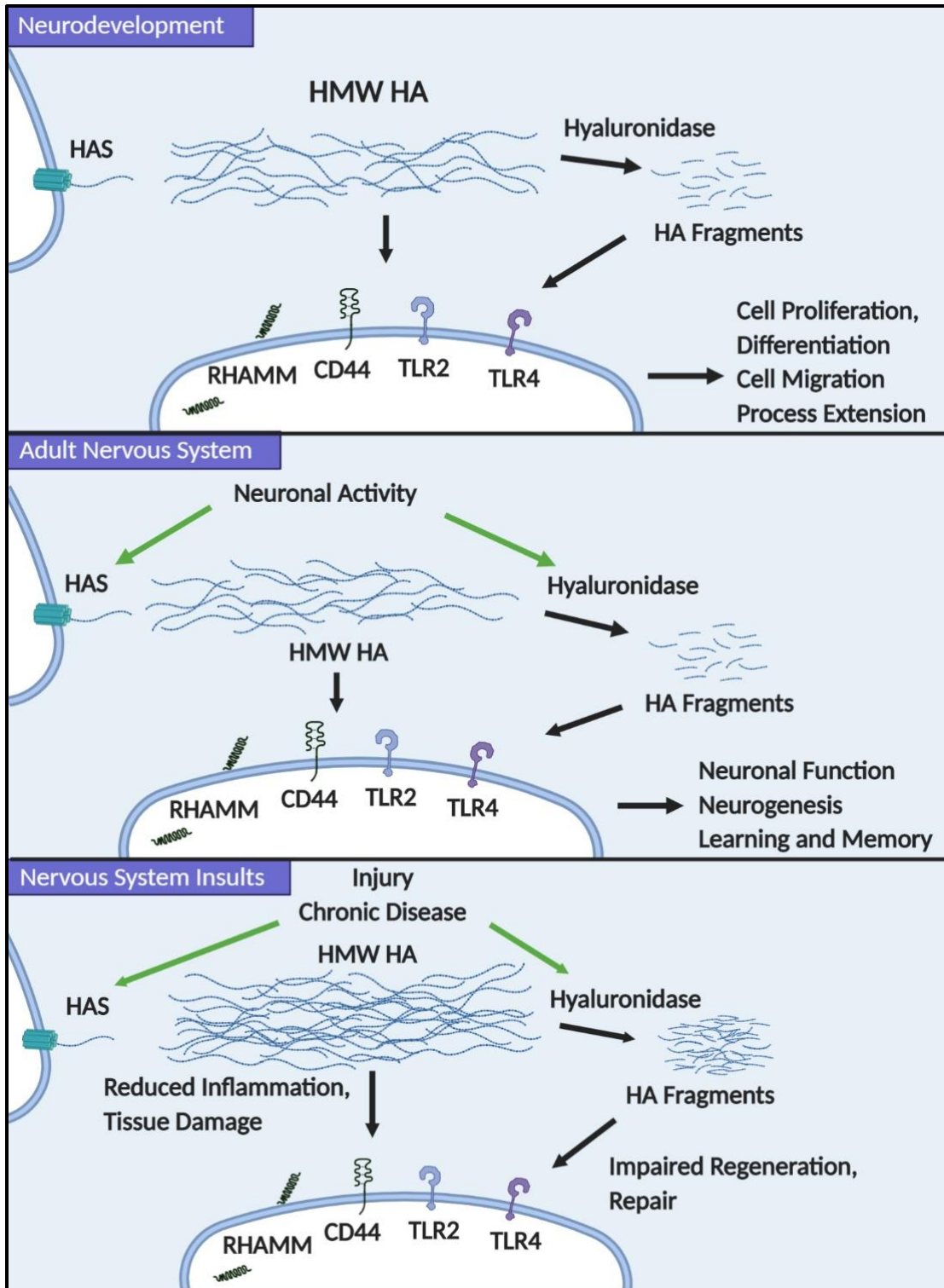


Figure 1. Hyaluronic acid (HA) has diverse functions in neurodevelopment, the adult nervous system, and in nervous system disease. During neurodevelopment, changes to HA in the extracellular matrix (ECM) through the modulation of HA synthases (*HAS*) and hyaluronidase expression and activity help regulate neural stem and progenitor cell proliferation and differentiation, as well as migration and process extension of different neural cell lineages. In the adult nervous system, neuronal activity can alter *HAS* and hyaluronidase expression to regulate neuronal function and adult neurogenesis. During insults to the nervous system, increased *HAS* expression and activity lead to high molecular weight (HMW) HA accumulation which can modulate neuroinflammatory events and provide protection from tissue damage; however, the buildup of HA fragments from hyaluronidase activity can inhibit the repair capacity of progenitor cells.

Rationale and hypotheses

How does hyaluronan metabolism influence remyelination during CNS inflammatory demyelination?

The Sherman lab studies the role of HA in inflammatory demyelination, including MS. MS is characterized by autoimmune-mediated targeting and destruction of CNS myelin and neuronal damage over time¹⁷⁶. Focal neuroinflammation and demyelination develop as immune cells (primarily T-cells, plasma cells, and macrophages) infiltrate the CNS and break down myelin, forming lesions that can be observed using magnetic resonance imaging (MRI) combined with a gadolinium contrast agent¹⁷⁷. In chronically active MS lesions, it has been found that OPCs accumulate at lesion sites but fail to differentiate into myelinating oligodendrocytes¹⁷⁸⁻¹⁸¹. Previous studies by the Sherman lab have found that HA and CD44 levels increase in MS lesions and in mice with EAE¹⁸². HMW HA was found to inhibit both the differentiation of oligodendrocyte progenitor cells *in vitro* and *in vivo* remyelination in a mouse model of focal demyelination¹⁸², but further studies found that it was HA fragments produced by

hyaluronidase activity that were more potent at inhibiting OPC differentiation and *in vivo* remyelination^{106, 107}.

Additionally, the Sherman lab has recently found a small molecule hyaluronidase inhibitor, S3, that blocks the activities of the PH20 and CEMIP hyaluronidases, but not HYAL1 or HYAL2¹³⁵. S3 also accelerated *in vitro* OPC differentiation in the presence of HMW HA, and functional remyelination after focal demyelination in the corpus callosum¹³⁵. These studies have demonstrated that hyaluronidase activity in active demyelinating lesions produces HA fragments that inhibit OPC differentiation and functional remyelination; however, the hyaluronidase(s) that produce these extracellular bioactive HA fragments remained to be identified. In this dissertation, I sought to determine how genes encoding enzymes directly involved in hyaluronic acid synthesis and catabolism (i.e. hyaluronic acid synthases and hyaluronidases) change during autoimmune-mediated inflammatory demyelination, and which hyaluronidase(s) are responsible for the production of extracellular inhibitory HA fragments that contribute to inhibiting remyelination rates. I hypothesized that at least one of the more recently discovered hyaluronidases, TMEM2 and CEMIP, were involved with the production of inhibitory HA fragments at lesion sites.

Is targeting hyaluronidase activity a tractable method for accelerating functional remyelination during inflammatory demyelination?

The findings that S3 can accelerate functional remyelination¹³⁵ supports the idea that hyaluronidase inhibitors could be used as a potential treatment for MS. S3 is a small molecule derived from the flavonoid apigenin, a natural plant extract that has previously shown to have anti-inflammatory effects in humans^{183, 184}. As part of my PhD research, I also sought to determine if other small molecules, both synthesized and naturally derived, inhibited hyaluronidase activity and accelerate *in vitro* OPC differentiation. My goal was to determine whether other compounds similar in structure to S3 and apigenin retained their biological activity or had different potencies. The overall goal of these studies was to reveal whether this class of compounds could be exploited to develop therapeutic strategies designed to accelerate functional remyelination in MS patients.

CHAPTER 2: THE CEMIP HYALURONIDASE IS ELEVATED DURING INFLAMMATORY DEMYELINATION AND PRODUCED BIOACTIVE HYALURONIC ACID FRAGMENTS THAT DELAY REMYELINATION

For submission to Annals of Neurology

Introduction

Multiple Sclerosis (MS) is the most common autoimmune disease of the central nervous system (CNS), affecting approximately 2 million individuals worldwide¹⁸⁵. Characterized by neuroinflammatory demyelination, MS can impair motor, sensory, and cognitive function in patients^{177, 185, 186}. Currently approved therapies for MS target the immune system to reduce the number of neuroinflammatory attacks, however demyelination still occurs and almost all patients experience disease progression¹⁷⁶.

CNS lesions in MS and other demyelinating diseases exhibit remyelination delay or remyelination failure despite the presence of intact axons. Remyelination failure is linked to the inability of oligodendrocyte progenitor cells (OPCs), which accumulate at lesion sites, to mature into myelinating oligodendrocytes (OLs)¹⁸⁷⁻¹⁹⁰. Changes in the microenvironments of demyelinating lesions are therefore likely to be the underlying cause of blocked OPC maturation and remyelination failure. One such change in the lesion microenvironment is the accumulation of the extracellular matrix glycosaminoglycan hyaluronan (HA; also called hyaluronic acid) at lesion sites¹⁸². HA is composed of unbranched, non-sulfated

repeating units of glucuronic acid and *N*-acetyl-glucosamine ranging in size from $\leq 2.5 \times 10^5$ Da to high molecular weight (HMW) sizes $\geq 4 \times 10^6$ Da. HA is synthesized at the plasma membrane by HA synthases (HAS1, HAS2, and HAS3) and catabolized by multiple hyaluronidases that generate distinct sizes of HA fragments. Several HA receptors have been identified, including the CD44 transmembrane glycoprotein, to regulate cell growth, migration and differentiation in response to HA¹⁹¹.

The increased synthesis of HMW HA paired with hyaluronidase activity in active demyelinating lesions produces bioactive HA fragments that impair OPC differentiation and remyelination^{15, 106, 107}. Blocking hyaluronidase activity using a small molecule inhibitor in a mouse model of lysolecithin-induced focal demyelination led to increased functional remyelination¹³⁵, demonstrating a potential method to promote remyelination in MS and other demyelinating lesions. However, the mechanisms of increased HA synthesis and which hyaluronidase(s) are elevated during neuroinflammatory demyelination to produce extracellular inhibitory HA fragments is unknown.

Here, I sought to identify how the expression of hyaluronan synthases, *Cd44*, and different hyaluronidases changed in CNS tissue during the course of neuroinflammatory demyelination, and to determine if a specific hyaluronidase is responsible for blocking OPC maturation and remyelination in demyelinating lesions. Among the hyaluronidases that were assessed, I found the greatest

increase in expression by the cell migration-inducing and hyaluronan-binding protein (CEMIP; originally named KIAA1199). CEMIP can digest HA although the mechanism is unclear¹⁹². Mutations in CEMIP lead to hearing deficits, and mice lacking *Cemip* demonstrate memory and learning deficits as well as increased HA levels in the brain^{132, 133}. CEMIP also plays roles in the progression and metastasis of a growing number of cancers¹⁹³, and one study suggested that CEMIP could be elevated in MS lesions¹⁹⁴. I found that *Cemip* is expressed by OPCs in demyelinating lesions and that it digests HMW HA into bioactive HA fragments that inhibit OPC maturation. Furthermore, I found that HA digested by CEMIP blocks remyelination. These data support the notion that CEMIP is a potential target for therapies that promote remyelination.

Materials and methods

All animal experiments were approved by the Institutional Animal Care and Use Committee at the Oregon Health & Science University.

Cell Culture

Human embryonic kidney 293T cells were cultured in Dulbecco's modified eagle medium (DMEM, Fisher) supplemented with 10% fetal bovine serum (FBS, Atlas Biologicals). 293T cells were subcultured using 0.25% trypsin (Fisher) to dissociate cells. Primary mouse oligodendrocyte progenitor cells (OPCs) derived from oligospheres were cultured as previously described^{107, 135}. Briefly, OPCs were cultured in DMEM:F12 (Gibco) supplemented with 0.1% bovine serum

albumin (BSA, Fisher), recombinant platelet-derived growth factor AA (PDGF-AA, Promega), and fibroblast growth factor-2 (FGF-2), B27 supplement without vitamin A (Gibco), N1 supplement (Sigma), and Biotin (Sigma). Cells were dissociated for subculturing using Accutase (Invitrogen).

RNA extraction, cDNA generation, and qPCR

RNA was extracted from tissue and cells using the Macherey-Nagel Nucleospin RNA Plus kit, and cDNA generated using an Applied Biosciences High Capacity cDNA Reverse Transcription Kit. qPCR was performed as previously described using SybrGreen (Fisher), and changes in gene expression were determined using the delta-delta-cycle threshold ($\Delta\Delta C_t$) method. Primers used to measure changes in gene expression, including housekeeping genes, are listed in Table 1.

Gene	Forward Primer (5' to 3')	Reverse Primer (5' to 3')
<i>IL-6</i>	CACTTCACAAGTCCGAGGCT	TGGTACTCCAGAAGACCAGAGG
<i>Tnfa</i>	GTTGTACCTTGTCTACTCCC	CTCCTGGTATGAGATAGC
<i>Ifny</i>	AACGCTACACACTGCATCTTGG	GCCGTGGCAGTAACAGCC
<i>Gfap</i>	CGAAGAAAACCGCATCACCAT	TCACCATCCCGCATCTCCA
<i>Mbp</i>	GCTCCCTGCCCCAGAAGT	GATGGAGGTGGTGTTCGAGG
<i>Pdgfra</i>	ACCTCCCACCAGGTCTTT	CTTCACTCTCCCCAACGCAT
<i>Cd44s</i>	CCATCAGAGTCCAGAGTCAT	CTGTTTCATCTTCATTTTCCTCA
<i>Iba1</i>	TCAGCTACTCTGACTTTTCTCA	CCTCTTGTGTTCTTTGTTTTTC
<i>Olig2</i>	CGCAGCGAGCACCTCAA	CGATGGGCGACTAGACAC
<i>Has1</i>	GTTAACTATCTACTGGGTAGG	CTCACAAGGACTCCTCCTTT
<i>Has2</i>	GGTGGTGTAAATTTTCACCATT	CATCAAGCACCATGTCATAC
<i>Has3</i>	TGTCCATCTGGGTGGCAGTT	TCCGCAAAAGCCAGGCTATA
<i>Hyal1</i>	GCACCCTCCAACCTGGGGCAG	CGGTGTGGAACGTACATCTG
<i>Hyal2</i>	GAGTTCCTGAGCTGCTACCA	GTCTCGTCCAGGTACACAGA
<i>Hyal3</i>	CTGGACGACCTGATGCAGAC	GGGCCCTAAAGTGCCCACTAA
<i>Ph20/Spam1</i>	GCGTCGGTGACAATGTTTGTAT	GTGGCAGATGGTACAGCACAT
<i>Cemip</i>	CAATGACCAAACTGGGCAGC	CAGTTTGAAAACCCGGGCAG
<i>Tmem2</i> (<i>Cemip2</i>)	TTGGAAACTACGTCCCTGTG	CATGCAGTCTGTGGTAGGCA
<i>Cyca</i>	GGCAAATGCTGGACCAAACACAA	GGTAAAATGCCCGCAAGTCAAAG
<i>Gapdh</i>	GCATTGTGGAAGGGCTCATG	AGCCCCACGGCCATCAC

Table 1: qPCR primer sequences

HA fragment generation and purification

Cemip expression vector (Catalog MR217955) and empty vector (Catalog PS100001) were purchased from Origene. All transfections were completed using Fugene HD (Promega).

6x10⁶ 293T cells were cultured on 10cm² polystyrene dishes (Fisher) overnight, and transfected with 10µg plasmid the following day (1:3 DNA to Fugene HD

ratio). 24 hours after transfection, culture medium was replaced with 10mg of high molecular weight hyaluronic acid (HMW HA, Lifecore Biomedical) dissolved in 10mL of dye free, serum free, DMEM (Fisher).

After 72 hours of incubation, conditioned medium was harvested and HA extracted using phenol:chloroform solution (1:1, both chemicals from Sigma). An equal volume of phenol:chloroform was added to the conditioned medium, and the solution was centrifuged at 12,000rpm for 45 minutes. The aqueous layer was harvested and dialyzed in pure water using a 20,000 Dalton molecular weight cutoff dialysis cassette (Fisher) for 24 hours, replacing the water with fresh pure water halfway through. The conditioned medium was then collected, dried overnight in a SpeedVac, and resuspended in pure water to reach a desired concentration for use in subsequent experiments. HA yield is thought to be >95%.

HA gel assay

HA and conditioned medium/HA fragments were analyzed using agarose gel electrophoresis as described previously^{107, 135}. HA fragments were separated by size in a 0.5% HGT agarose gel (SeaKem) in tris-borate EDTA (Fisher). The gel was then stained in 0.005% Stain-all (Fisher) in 50% ethanol overnight, and washed in 10% ethanol overnight in the dark. Gels were de-stained in light then imaged. High, medium, and low HA ladder was purchased from Echelon Biosciences.

Differentiation experiments

OPC differentiation experiments were performed as previously described^{106, 107, 135, 182}. OPCs were plated on poly-ornithine (Sigma) coated coverslips in 24-well plates at 3×10^4 cells per coverslip. The following day, OPC culture medium was replaced with DMEM:F12 supplemented with B27 supplement (Fisher), N-acetyl cysteine (NAC, Sigma), and triiodothyronine (T3, Sigma) with and without HMW HA and conditioned medium/HA fragments from 293T cells overexpressing either empty vector or *Cemip* (final concentration for all HA conditions is $50 \mu\text{g/mL}$). Differentiation medium was replaced daily for five days, then cells were fixed in 4% PFA. Immunocytochemistry was used to determine relative amounts of PDGFR α^+ OPCs and MBP $^+$ oligodendrocytes, and percent area coverage of each marker was calculated using ImageJ to determine the ratio of MBP/PDGFR α expression. Percent delay in differentiation when compared to untreated control was calculated from MBP/PDGFR α levels. At least three biological replicates consisting of three coverslips per condition were used. Six images per coverslip encompassing approximately 9mm^2 (~70% of the coverslip) were generated for analysis of OPC differentiation rates.

To induce *Cemip* overexpression, OPCs were plated on coated coverslips at 2×10^4 cells per coverslip. The following day, cells were transfected with 125ng of either empty vector or *Cemip* expression vector (Origene, above) using Fugene HD at a 1:6 DNA to reagent ratio. Cells were induced to differentiate for 5 days in

the presence and absence of HMW HA and analyzed for changes in differentiation rates using immunocytochemistry as previously described^{106, 107, 182}.

For differentiation experiments OPCs were plated in polyornithine coated 6-well plates (Fisher) at a density of 1×10^6 per well. Individual wells had medium replaced with differentiation medium for 1, 2, 3, or 4 days, starting with the longest so that all wells were harvested for RNA extraction, cDNA generation, and qPCR.

TNF α Treatment

OPCs were plated at 3×10^6 cells per well in a poly-ornithine coated polystyrene 6-well plate (Fisher) in growth medium. The following day, cells were treated with either vehicle (PBS) or TNF α at 10ng/mL. Cells were incubated for 24 hours, then harvested for RNA extraction and qPCR. N=9 per condition.

Embryological studies

Mice were paired for timed matings for 9.5, 10.5, 13.5, or 18.5 days. Presence of an ejaculatory plug and weight gain were used to verify pregnancies. Embryos were collected and brains dissected from embryos for RNA extraction and qPCR. Four brains were used per timepoint for E10.5, E13.5, and E18.5. Due to size, heads of E9.5 embryos were collected, and three heads pooled per replicate (N=4) to ensure adequate amounts of tissue for RNA extraction.

Morphological analysis was used to confirm embryological developmental day/stage.

Induction of EAE

Induction of EAE was performed by Kanon Yasuhara, a Research Assistant in the Sherman lab.

Experimental autoimmune encephalomyelitis was induced in 3-4 month old female C57Bl/6J mice with myelin oligodendrocyte glycoprotein 35-55 (MOG, Peptides International) in complete Freund's adjuvant¹⁰³. Pertussis toxin (List Labs) was injected the day of inoculation and 2 days post inoculation. Clinical scores were evaluated as previously described^{103, 182}. Cumulative disease index of mice was calculated as the sum of clinical scores of mice between 7 and 21dpi. Lumbar spinal cords were extracted at the indicated times post inoculation for RNA extraction or fixation and tissue processing. Four mice were harvested per condition.

Focal demyelination with lysolecithin

Focal demyelination was induced in the rostral corpus callosum in 3-4 month old mice as performed previously^{107, 182}. 2% Lysolecithin (Sigma) mixed with PBS (vehicle), and HA fragments purified from either vector expressing or *Cemip* expressing cells and injected at the following coordinates from Bregma: AP: +0.5mm, LAT: -0.6mm, and Z: -2.4mm. Brains were harvested at 7 days post

injection for CAP recordings, followed by fixation in 4% PFA and tissue processing.

Compound action potential (CAP) recordings

CAP recordings were performed by Dr. Steven Matsumoto with the author's assistance.

After tissue harvesting, brains were submerged in ice-cold artificial cerebrospinal fluid (aCSF) comprising of 124mM NaCl, 5mM KCl, 26mM NaHCO₃, 1.25mM NaH₂PO₄, 1.3mM MgSO₄, 2mM CaCl₂, and 10mM glucose at pH 7.4, saturated with a 95% O₂/5% CO₂ gas mixture. A 400µm section containing the lesion site was cut using a vibratome and incubated in aCSF with aeration at room temperature for one hour. CAP recordings across the corpus callosum were recorded as previously described¹³⁵. For each recording session 2 animals per group were analyzed.

Tissue processing

Cells were fixed in 4% PFA for 15 minutes, followed by 3 washes in PBS for 5 minutes each. Brains and spinal cords were fixed in 4% PFA for 24 hours at room temperature, followed by five 2-hour washes in PBS. Tissue was then put through an ethanol series (first with 5%, then 10% followed by increments of 10% until a final concentration of 70%) before being embedded in paraffin. 10µm tissue sections were used in downstream applications, including immunofluorescent experiments.

Immunohistochemistry

Tissue sections were de-paraffinized in xylene, followed in rehydration in graded ethanol. Sections were treated with Protease Plus solution (ACDBio) for 30 minutes at 40C, washed 2 times in ddH₂O, and treated with 0.1% Sudan Black (Sigma) solution in 70% ethanol for 1 minute, followed by 3 rinses in PBS.

Cells and tissue sections were permeabilized in 0.1% Triton X-100 (Sigma) in PBS for 15 minutes, followed by blocking for 2 hours in either 5% normal goat serum or normal donkey serum, depending on primary antibody selection (both from Jackson ImmunoResearch). Blocking solution was replaced with primary antibody mixture and incubated at 4C overnight. Primary antibodies used are listed in table 2. The following day, cells/tissue were washed three times with 0.05% Triton X-100 PBS for 5 minutes each, then incubated in appropriate secondary antibody solution for 2 hours at room temperature. Following this, slides were treated with DAPI (4',6-diamidino-2-phenylindole) (Fisher) at 1µg/mL in PBS for 5 minutes, then washed in 0.05% Triton PBS four times for 5 minutes each. Slides were mounted with Fluoromount-G (Southern Biotech) and Fisher coverglass.

Manufacturer	Catalog	Host	Target	Dilution
Sigma	G3893	Mouse	GFAP	1:5000
BioLegend	808402	Mouse	MBP	1:800
BD Pharmigen	558774	Rat	PDGFR α	1:100
Novus	NB600-144155	Rabbit	CD3	1:100
Wako	019-19741	Rabbit	Iba1	1:300
Sigma	SAB2105467	Rabbit	CEMIP	1:100
R&D Systems	AF2418	Goat	OLIG2	1:250
R&D Systems	AF1062	Goat	PDGFR α	1:20
R&D Systems	AF1002	Goat	VE-Cadherin	1:250

Table 2: Primary antibody list.

Imaging

Stained cells and tissues were imaged using an Olympus VS 120 SlideScanner with the following objectives: 2x/0.08NA Olympus Plan ApoN, 10x/0.40NA Olympus UPlanSApo, 20x/0.75NA Olympus UPlanSApo, and 40x/0.95NA UPlanSApo. The 2x objective was used for overview scans. Cells were imaged at 20x on one plane. EAE and MS tissue sections were imaged either at 20x on one plane, or at 40x with a 10 μ m Z-stack at 2 μ m intervals (5 slices). Maximum Z projection images were generated using CellSens software (Olympus), and all other analyses were performed using Fiji/ImageJ (National Institute of Health).

Luxol fast blue staining

Luxol fast blue staining was performed as previously described¹⁹⁵. Deparaffinized sections were placed in luxol fast blue (0.1% dissolved in 95% ethanol, Sigma) solution at 56C overnight. Slides were then rinsed in 95% ethanol and then water, then differentiated first in 0.05% lithium carbonate

(Sigma) for 30-60 seconds, then in 70% ethanol for approximately 60 seconds, then counterstained in 0.1% cresyl violet solution (Sigma) for 6 minutes. Slides were then dehydrated first in ethanol, then xylene, and then mounted in Fluoromount-G.

Human MS samples

Human MS samples were acquired from the University of Washington. All patients tested had relapsing-remitting MS. Patient information can be found in Table 3.

Patient	Age at death	Sex
1	93	Female
2	96	Female
3	74	Female
4	45	Male

Table 3: MS patient information.

Statistics

Statistically significant differences were tested using either an uppaired Student two-tailed T test (HA fragment sizes in CM analyzed by solid state nanopore assay) or an unpaired Student two-tailed T test with Welch's correction (differences in *Cemip* transcription in OPCs treated with TNF α) for two groups. A one-way ANOVA followed by Tukey's multiple comparison test was used to test for significance for experiments involving more than two conditions. A P-value below 0.05 was considered statistically significant.

Results

HA synthases, CD44, and hyaluronidases are elevated during peak neuroinflammatory demyelination

To explore the role of HA synthesis, signaling, and catabolism in inflammatory demyelinating disease, I examined the expression of HA synthases, *Cd44*, and hyaluronidases in demyelinating lesions in the C57Bl/6J-MOG model of experimental autoimmune encephalomyelitis (EAE), a model of MS. In this model, mice develop increasing ascending disability, starting with tail weakness, followed by partial motor recovery. In my experience with this model, peak disease is reached between 14 and 21 days post-inoculation (dpi; Fig. 2A, B). Lumbar spinal cord tissue, which demonstrates the greatest pathology in this model, was harvested from healthy C57Bl/6J mice and mice at multiple EAE stages (7 dpi, before motor symptoms develop; 14 dpi, when motor symptoms are worsening; and 21 dpi just after peak disease). RNA was extracted from these tissues, and quantitative polymerase chain reaction (qPCR) was used to determine changes in the expression of genes coding for HA synthases (*Has1*, *Has2*, and *Has3*), *Cd44*, and hyaluronidases (including the transmembrane protein-2 (*Tmem2*, also known as *Cemip2*), *Hyal1*, *Hyal2*, *Hyal3*, and *Cemip*; Fig. 2C). From the same RNA samples, genes involved in remyelination, astrogliosis, microglial activation, and various inflammatory mediators were also analyzed (Fig. 2D).

I found no significant changes in spinal cord gene expression at 7 dpi (Fig. 2C, D). However, at 14 dpi, I found significant increases compared to healthy controls in *Has1* ($p < 0.01$) and *Has2* ($p < 0.0001$) but not *Has3* (Fig. 2C). *Cd44* was also significantly elevated ($p < 0.0001$). This is consistent with previous studies showing that CD44 expression is increased and HA accumulates in EAE and MS lesions¹⁸². Interestingly, among hyaluronidase transcripts, only *Cemip* was elevated at this timepoint ($p < 0.001$). At 21 dpi, only *Has2* remained significantly elevated ($p < 0.001$) among the HA synthases. *CD44* remained elevated ($p < 0.0001$) along with *Cemip* ($p < 0.0001$), while another hyaluronidase, *Hyal2*, was slightly elevated ($p < 0.01$; Fig. 2C).

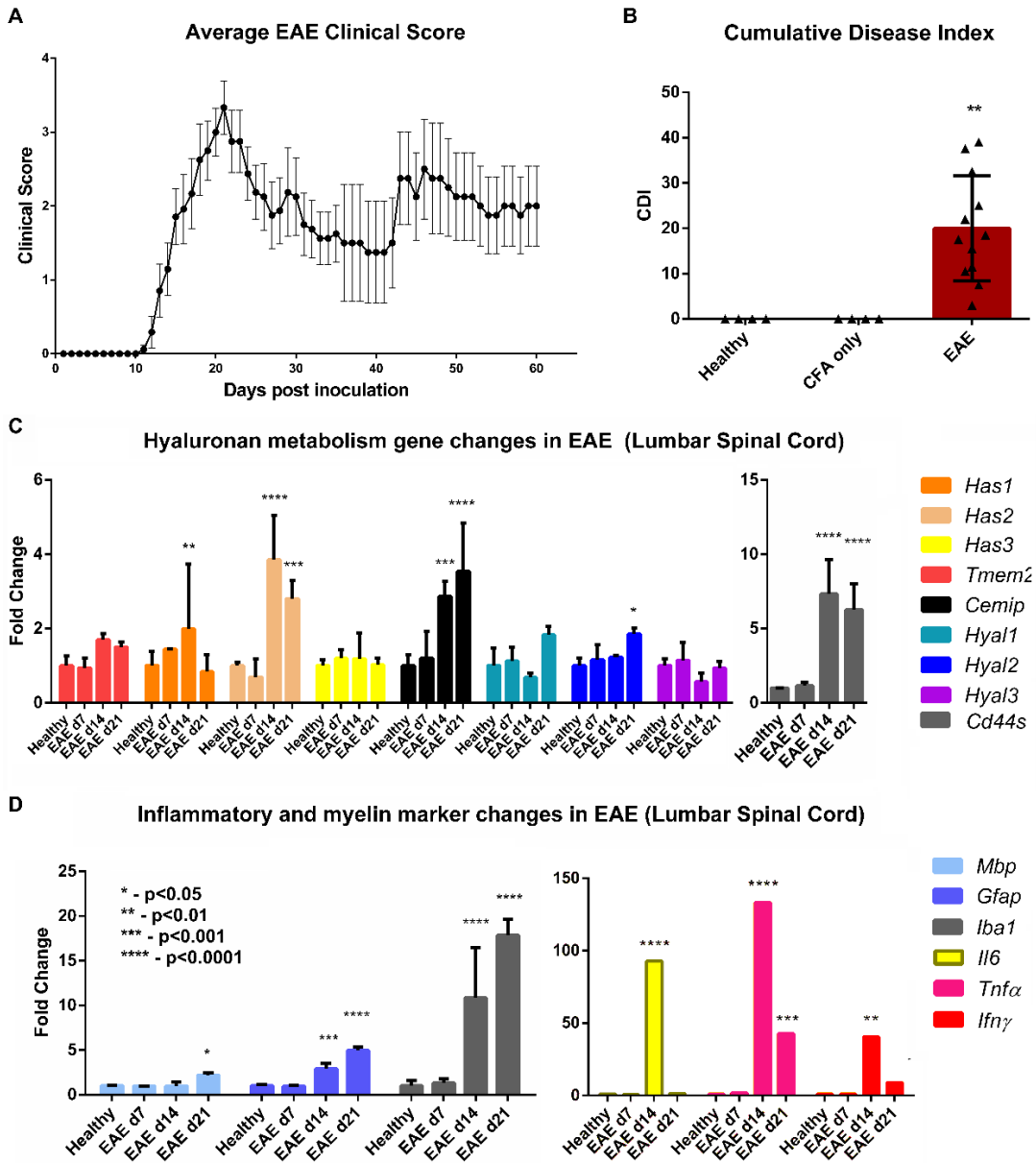


Figure 2: *Cemip* transcription is increased during EAE. C57Bl/6J mice induced to have EAE presented with a typical disease course (A,B). At indicated timepoints, lumbar spinal cords were extracted from mice, RNA and cDNA prepared, and qPCRs performed to detect changes in genes involved with hyaluronan metabolism (C) or myelin and neuroinflammatory genes (D). *Has1* and *Has3* transcripts were increased at times in EAE, and among hyaluronidases *Cemip* was the only one that increase coincident with neuroinflammatory genes. *Ph20* transcripts were not detected at any time. * - $p < 0.05$, ** - $p < 0.01$, *** - $p < 0.001$, **** - $p < 0.0001$.

Coincident with increased *Has1*, *Has2*, *Cd44*, and *Cemip* expression at 14 dpi, I observed significant increases in glial fibrillary acidic protein (*Gfap*; $p < 0.001$), a marker of astrogliosis, and ionized calcium binding adaptor molecule 1 (*Iba1*; $p < 0.0001$), a marker of microglia activation. Both *Gfap* and *Iba1* remained elevated through 21 dpi. These genes are typically elevated in demyelinating lesions. Myelin basic protein (*Mbp*), a marker of mature, myelinating OLs, was slightly elevated at 21 dpi ($p < 0.01$), indicating that at least some OPCs were maturing into myelinating OLs at this time. In addition, at 14 dpi I observed elevated levels of the inflammatory mediators interleukin-6 (IL6; $p < 0.0001$), tumor necrosis factor- α (*Tnfa*; $p < 0.0001$), and interferon- γ (*Ifny*; $p < 0.001$). Among these, only *Tnfa* remained significantly elevated through 21 dpi. These findings support the hypothesis that *Cemip* is transcriptionally upregulated in demyelinating lesions coincident with increased HA synthesis and *Cd44* expression during peak periods of demyelination and neuroinflammation.

Cemip expression localizes to areas of demyelination and reduced HA

The increase in *Cemip* RNA levels observed by qPCR analysis of spinal cord tissues from mice with EAE was validated by comparing *Cemip* transcript expression in healthy and EAE lumbar spinal cord sections (at 21 dpi) using RNAscope *in-situ* hybridization. I confirmed that *Cemip* transcription increased compared to healthy controls in the spinal cords of mice with EAE, both in the

parenchyma of white matter and in parameningeal areas (Fig. 3A-F). I then used combined immunohistochemistry and *in situ* hybridization to identify commercial antibodies that accurately immunolabeled CEMIP protein in tissues (Fig 4). I identified one such antibody and used it to compare *Cemip* expression with MBP to label myelin and a biotinylated HA-binding protein (HABP) to localize HA in spinal cord tissues. I found that in lumbar spinal cord sections of animals over all stages of EAE where motor symptoms are present, CEMIP protein localized to EAE lesion areas that exhibited demyelination and reduced levels of HA when compared to white matter from healthy controls, controls treated with CFA alone, and normal appearing white matter adjacent to lesion sites (Fig. 3G-S). I also examined sections of demyelinated lesions from four patients who had relapsing-remitting MS, staining one section from each case with Luxol Fast Blue to identify areas of demyelination, and adjacent sections with DAPI (to label cell nuclei), anti-MBP, and anti-CEMIP antibodies. Consistent with the findings in EAE lesions, I observed CEMIP-positive cells within areas of demyelination in each of the MS cases (Fig. 3T-X)

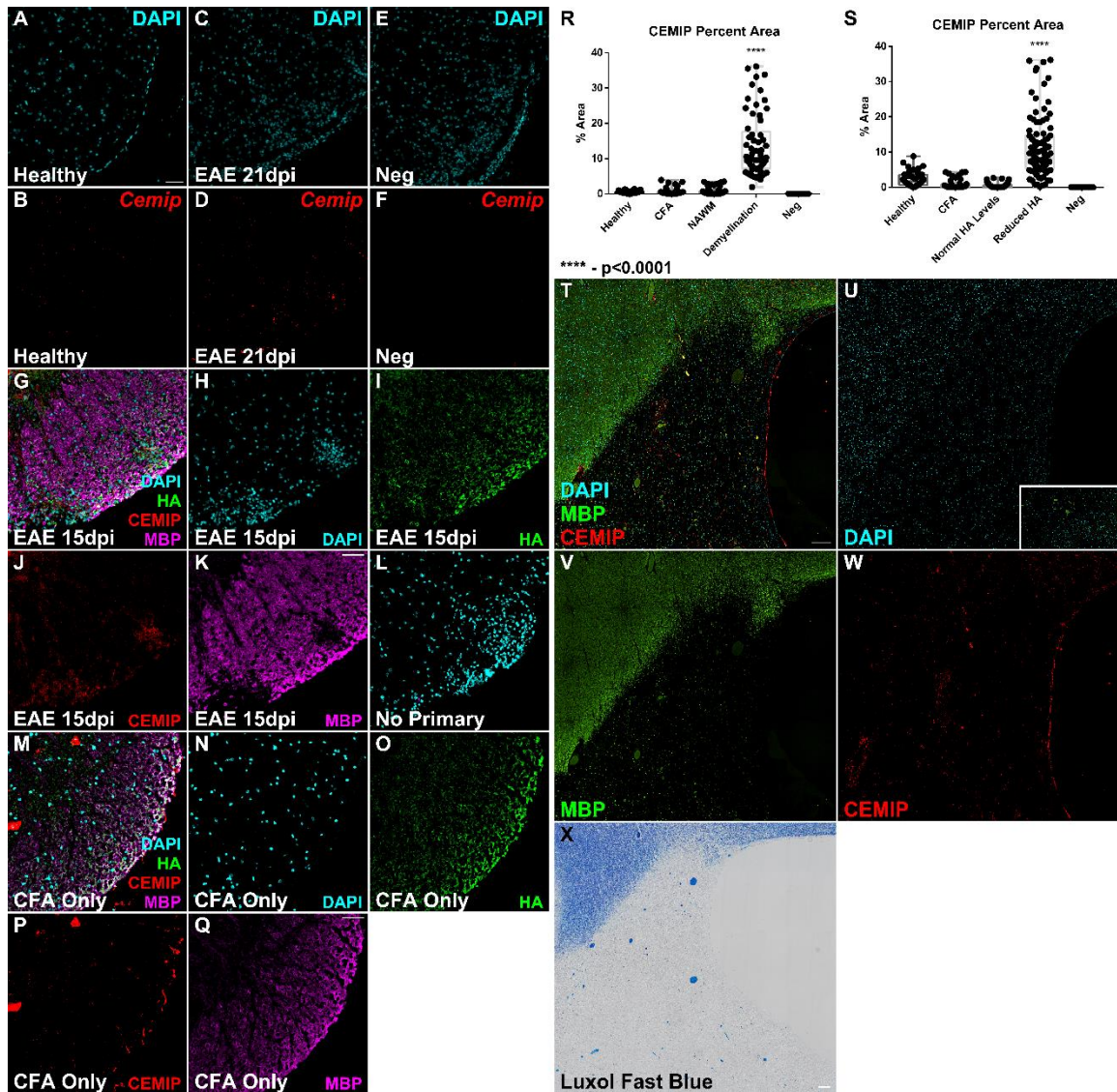


Figure 3: RNAscope *in situ* hybridization experiments targeting *Cemip* reveal that elevated *Cemip* transcription in EAE lumbar spinal cord sections localize to parameningeal areas and areas of hypercellularity, a sign of inflammation and active demyelination (A-F, Neg – negative control probe). Immunofluorescent labelling of CEMIP, MBP, and HABP reveal that elevated CEMIP protein localizes to areas of demyelination and less HA (G-K, L – no primary control, M-Q – CFA-only control). Comparing the percent area of *Cemip* expression between healthy tissue, CFA-only controls, areas of demyelination and reduced HA, and adjacent normal appearing white matter areas reveal that CEMIP is only elevated at lesion sites in EAE. Labeling of CEMIP and MBP in human MS tissue sections show that CEMIP also localized to lesion areas (T-W, X – luxol fast blue stain of adjacent section). Scale bars for mouse tissue images are 50µm, 200µm for human IF images, and 100µm for LFB image. **** - $p < 0.0001$.

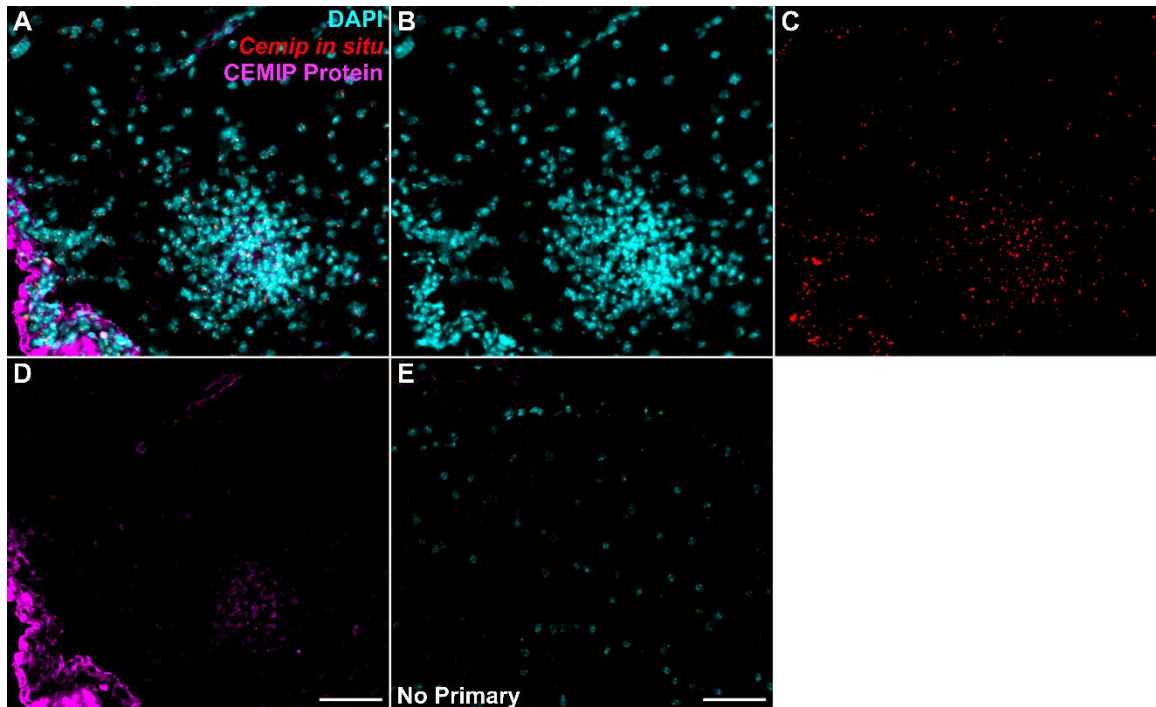


Figure 4: Co-staining of CEMIP protein and *Cemip* transcript using RNAScope reveal signal that largely co-localize in space. RNAScope seems to have a greater sensitivity to detect CEMIP expression. Scale bar = 50 μ m.

Oligodendrocyte progenitor cells express Cemip

I next determined which cells expressed *Cemip* within demyelinating lesions. I first assessed *Cemip* expression using the Barres lab Brain RNA-seq project database¹⁹⁶ and found that OPCs have the highest *Cemip* expression of any cells in the brain, followed by at least a subset of neurons, with weak expression in endothelial cells (Fig. 5A). Astrocytes and microglia did not express *Cemip*. To validate these findings, I performed qPCR analyses of mouse OPCs grown *in vitro*. OPC cultures expressed *Cemip*, and this expression decreased over time as the cells differentiated into myelinating OLs as indicated by decreased *Pdgfra* expression and increased *Mbp* expression (Fig. 5B-D). I then

co-stained for CEMIP and PDGFR α or Olig2 (both markers for OPCs) in lumbar spinal cord sections from mice with EAE, and found that a subset of *Cemip* expressing cells within lesions also express *Olig2* and *Pdgfra* (Fig. 5E-L). I also observed CEMIP protein levels in vascular endothelial cells that also VE-cadherin (Fig. 5M-R). I did not observe *Cemip* expression in microglia (Fig. 5S-V). Furthermore, in contrast to a previous report¹⁹⁴ but consistent with the RNAseq findings, CEMIP protein did not co-localize with GFAP, indicating that astrocytes do not express *Cemip* at these EAE stages (Fig. 5M-R).

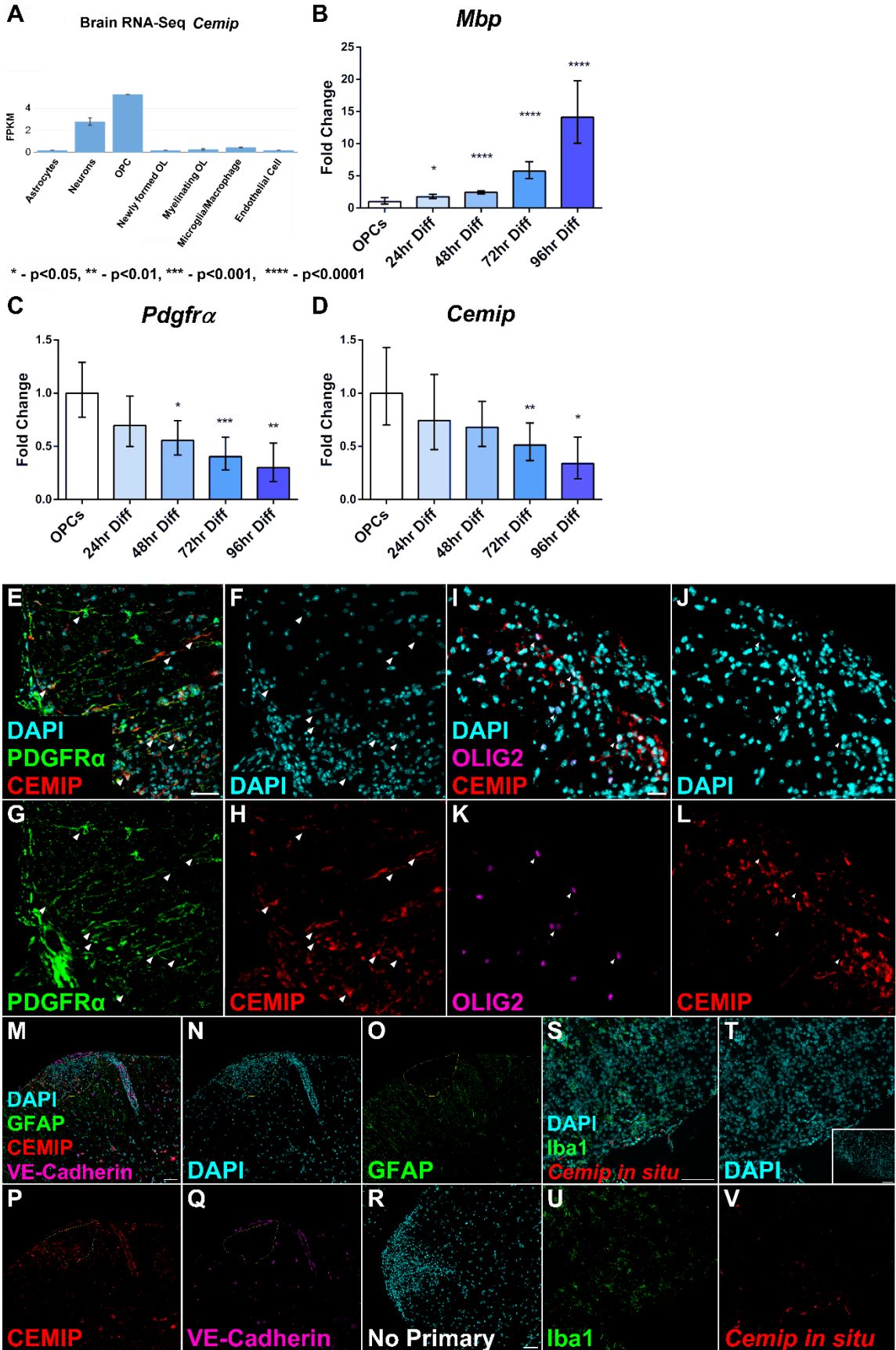
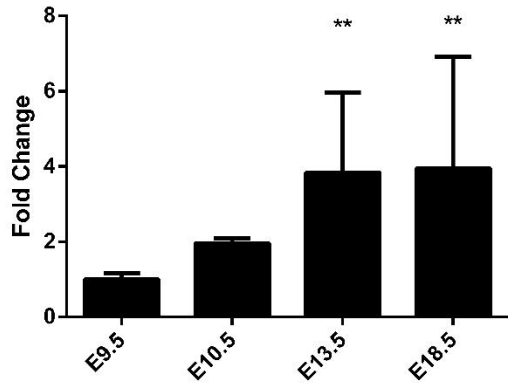


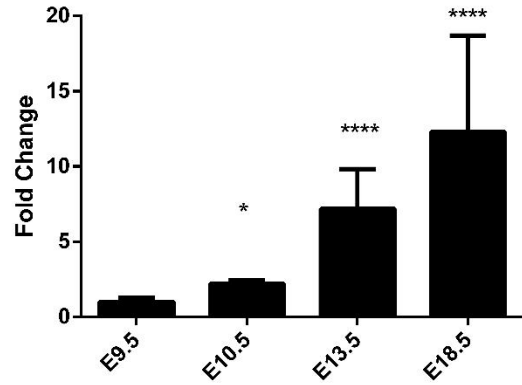
Figure 5: Barres mouse brain RNA sequencing database show that CEMIP is expressed by neurons, OPCs, and endothelial cells (A). qPCR results of OPCs induced to differentiate into oligodendrocytes for indicated time periods show that *Cemip* expression decreases as *Pdgfra*⁺ OPCs differentiate into *Mbp*⁺ oligodendrocytes (B-D). Immunofluorescent labelling of mouse EAE tissue sections (21dpi) show that CEMIP expression colocalizes with both PDGFR α and OLIG2, suggesting that OPCs express CEMIP in these lesions (E-L). Co-labelling for CEMIP transcript using RNAscope and Iba1 reveal that CEMIP is largely absent from microglia as well (M-P, inset is no primary and negative probe control). GFAP expression was largely absent from CEMIP positive lesion sites, while VE-cadherin did colocalize with CEMIP (Q-U, V – no primary control). Scale bars = 50 μ m. * - p<0.05, ** - p<0.01, *** - p<0.001, **** - p<0.0001.

Because OPCs expressed *Cemip* *in vitro* and in demyelinating lesions, I sought to determine if *Cemip* was also expressed by OPCs during development or in the healthy adult brain. Using qPCR, I found that *Cemip* transcript levels increased in the brains of mouse embryos with increasing age at the same time as *Olig2* transcript levels are increasing (Fig. 6A,B). Immunofluorescence experiments revealed that PDGFR α -expressing OPCs co-express *Cemip* in a variety of areas throughout the developing and adult brain, including the median eminence, an area of adult oligodendrogenesis in mice (Fig. 6C-F)¹⁹⁷, as well as in other areas of the hypothalamus such as the arcuate nucleus (Fig 6G-J).

A *Olig2* mRNA in developing CNS



B *Cemip* mRNA in developing CNS



* - $p < 0.05$, ** - $p < 0.01$, **** - $p < 0.0001$

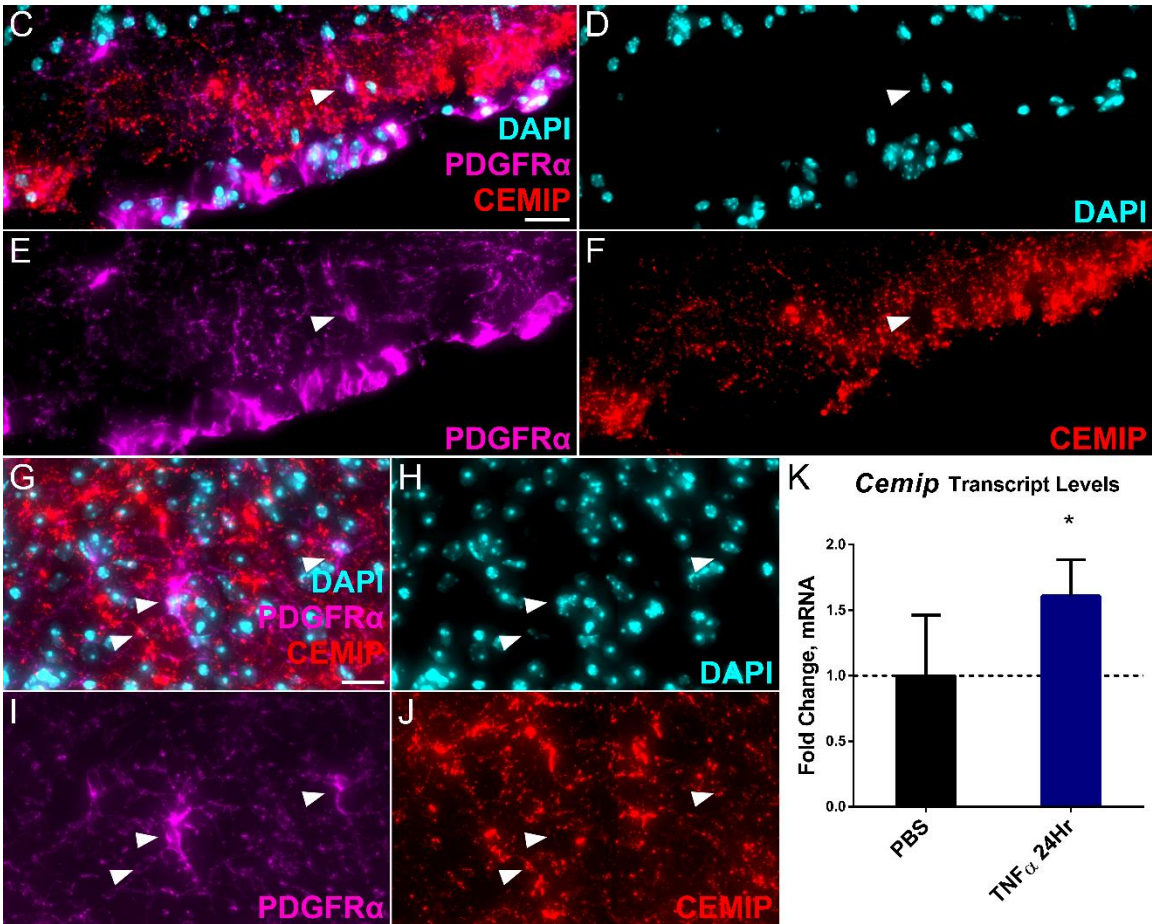


Figure 6: qPCR results from developing brains of mouse embryos at indicated embryonic days indicate that *Cemip* transcript levels increase in the developing CNS coincident with *Olig2*, a marker for oligodendrocyte lineage cells (A,B). Immunofluorescent labelling of CEMIP and PDGFR α , a marker for OPCs, in the median eminence (C-F) and arcuate nucleus (G-J) show that OPCs also express CEMIP in an adult area of oligodendrogenesis. Treating cultured OPCs with TNF α , one of the cytokines found to be elevated in EAE, leads to elevated CEMIP transcription (K). * - $p < 0.05$, ** - $p < 0.01$, *** - $p < 0.001$, **** - $p < 0.0001$

TNF α induces increased Cemip transcription in OPCs

Given that at least some OPCs express *Cemip* in the developing and healthy adult brain, and that *Cemip* expression is greater in demyelinating lesions than in adjacent normal appearing tissues and in healthy tissues, I tested the possibility that inflammatory signals within lesions could increase *Cemip* expression by OPCs. Similar to what was observed in EAE spinal cord tissue (Fig. 2C, D), I found that treatment with 10ng/mL TNF α elevated *Cemip* transcription in cultured OPCs ($p < 0.05$; Fig. 6K).

CEMIP generates bioactive HA fragments that block OPC maturation

To study the effects of elevated *Cemip* expression on OPC maturation, I transiently overexpressed *Cemip* in OPC cultures under conditions that promote maturation to OLs. After five days, cultures were fixed and stained for PDGFR α and MBP, and the ratio of MBP:PDGFR α expression was determined. Compared to untransfected or empty vector transfected controls, cells that overexpressed *Cemip* demonstrated reduced OPC maturation in the presence and absence of added HMW HA (Fig. 7A-G, $p < 0.05$).

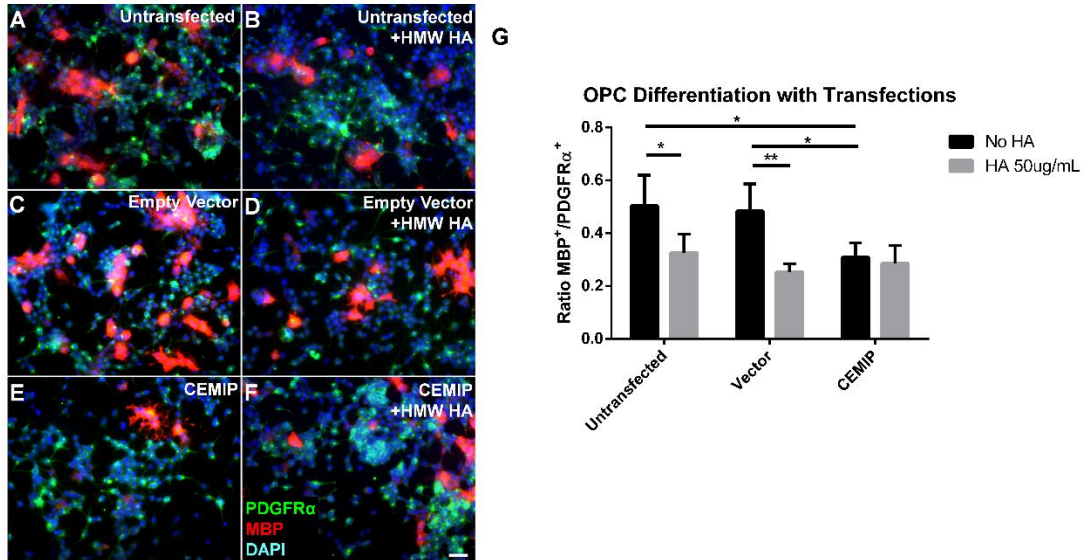


Figure 7: OPCs were induced to overexpress *Cemip* or empty vector, and differentiated in the presence and absence of high molecular weight HA (HMW HA) for five days. Cells were then immunofluorescently labelled to show numbers of PDGFR α ⁺ OPCs, and MBP⁺ OLs (A-F). Cell counts reveal that *Cemip* overexpression delays OPC differentiation in the presence and absence of HMW HA (G). Scale bar = 20 μ m * - p<0.05, ** - p<0.01

It was previously found that HA fragment sizes between 175 kDa and 300 kDa attenuated OPC maturation¹⁰⁶. Given my observation that CEMIP is expressed in demyelinating lesions with reduced HA staining, and that elevated CEMIP blocks OPC maturation, I hypothesized that CEMIP generates HA fragments in this bioactive size range. I therefore added HMW HA to cultures of cells transfected with either an empty vector or a *Cemip* expression vector then collected the conditioned medium after 72 hours. I extracted HA from the medium through phenol/chloroform extraction followed by dialysis in pure water. The distribution of HA sizes was determined using two methods: first, through agarose gel electrophoresis combined with staining with Stains-All to demonstrate the overall distribution of HA sizes; then using a nanopore assay¹⁹⁸. Both methods revealed

that, when compared to HMW HA in solution or conditioned medium from vector-transfected cells, *Cemip* overexpression leads to the catabolism of HMW HA to fragments with peak sizes between approximately 210 kDa and 500 kDa, overlapping with the sizes of HA previously reported to inhibit *in vitro* OPC differentiation (Fig. 8A, B). Furthermore, when these CEMIP-produced HA fragments were added to OPC cultures under conditions that promote OPC maturation, they blocked OPC maturation to a greater degree than HMW HA alone (Fig. 8C-H).

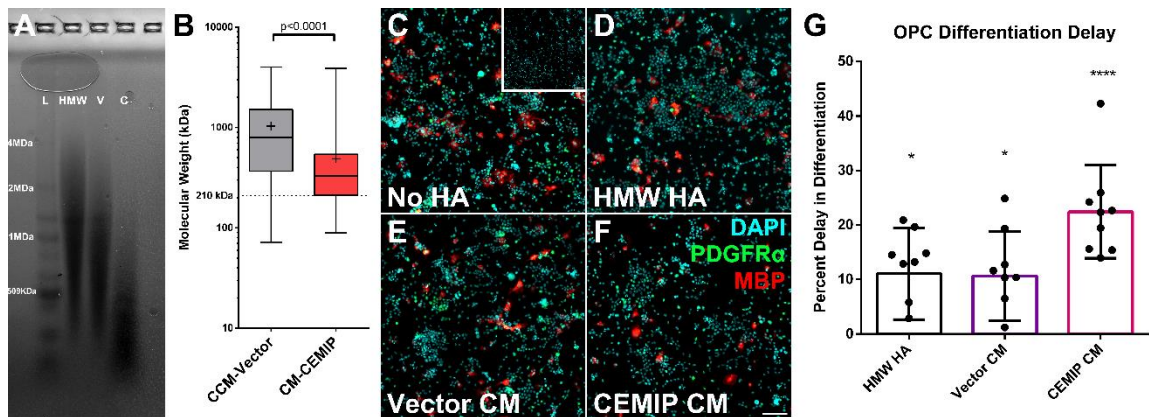


Figure 8: Cells were induced to overexpress *Cemip*, and HMW HA was added to culture medium for 3 days. HA was then extracted from conditioned medium using phenol/chloroform, and dialyzed with water to purify HA. The sizes of the resulting HA was determined using agarose gel electrophoresis (A, L – ladder, HMW – HMW HA, V – Vector conditioned medium, C – CEMIP conditioned medium) and a solid-state nanopore assay (B). Both assays revealed that *Cemip* overexpression leads to the digestion of HMW HA to sizes previously found to delay OPC differentiation, approximately 100-500 kDa range. Treating differentiating cultured OPCs with these fragments leads to a delay in differentiation that is larger than HMW HA (C-G, p values are from comparing differentiation rates between no HA control and each condition, inset is no primary control). Scale bar = 100 μ m. * - $p < 0.05$, **** - $p < 0.0001$.

HA fragments produced by CEMIP delay functional remyelination

I have established that HA fragments produced by CEMIP activity inhibit *in vitro* OPC maturation. To determine if these fragments influence functional remyelination *in vivo*, I induced focal demyelination in the corpus callosum of mice by stereotactic injection of lysolecithin, co-injecting either PBS (vehicle), or purified HA fragments from either vector transfected or *Cemip* transfected cells. Seven days-post injection, brains were harvested and slices that included the lesion area were analyzed for changes in conduction velocities using compound

action potential (CAP) recordings. Following recordings, tissues were analyzed by immunohistochemistry for MBP¹³⁵. Compared to PBS or vector fragment controls, mice co-injected with CEMIP-produced HA fragments exhibited reduced conduction velocities and reduced MBP immunolabeling, consistent with delayed remyelination (Fig. 9A-I).

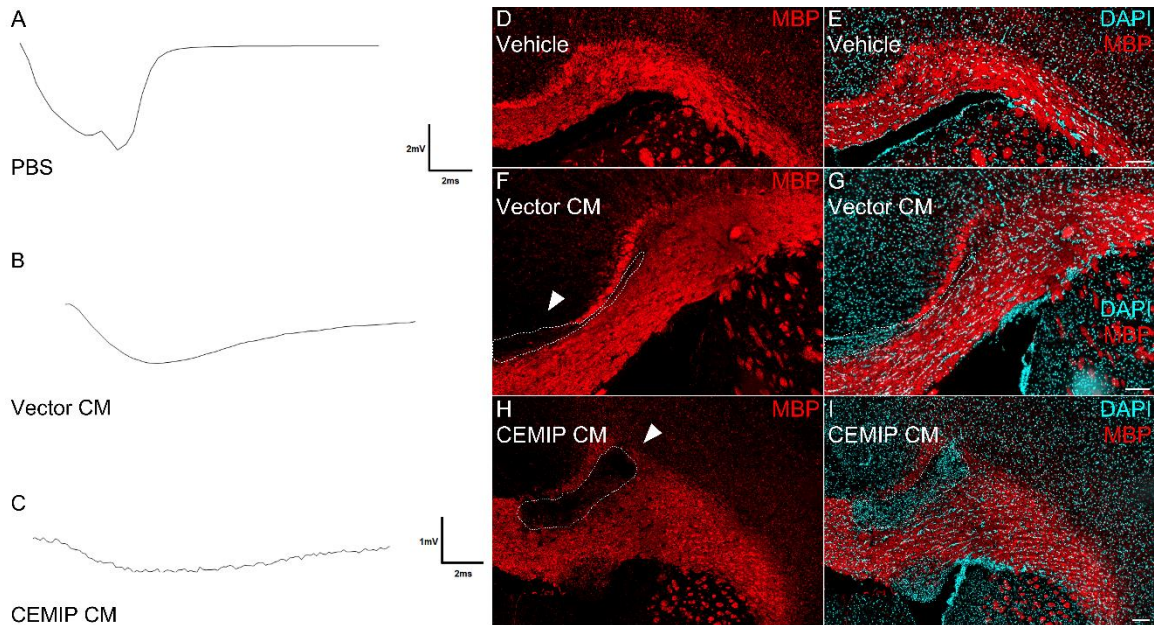


Figure 9: Lysolecithin and vehicle (PBS), and HA fragments purified from either vector CM or CEMIP CM (100 μ g/mL) were co-injected into the corpus callosa of mice. 7 days later, brains were harvested and assessed for remyelination using compound action potential recordings (A-C) and immunolabelling of MBP in fixed brain sections (D-I). Brains co-injected with HA fragments produced by CEMIP activity show delayed remyelination rates when compared to both PBS control and Vector CM (mainly HMW HA). Arrowheads and dotted lines denote lesion areas Scale bar = 100 μ m.

Discussion

There is an unmet need for therapeutic interventions that promote remyelination in demyelinating diseases, including MS. I have found that the CEMIP hyaluronidase is transcriptionally elevated in demyelinating lesions in

mice with EAE and in MS patients. Furthermore, cultured OPCs had increased expression of *Cemip* after treatment with TNF α , supporting a role for pro-inflammatory mediators in regulating *Cemip* expression. I also found that elevated CEMIP levels in OPCs generates HA fragments that can block OPC maturation and delay functional remyelination. These findings support the notion that hyaluronidase activity, and particularly CEMIP, in demyelinating lesions contributes to remyelination failure in inflammatory demyelinating diseases.

I found that *Cemip* is elevated coincident with *Has1* and *Has2* expression in the lumbar spinal cord during EAE progression. This is consistent with previous studies showing that HA accumulates in demyelinating lesions⁹. A previous study reported increased expression of *Has3* in demyelinating lesions using immunohistochemistry, but did not examine *Has1* or *Has2* expression. I did not observe significant levels of *Has3* transcription at any stage of EAE progression. It is unclear, therefore, the degree to which HAS3 contributes to HA accumulation in demyelinating lesions. Nonetheless, I propose that HA accumulates in lesions and is catabolized by CEMIP expressed by OPCs recruited to areas of demyelination. When there are sufficiently high levels of HA, CEMIP-generated HA fragments reach levels that feed back on OPCs, blocking their maturation. My findings here suggest that CEMIP generates sizes of HA that have been shown to block OPC maturation through a toll-like receptor-4 based mechanism via inhibition of AKT signaling¹⁰⁶. Consistent with this idea, a hyaluronidase inhibitor

whose targets include CEMIP activity reverses the effects of HMW HA on AKT phosphorylation¹³⁵.

In addition to *Cemip*, *Hyal2* also demonstrated significant increases in expression in spinal cord tissues from mice with EAE. However, this increase was only observed at 21 dpi. HYAL2 is a glycosylphosphatidylinositol-anchored enzyme located at the cell surface¹⁹⁹. In at least some cell types, HYAL2 digests HMW HA into fragments of approximately 10–20 kDa²⁰⁰. These fragments are taken up into cells through receptor-mediated endocytosis. Given the later time at which *Hyal2* is induced during EAE progression, and the sizes of HA fragments generated by HYAL2, it is unlikely that digestion of HA by HYAL2 contributes to the inhibition of OPC maturation. Two other hyaluronidase, TMEM2 and PH20/SPAM1, have also been implicated in regulating OPC morphology^{107, 201}. However, it is unclear if either function as hyaluronidases in the CNS. I did not observe any changes in *Tmem2* transcription during EAE progression and I did not detect the expression of *Ph20* in these tissues via qPCR.

My data showing that CEMIP is elevated in demyelinating EAE and MS lesions are in agreement with a previous study that also found that CEMIP was present in areas of reduced myelin and reduced HA¹⁹⁴. However, this earlier study reported that *Cemip* expression was predominantly in astrocytes. I found that astrocytes from healthy brain tissue lack *Cemip* transcripts based on RNAseq analyses, and I did not observe *Cemip* expression in GFAP-immunolabeled

astrocytes in demyelinating lesions or in healthy tissues. I validated the expression of *Cemip* using multiple approaches including (1) qPCR analyses of tissues and cells grown *in vitro*; (2) staining CEMIP-negative cells transfected with a *Cemip* cDNA; and (3) co-staining cells and tissues with antibodies and *in situ* hybridization probes. It is possible that the antibody used in the previous study was not specific for CEMIP. It is also possible that under some conditions, astrocytes may transiently express *Cemip*, however I did not observe such expression at any stage of EAE. My data also suggest that *Iba1*-expressing microglia and *Cd3* expressing lymphocytes largely lack CEMIP expression, while OPCs and endothelial cells are CEMIP-positive. Other cell types, including immune cells, may also express *Cemip* but I was unable to identify positive cells in those populations.

Interestingly, in addition to observing elevated *Cemip* expression within demyelinated lesions in MS cases, I also observed CEMIP protein around blood vessels and at the borders of some lesions. At least some of the staining around blood vessels appears to involve brain vascular endothelial cells, consistent with the RNAseq findings that endothelial cells express *Cemip*. This finding suggests that CEMIP may play a role in regulating brain vascular endothelial cell function and integrity, which could influence disease progression by altering how immune cells enter the CNS. In addition, the patterns of CEMIP staining in MS cases were distinct from what was observed in mice with EAE. The lesions in the MS cases that were analyzed were mostly inactive and therefore might not include as

many OPCs or other cells with elevated *CEMIP* expression. Future studies will elucidate the differences in *CEMIP* expression between MS and EAE, as well as the role of elevated CEMIP in vascular endothelial cells.

Given that TNF α and the other pro-inflammatory mediators that are elevated in inflammatory demyelination are also involved in a variety of other CNS insults including stroke, seizures, and traumatic brain injury²⁰²⁻²⁰⁴, it remains to be determined if *CEMIP* expression is altered in these conditions as well, and whether bioactive HA fragments produced by CEMIP influence the progression of these conditions. Interestingly, a recent study of perinatal brain injury in sheep found that S3, which can inhibit CEMIP activity, prevented seizures²⁰⁵. This finding is interesting given that chronic demyelination can lead to seizures in neonates²⁰⁶.

My studies have highlighted CEMIP as a tractable target for small molecule inhibitors to accelerate functional remyelination. Indeed, it was previously found that a small molecule inhibitor that blocks CEMIP activity accelerates functional remyelination¹³⁵. Receptors and their downstream mediators that signal in response to HA fragments produced by CEMIP could also be targets to accelerate OPC maturation and remyelination at lesion sites. This could be paired with current and future immunomodulatory therapies to both reduce the number of MS attacks and increase remyelination rates. I propose that such a strategy has the potential to limit disease progression while promoting CNS

repair, potentially reversing neurological impairments for the many patients who live with demyelinating diseases.

CHAPTER 3: DISTINCT CHEMICAL STRUCTURES INHIBIT THE CEMIP HYALURONIDASE AND PROMOTE OLIGODEDROCYTE PROGENITOR CELL MATURATION

For submission to the Journal of Biological Chemistry

Note: the work involving data collection and analysis to generate Tables 4 and 5, as well as figures 10 and 11, were not completed by the author but by collaborating laboratories. The structural analysis of tested compounds to identify functional groups important to inhibitory activity was performed by collaborators.

Introduction

Dynamic changes in the composition of the extracellular matrix (ECM) are implicated in the regulation of a wide variety of cellular activities including cell division, migration, differentiation, and survival. For example, the ECM can influence the behaviors of cells during embryonic development but also the proliferation and metastasis of cancer cells²⁰⁷. In the central nervous system (CNS), alterations in the ECM contribute to neuroplasticity but can also limit repair processes in neurodegenerative diseases^{98, 207-209}.

Glycosaminoglycans and proteoglycans are major components of the ECM that can influence each of these cellular processes. In particular, increased synthesis of the extracellular glycosaminoglycan hyaluronan (also called hyaluronic acid; HA), accompanied by HA catabolism through hyaluronidase activity, is associated

with cancer progression and poor prognosis, as well as delayed recovery in CNS insults, including multiple sclerosis (MS) and ischemic injury^{191, 210}. These pathological effects are linked to the accumulation of HA fragments of various sizes that have distinct biological activities¹⁹¹. Inhibiting hyaluronidase activity using a small molecule-based therapy may therefore be a tractable method to improve patient outcomes in cancer, CNS diseases, and other conditions.

Elevated expression of the hyaluronidase Cell Migration Inducing and hyaluronan binding Protein (CEMIP) has been associated with increased metastasis and poor prognosis in multiple cancer types, including colorectal^{211, 212}, thyroid²¹³, gastric²¹⁴, and hepatic cancers^{215, 216}. Furthermore, *Cemip* expression in tumor exosomes increases metastases to the brain in mice, and increased *CEMIP* expression in human tumors is associated with increased numbers of brain metastases in patients²¹⁷. CEMIP has also been implicated in the pathogenesis of MS, a disease characterized by inflammatory demyelination in the CNS, leading to sensory, motor, and cognitive dysfunction^{185, 218}. Chronically demyelinated MS lesions exhibit an accumulation of oligodendrocyte progenitor cells (OPCs) that fail to differentiate into myelinating oligodendrocytes. This is in part due to elevated hyaluronidase activity, producing bioactive HA fragments that directly inhibit OPC differentiation^{182, 189, 190}. *CEMIP* expression is reported to be elevated in demyelinating MS lesions¹⁹⁴, and an inhibitor that blocks the activities of some hyaluronidases, including CEMIP, increased functional recovery in a rodent model of MS¹³⁵. Targeting CEMIP hyaluronidase

activity with therapeutic small molecule inhibitors may therefore be an efficacious method to promote repair following CNS insults, reduce cancer cell metastasis to the brain, and reverse other pathological conditions linked to elevated HA catabolism.

Numerous hyaluronidase inhibitors have been characterized with varying degrees of efficacy in blocking HA digestion²¹⁹. These include synthetic and plant-derived compounds, proteins, polysaccharides, fatty acids, and glycosaminoglycans. Among plant-derived inhibitors, flavonoids, their biosynthetic precursors chalcones, and the closely related compound class of aurones, have been found to have anti-cancer, anti-inflammatory, and hyaluronidase inhibitory activities^{184, 220-224}. Recently, a structural derivative of the flavone apigenin was described that selectively inhibited CEMIP activity over other hyaluronidases¹³⁵. Named S3, the flavone was also found to accelerate functional remyelination in a mouse model of demyelinating disease¹³⁵.

Although S3 inhibited hyaluronidase activity, it only poorly crosses the blood-brain barrier, is relatively insoluble, and requires relatively high doses to block CEMIP activity. S3, therefore, is unlikely to be useful as an intravenous or oral drug to treat elevated CEMIP activity that contributes to disease pathogenesis. Here, I took a two-pronged approach to identify novel CEMIP inhibitors to better understand the chemistry of hyaluronidase inhibitors and to identify potential lead compounds for therapeutic use. I screened a library of novel, synthetic

compounds and also screened a large number of plant extracts for novel agents that block CEMIP activity. I then compared the agents I identified to S3 with regards to their anti-hyaluronidase activity in both a tumorigenic cell line and in primary cultures of OPCs, then examined the best of these compounds for their ability to influence cell proliferation, survival and differentiation.

Materials and Methods:

Identification of Novel Hyaluronidase Inhibitors

Inhibitors were chemically synthesized and screened for inhibitory activity as described previously²²⁵.

Orange dahlia flowers were obtained from a local garden and were quickly frozen. The petals were crushed and about 500 grams (125 g dry weight) were extracted 3 times with methanol at room temperature on a shaker for 6 to 10 hours each. Solvent was filtered and evaporated under reduced pressure to obtain about 55 g of residue. 50 mL of water was added to the residue which was extracted with ethyl acetate.

The ethyl acetate extract was dried under reduced pressure to yield about 15 g. The residue was dissolved in ethyl acetate and methanol, added to silica gel and dried. It was separated using silica gel flash chromatography system (Reveleris, Buchi) using a gradient of hexane to ethyl acetate to methanol. Fractions were collected, visualized with silica gel thin layer chromatography after eluting with

7:1 chloroform: methanol to yield 14 fractions and fumed with iodine to identify flavonoids.

The fractions were assayed for their ability to inhibit the activity of hyaluronidase. Active fractions were pooled and chromatographed as before with flash chromatography. Fractions eluting with 40-80% ethyl acetate in methanol were most active against hyaluronidase. Fraction 7 was a yellow powder identified as sulfuretin (molar mass, 270.24, melting point 300-303°C). Other flavonoid fractions contained apigenin, luteolin, naringenin, eriodictyol and butein.

Cell Culture

Human embryonic kidney 293T cells were cultured in Dulbecco's modified eagle medium (DMEM, Gibco) supplemented with 10% fetal bovine serum (FBS, Atlas Biologicals). 293T cells were passaged using 0.25% trypsin (Gibco) for cell detachment/dissociation. Primary mouse oligodendrocyte progenitor cells (OPCs) derived from oligospheres were cultured as described previously¹⁰⁷. Briefly, OPCs were cultured in DMEM:F12 (Gibco) supplemented with 0.1% bovine serum albumin (BSA, Fisher), recombinant platelet-derived growth factor AA (PDGF-AA, Promega), and fibroblast growth factor-2 (FGF-2), B27 supplement without vitamin A (Gibco), N1 supplement (Sigma), and Biotin (Sigma). Cells were passaged using Accutase (Invitrogen).

Viability Assay

Cell viability was assayed using crystal violet adapted from²²⁶. Briefly, 12-well plates (Corning) were seeded with 2×10^5 293T cells or OPCs per well. The next day, DMSO (vehicle, Fisher) or inhibitors were added to the culture medium. Cells were grown for three days, fixed in Zamboni's fixative (4% PFA with picric acid, see ²²⁷), and stained with 0.5% crystal violet (Fisher). Stained cells were washed in distilled water, and imaged on a scanner. Changes in viability were determined by measuring differences in percent area cell coverage between wells in ImageJ.

Proliferation Assay

5-Bromo-2-deoxyuridine (BrdU) uptake and Ki67 expression were measured to determine cell proliferation¹². Cells were seeded on coverslips (Carolina) in 24-well plates (Corning), at 1×10^5 per well for both 293T cells and primary OPCs. 293T cells were plated on uncoated coverslips, while OPCs were plated on poly-L-ornithine (Sigma) coated coverslips²²⁸. The following day, the appropriate amount of DMSO or inhibitors were added to wells. 24 hours later, BrdU (Sigma) was added to wells at a final concentration of 10 μ M. 293T cells were allowed to incubate for 4 hours, while OPCs were incubated with BrdU for 12 hours. Cells were fixed in Zamboni's fixative (see above in *Viability Assay*) and assayed for BrdU and Ki67 expression using immunocytochemistry (described below). Changes in numbers of Ki67 and BrdU expressing cells were measured using ImageJ.

HA Digestion Assay

Cemip expression vector (Catalog MR217955) and empty vector (Catalog PS100001) were purchased from Origene. All transfections were completed using Fugene HD (Promega). To test for hyaluronidase activity in live cells, 6×10^6 293T cells or 3×10^6 OPCs were cultured on 10cm^2 polystyrene dishes (Fisher) overnight for transient transfection. The following day, cells were transfected with $10 \mu\text{g}$ plasmid using Fugene HD at a ratio of 1:3 DNA to transfection reagent for 293T cells, and 1:6 for OPCs. The next day, the cell culture medium was replaced. 48 hours after transfection, cells were re-plated into 24-wells plates, at a concentration of 1×10^5 per well for 293T cells and 2×10^5 per well for OPCs.

The following day, cell culture media was replaced with dye-free, serum-free medium containing high molecular weight hyaluronic acid (Lifecore Biomedical) at $50 \mu\text{g}/\text{mL}$ with and either no other additions, dimethyl sulfoxide (DMSO, vehicle), or each inhibitor at the indicated concentrations. Culture medium was collected 72 hours later and used directly in agarose gel electrophoresis assays.

HA was separated by size using agarose gel electrophoresis and analyzed by densitometry as previously described¹³⁵. Briefly, size separation was achieved in 0.5% HGT agarose gel (SeaKem) in tris-borate EDTA. The gel was stained in 0.005% Stains-all (Fisher) in 50% ethanol overnight, and washed in 10% ethanol, all in the dark. Gels were de-stained in light and then photographed.

Densitometry was used to determine percent CEMIP inhibition in ImageJ as

described previously¹³⁵. Briefly, pixel density of HMW HA was determined for each lane, and absorbance normalized to a 0-100% scale, HMW HA pixel density in the CEMIP lanes (no additions) being 0% and pixel density in the vector-transfected lanes being 100%. A CEMIP inhibition value of above 100% means the absorbance is above that seen in the vector-transfected lane.

OPC Differentiation Assay

OPCs were differentiated *in vitro* as described previously^{106, 107, 135, 182}. OPCs were plated on poly-ornithine (Sigma) coated coverslips in 24-well plates at 3×10^4 cells per coverslip. The following day, OPC culture medium was replaced with DMEM:F12 supplemented with N-acetyl cysteine (NAC, Sigma) and triiodothyronine (T3, Sigma) with and without HMW HA, vehicle, or each inhibitor at indicated concentrations. Differentiation medium was replaced daily, and cells were fixed in Zamboni's fixative (4% PFA in phosphate buffer and aqueous picric acid, see above). Immunocytochemistry was used to determine relative amounts of $\text{PGFR}\alpha^+$ OPCs and MBP^+ oligodendrocytes as described previously, and percent area coverage of each marker was calculated using ImageJ to determine the ratio of $\text{MBP}/\text{PDGFR}\alpha$ expression.

Immunocytochemistry

Immunocytochemistry was performed on fixed cells as described previously^{106, 107, 135}. Cells were permeabilized with 0.5% triton X-100 (Sigma) in 1X phosphate buffered saline (PBS) for 15 minutes, and then blocked in 5%

normal goat serum (Fisher) in 1X PBS for two hours. Blocking buffer was replaced with blocking buffer and appropriate primary antibodies, and incubated at 4°C overnight. The following day, cells were washed in 0.05% triton X-100 in 1X PBS times for five minutes each, and then secondary antibody was added for two hours at room temperature. Cells were then washed three times with 0.05% triton in 1X PBS, counterstained with DAPI (Molecular Probes, 1:5000 concentration in 1X PBS for 3 minutes) and mounted onto glass slides (Fisher) using Fluoromount-G (Southern Biotech).

The following primary antibodies were used: PDGFR α (BD Pharmingen Catalog No. 558774, 1:100 dilution); MBP (Biolegend Catalog No. 808402, 1:800 dilution); Ki67 (Invitrogen Catalog No. MA5-14520, 1:250 dilution); BrdU (Invitrogen Catalog No. B35128, 1:250 dilution). The following secondary antibodies were used, all purchased from Invitrogen and used at a 1:1000 dilution: Goat anti-mouse AF488 (Catalog No. A11029); goat anti-mouse AF546 (Catalog No. A11003); goat anti-rabbit AF546 (Catalog No. A11035); goat anti-rat AF488 (Catalog No. A11006).

Imaging

Stained cells were imaged using an Olympus VS 120 SlideScanner with the following objectives: 2x/0.08NA Olympus Plan ApoN, 10x/0.40NA Olympus UPlanSApo, 20x/0.75NA Olympus UPlanSApo, and 40x/0.95NA UPlanSApo. The

2x objective was used for overview scans. Cells were imaged at 20x on one plane. Analyses were performed using Fiji/ImageJ (National Institute of Health).

Statistics

A statistically significant difference between conditions were determined using a one-way ANOVA with Tukey's multiple comparison test for all assays performed. Statistical calculations were made in GraphPad Prism. A p-value below 0.05 was considered significant.

Results

Identification of novel hyaluronidase inhibitors

To understand the range of chemical structures that can block CEMIP activity, collaborators first screened for both naturally occurring and synthetic agents that could block the activity of a similar hyaluronidase, bovine testicular hyaluronidase, the activity of which is mostly linked to the PH20 hyaluronidase in sperm²²⁹⁻²³¹. For the natural products screen, bovine testicular hyaluronidase (50 U/ml) was mixed with high molecular weight (HMW) HA (>1 MDa) as a substrate along with fractionated extracts from a variety of plants. The extracts were tested for their ability to block HA digestion as assessed by gel electrophoresis and labeling with Stains-All as previously described²³². Several fractions were identified different plants that were able to block hyaluronidase activity at least partially (Table 4). Using NMR spectroscopy, it determined that the active molecules in each fraction were flavonoids. The most active fraction, compound

F (Table 4), was the aurone sulfuretin (Fig. 10A, Table 5) which had not previously been isolated from coreopsis (tickseed) flowers. Previous studies suggested that sulfuretin has anti-inflammatory, neuroprotective, and anti-cancer activities²³³⁻²³⁷, but none had supported a role for sulfuretin as a hyaluronidase inhibitor. Analyzing the chemical structures of the naturally derived compounds reveals multiple similarities and differences between the structures (Fig. 10).

Extract	Source
A	Primula
B	Apple
C	Rose
D	Geranium
E	Glycyrrhiza
F	Coreopsis
G	Marigold
H	Alfalfa
I	Columbine B6
J	Dahlia 1 #5
K	Dahlia 1 #9
L	Columbine 2
M	Dahlia 3

Table 4: Extracts and plant sources

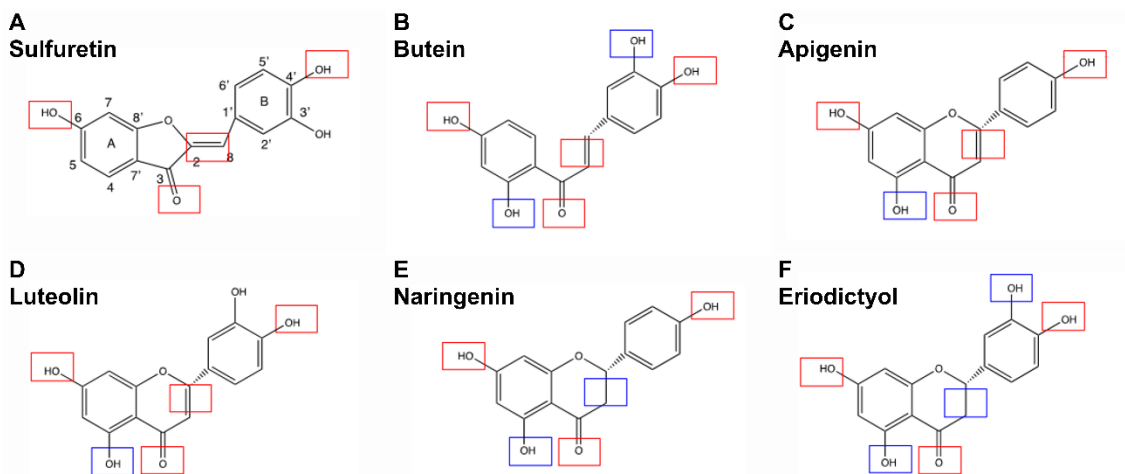


Figure 10: Structures of flavonoids extracted from Dahlia flower. Red boxes denote similarities between compound structures and A) sulfuretin, while blue boxes denote differences.

Compound Name	Flavonoid Class	Molecular Formula	Molecular Weight	CAS number
Sulfuretin	Aurone	C ₁₅ H ₁₀ O ₅	270.24	120-05-8
Butein	Chalcone	C ₁₅ H ₁₂ O ₅	270.25	487-52-5
Apigenin	Flavone	C ₁₅ H ₁₀ O ₅	270.24	520-36-5
Luteolin	Flavone	C ₁₅ H ₁₀ O ₆	286.24	471-70-3
Naringenin	Flavanone	C ₁₅ H ₁₂ O ₅	272.26	480-41-1
Eriodictyol	Flavanone	C ₁₅ H ₁₂ O ₆	288.26	552-58-9

Table 5: Flavonoids isolated from dahlia and coreopsis that were found to actively inhibit PH20 hyaluronidase activity.

As a complementary strategy to identify additional hyaluronidase inhibitors, collaborators screened a compound library for additional molecules with hyaluronidase inhibitor activity as previously described²²⁵. Two molecules, BIC-1A and BIC-4A, were found that had strong inhibitory activity (Fig. 11A,B).

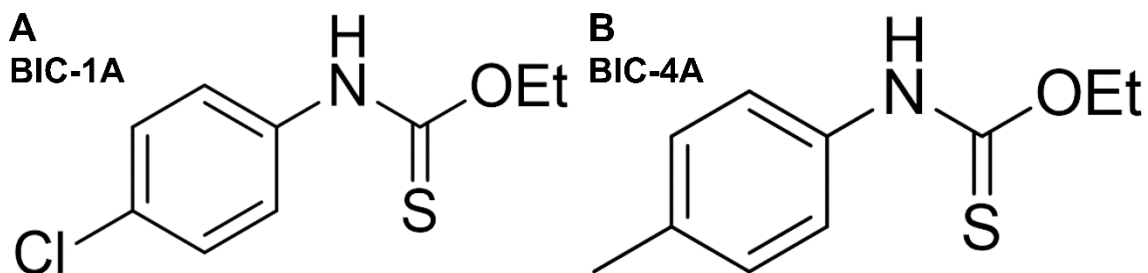


Figure 11: Chemical structures of the synthetically-derived compounds A) BIC-1A and B) BIC-4A.

Both synthetic and natural hyaluronidase inhibitors block CEMIP activity in live cells

I tested the CEMIP hyaluronidase inhibitory activity of sulfuretin, BIC-1A, and BIC-4A in live tumorigenic 293T cells and primary cultures of OPCs induced to express *Cemip*, and compared their activities to the S3 hyaluronidase inhibitor as previously described¹³⁵. I found that sulfuretin, BIC-1A, and BIC-4A demonstrated inhibitory activity that is superior to S3 (Fig.12). In the 293T cell line, I found that the BIC-1A and sulfuretin were both potent CEMIP hyaluronidase inhibitors (Fig.12A and B, upper). Surprisingly, in primary oligodendrocyte progenitor cells (OPCs), sulfuretin was distinct in its ability to inhibit CEMIP hyaluronidase activity even at lower concentrations (Fig.12B, lower). These differences in results likely reflect differences in the cell tolerances to the compounds, and well as differences in drug uptake/exposure to CEMIP between the two cell types.

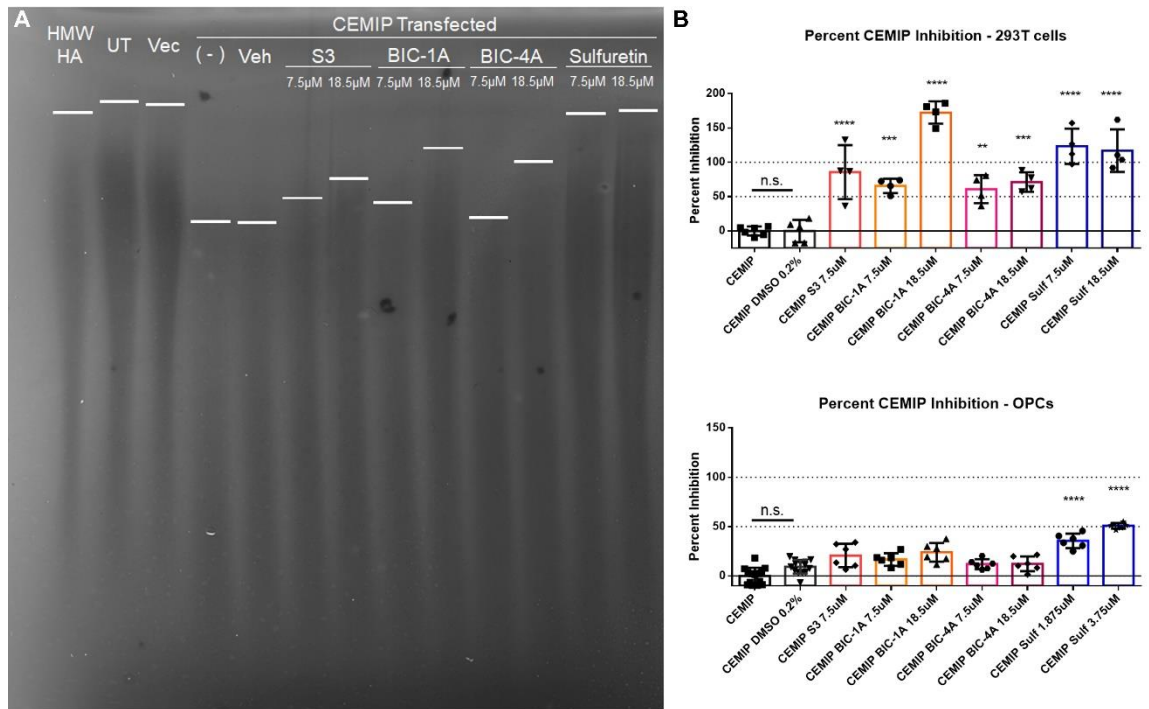


Figure 12: Synthetically and naturally derived compounds inhibit CEMIP hyaluronidase activity. A) Representative HA agarose gel showing 293T cells overexpressing CEMIP degrade HMW HA, and multiple compounds (BIC-1A, BIC-4A, and sulfuretin) block this hyaluronidase activity. B) Quantification of inhibitory activity of each compound in comparison to S3 in 293T cells (upper) and culture OPCs (lower). * - $p < 0.05$, ** - $p < 0.01$, *** - $p < 0.001$, **** - $p < 0.0001$, n.s. – not significant.

Cell viability, and not proliferation, is differentially affected by hyaluronidase inhibitors in different cell types.

Given that previous studies have suggested roles for CEMIP in tumor growth, I sought to determine if the compounds influence cell survival and/or altered cell proliferation at the concentrations that demonstrate CEMIP inhibitory activity. I grew 293T cells and OPCs in the presence of each compound and assayed cell viability using a crystal violet assay. I found that S3 greatly reduced the amount of viable 293T cells at higher concentrations (18.5μM; $p < 0.0001$),

while OPCs were more resistant to cell death ($p < 0.05$; Fig. 13). In contrast, 293T cell viability was not altered in the presence of any concentration of sulfuretin that was tested, while OPCs had reduced viability at both 7.5 μM and 18.5 μM (Fig. 13B, lower). Synthetically-derived BIC-1A and BIC-4A did not appreciably change cell viability in either cell type at any concentration tested.

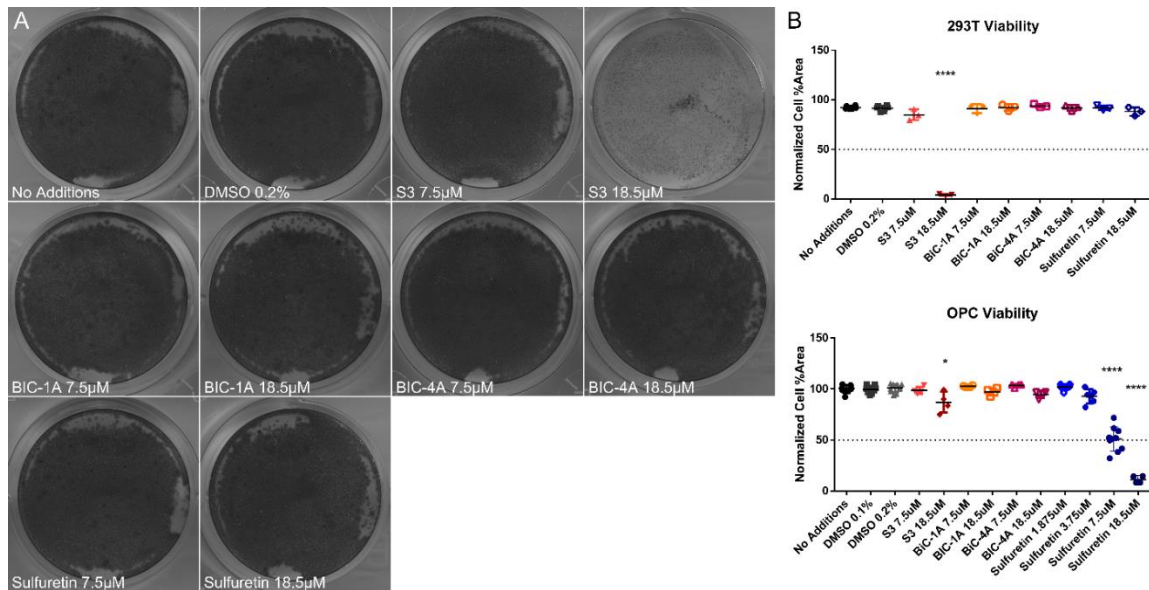


Figure 13: Viability assay of cells exposed to hyaluronidase inhibitors. A) Representative images displaying 293T cell amounts under normal growth conditions with indicated inhibitor amounts. B) Quantification of cell viability of 293T cells (upper) and OPCs (lower). * - $p < 0.05$, **** - $p < 0.0001$.

To determine if cell proliferation was affected by any of the CEMIP inhibitors, I measured changes in the amount of 5-bromo-2-deoxyuridine (BrdU) uptake and Ki67 expression in both cell types. I found no significant change in the percentages of Ki67⁺ (not shown, the vast majority of cells were positive in all conditions) or BrdU⁺ cells for any tested condition in both cell types (Fig. 14).

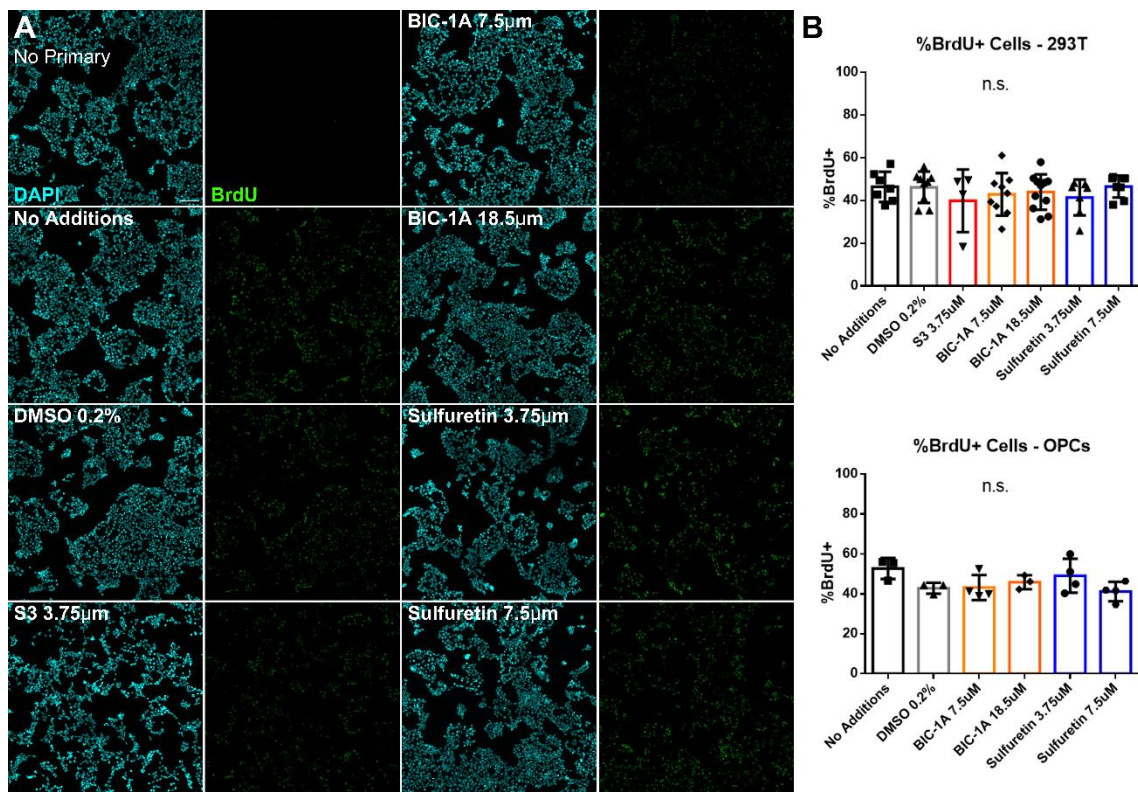


Figure 14: Cell proliferation rates remain unchanged when exposed to hyaluronidase inhibitors. A) Representative images of 5-bromo-2-deoxyuridine (BrdU) uptake of cells exposed to indicated concentrations of hyaluronidase inhibitors. B) Percentages of BrdU⁺ cells do not change under any condition for both cell types. Scale bar = 100µm. n.s. – not significant.

CEMIP inhibitors rescue in vitro oligodendrocyte differentiation in the presence of HMW HA

The *in vitro* differentiation of OPCs into mature oligodendrocytes is inhibited by HMW HA^{106, 135, 182}. Inhibiting hyaluronidase activity with the flavonoid S3 restored OPC differentiation *in vitro* and functional remyelination rates *in vivo*¹³⁵. I sought to determine if sulfuretin, BIC-1A, or BIC-4A could also accelerate OPC differentiation in the presence of HMW HA. I differentiated OPCs

in the presence of HMW HA and each of the inhibitors. OPC differentiation was determined using immunocytochemistry to differentially mark platelet derived growth factor receptor alpha (PDGFR α) expressing OPCs and myelin basic protein (MBP) expressing mature oligodendrocytes, and the ratio of MBP to PDGFR α expression was used to determine the percentages of cells that differentiated^{106, 135, 182}. I found that at 18.5 μ M, both BIC-1A and BIC-4A significantly promoted OPC differentiation in the presence of HMW HA ($p < 0.05$ for both compounds; Fig. 15A, B). I did not test the influence of S3 at this concentration, as it is toxic to OPCs at concentrations $> 10 \mu$ M. Sulfuretin rescued differentiation rates at a much lower concentration (3.75 μ M; $p < 0.05$, Fig. 15C, D), while S3 had no significant impact on OPC differentiation rates at comparable concentrations. Altogether, these data confirm that agents that can block CEMIP activity are capable of promoting OPC maturation, and support the notion that CEMIP inhibitors have the potential to be used to promote OPC maturation and remyelination in demyelinating diseases.

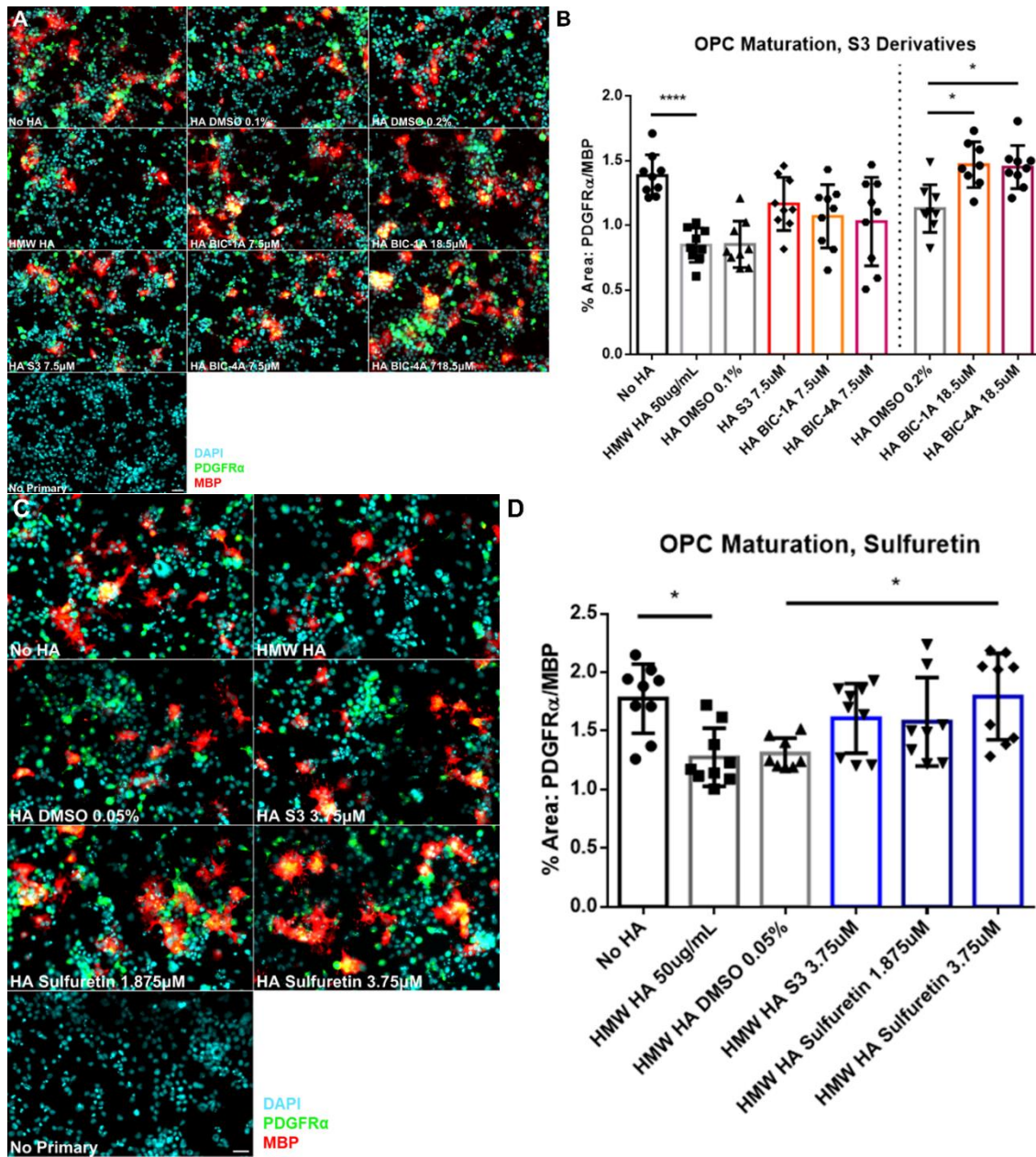


Figure 15: Hyaluronidase inhibitors rescue *in vitro* OPC differentiation rates in the presence of HMW HA. A,C) Representative images showing amounts of PDGFRα+ OPCs and MBP+ oligodendrocytes when exposed to HMW HA, or HMW HA with indicated inhibitor concentrations. B,D) Quantifications of OPC differentiation rates in the presence of HMW HA, S3, synthetically-derived hyaluronidase inhibitors. B) BIC-1A and BIC-4A both accelerate OPC differentiation in the presence of HMW HA at a concentration of 18.5μM, while S3 is toxic to cells at this level. D) Sulfuretin is more potent than S3 at rescuing OPC differentiation rates when exposed to HMW HA. Scale bars = 30μm. * - p<0.05, **** - p<0.0001.

Discussion

I found that multiple synthetic agents and natural flavonoids act as potent inhibitors of CEMIP, a novel hyaluronidase implicated in a number of pathological processes. The molecules I tested differed in their abilities to inhibit CEMIP activity in two cell types. The synthetic inhibitor BIC-1A had the greatest inhibitory activity in 293T cells, while sulfuretin was much more potent in primary OPCs. Although these differences may be explained, in part, by different levels of CEMIP expression and hyaluronidase activity in the different cell types, other factors, including CEMIP subcellular localization or cell type-specific differences in protein-protein interactions could explain why these agents demonstrate different activities in different cells. Importantly, these differences suggest that different classes of inhibitors are needed for different cell types.

My findings add to the list of previous flavonoid and related compounds found to act as hyaluronidase inhibitors. Sulfuretin had not previously been reported to have hyaluronidase inhibitory activity, and it blocks CEMIP activity at a lower concentration and with less toxicity than the S3 synthetic flavonoid. The structure of S3 is based on the structure of another flavonoid, apigenin, that has weak activity as a broad hyaluronidase inhibitor²²⁰⁻²²². These data indicate that flavonoid structures can be modified to increase hyaluronidase inhibitory activity and specificity, and that such structures could be further developed for therapeutic applications.

Phenols and polyphenols are known to inhibit the activity of hyaluronidases²³⁸. Proposed interactive sites between hyaluronidases and these compounds have been suggested by docking studies and structure-activity relationships^{219, 239, 240}. Based on these results from my and collaborators experiments and these previous studies, it is suggested that the following structural features should be considered when evaluating flavonoids for anti-hyaluronidase activity.

The hydroxyl groups on carbons 6 and 4' (Fig. 10A) and a carbonyl group on carbon 3 appear to be essential for inhibitory activity. A double bond between carbons 2 and 3 and hydroxyl groups on carbons 4 and 5' appear to be involved in biological activity, but are non-essential.

In addition to cell type-specific differences in hyaluronidase inhibitory activity, I found that different inhibitors had distinct effects on cell survival, while none of the inhibitors tested significantly influenced cell proliferation. These different effects on cell survival raise the possibility that different classes of CEMIP inhibitors are selectively toxic to certain cell types. Further investigations will determine whether such selective toxicity could be effective in treating tumors or other hyperproliferative conditions.

HA digestion products of specific sizes, and not HMW HA, have been shown to inhibit OPC differentiation^{106, 107}. Cells of the oligodendrocyte lineage have hyaluronidase activity^{15, 107}, and inhibiting this endogenous activity is a likely

mechanism to restore OPC differentiation rates in the presence of HMW HA. The synthetic flavonoid S3 has previously been shown to accelerate OPC differentiation in the presence of HMW HA and to promote functional remyelination¹³⁵. I have found that each of the three compounds tested increased OPC differentiation at a greater rate than S3 at similar as well as lower concentrations, suggesting that these agents have the potential to be developed for therapeutics that target CEMIP activity in demyelinating diseases. This may be especially true for BIC-1A and BIC-4A, which are predicted to cross the blood-brain barrier (BBB) more readily than S3.

CEMIP expression is correlated with increased tumor metastases and poor prognosis in numerous cancers^{193, 211-216}, suggesting that CEMIP hyaluronidase activity may be contributing to the ability of tumor cells to migrate and colonize other tissues. This may be due to the generation of HA digestion products. HA fragments can induce tumor angiogenesis by stimulating endothelial cell proliferation^{104, 105}. In addition, HA fragments can influence tumor cell migration and the expression of matrix metalloproteases that have been implicated in tumorigenesis and metastasis^{210, 241}. Consistent with these activities of HA digestion products that can be generated by hyaluronidases, knockdown of *Cemip* expression in tumor cells greatly reduces their ability to metastasize to the brain and not other organs²¹⁷. My findings in tumorigenic 293T cells indicate that CEMIP inhibition does not influence tumor cell proliferation under the cell culture conditions utilized in this study. It is possible, therefore, that CEMIP activity only

contributes to cancer cell metastasis but not tumor growth, although studies of the effects of blocking CEMIP activity *in vivo* are needed to confirm these findings. Nonetheless, my findings, in conjunction with previous studies, suggest that cell-type specific CEMIP inhibitors have the potential to treat metastatic disease. Further explorations into the chemistry of flavonoids and other agents similar to those identified here will reveal the potential of this strategy.

Chapter 4: Conclusions

Cemip is elevated during inflammatory demyelination

Through multiple methods, I have demonstrated that CEMIP is elevated during inflammatory demyelination in mouse and human lesions. In mice, *Cemip* is expressed by OPCs and endothelial cells, and not by GFAP⁺ astrocytes nor Iba1⁺ microglia. In fact, *Gfap* expression seems to be mostly absent from active lesions in mice with experimental autoimmune encephalomyelitis that have elevated *Cemip* expression. *CEMIP* expression is also elevated in lesion areas of inactive MS lesions in humans.

What remains to be seen is if other cell populations express *CEMIP* during inflammatory demyelination, and if these cell types change over time as active lesions either begin to remyelinate or transition to inactive lesions. While CD3-expressing T cells do not express *Cemip* in EAE, other immune cell types might, including humoral cells and macrophages. It is also possible that pericytes express *CEMIP/Cemip* in MS and EAE lesions. More studies need to be performed to determine the evolution of *CEMIP* expression over the course of lesion formation and resolution.

It is also unknown if *CEMIP* expression changes in other CNS insults. Like with EAE, qPCR, single-cell RNA-Seq, *in situ* hybridization, and immunofluorescence experiments could be used to begin to explore changes in CEMIP levels in other conditions such as perinatal white matter injury, ischemia, traumatic brain injury,

and spinal cord injury. Generating a CEMIP reporter mouse line (i.e. *Cemip* promoter followed by an *eGFP* open reading frame) may help determine how *Cemip* expression changes in cell types due to different CNS insults. Additionally, given that the cytokine TNF α increased *Cemip* transcription in cultured oligodendrocyte progenitors, it would be interesting to see if TNF α and other inflammatory cytokines alter *Cemip* expression in other neural cell types.

The functions of CEMIP in MS and EAE lesions is also currently not completely understood. I found that *Cemip* transcript and protein levels were elevated at EAE lesion sites as well as in meningeal tissue. CEMIP may have a role in immune cell extravasation and infiltration into CNS tissue during EAE. It would be interesting to test if genetic ablation of *Cemip* in different cell types, such as in endothelial cells or lymphocytes, changes the severity or onset time of EAE in mice. Total *Cemip* knockout mice currently exist¹³², making these experiments readily feasible, as *Cemip* ablation is not embryonic lethal.

Oligodendrocyte progenitor cells express Cemip in health and disease

I found that 1) cultured OPCs express *Cemip*, and this expression decreases as they differentiate into oligodendrocytes, 2) PDGFR α ⁺ and OLIG2⁺ cells express *Cemip* in EAE lesions, and 3) *Cemip* transcription in developing mouse embryos increases coincident with *Olig2*, and 4) PDGFR α ⁺ cells express *Cemip* in the mouse hypothalamus, including the oligodendrogenic niche the

median eminence. These results demonstrate that OPCs express *Cemip* in healthy tissue, and this expression is elevated in disease.

What currently remains unclear is the function of CEMIP in OPCs at different times. CEMIP in part was given this name for inducing cell migration and metastasis in cancers such as colorectal cancer^{192, 193}. CEMIP may also promote cell migration in CNS cell types, including OPCs. Given that the CNS extracellular matrix is largely HA-based, local degradation of HMW HA by increased CEMIP activity may help allow migrating cells to proceed to their destinations. It will be interesting to test whether genetic ablation of *Cemip* changes how OPCs migrate to lesion sites. Previous studies found that CD44 ablation in OPCs prevented their directed migration to a demyelinated lesion in mice¹⁵⁴, and it remains to be seen if CEMIP is also required for successful OPC migration to lesion sites.

There also may be other roles of CEMIP in the developing and adult CNS, such as in neurogenic and oligodendrogenic niches, that remain to be elucidated. For example, what is the function of CEMIP in the median eminence and other hypothalamic nuclei? EAE does change oligodendrogenesis rates in the median eminence¹⁹⁷, and the role of CEMIP in this process is currently not known. Do EAE and other inflammatory demyelination states change *Cemip* expression in other brain areas, and is this change brought about by exposure to inflammatory cytokines as it seems to occur in local EAE lesions?

CEMIP hyaluronidase activity produces bioactive HA fragments

I also determined that in two different cell types, the 293T cell line and cultured primary OPCs, elevated *Cemip* expression leads to the catabolism of HMW HA to bioactive sizes (approximately 100-500kDa). Previous studies determined that similar HA fragment sizes (between 175 and 300kDa) delayed OPC differentiation *in vitro*¹⁰⁶. These fragments seem to initiate cellular signaling cascades by binding to TLR4 on OPCs, leading to persistent depression of phospho-AKT levels and the dissociation of the chromatin remodeling factor BRG1 and the transcription factor OLIG2 from promoters of myelin genes such as MBP¹⁰⁶.

HA fragments produced by CEMIP activity delayed OPC differentiation *in vitro* and *in vivo* remyelination rates. Further studies should be conducted to determine whether these fragments have the same mechanism of action as other HA fragments. Both pharmacological inhibition and genetic ablation of *Tlr4* in cultured OPCs could be used to see if CEMIP HA fragments signal through TLR4 to delay OPC differentiation. For example, a TLR4 inhibitor could be tested to see if it accelerates *in vivo* remyelination in the presence of CEMIP generated HA fragments. These future studies would help determine if TLR4 inhibitors could be used to accelerate functional remyelination in MS and other forms of demyelination.

Further studies could also be conducted to determine if CEMIP-generated HA fragments lead to phospho-AKT depression in OPCs, as well as changes in the binding of Brg1 and OLIG2 to myelin genes. A combination of western blotting and chromatin immunoprecipitation followed by high-throughput sequencing could be used to begin to determine if CEMIP-produced HA fragments delay OPC differentiation using the same mechanisms as previously tested HA fragments¹⁰⁶

My results have led to the hypothesis that *Cemip* expression is abnormally elevated in EAE, at least by OPCs and endothelial cells, due to the local release of inflammatory cytokines such as TNF α , leading to an increase in the levels of the products produced by CEMIP hyaluronidase activity (i.e. bioactive HA fragments, Figure 16). These fragments then directly interact with local OPCs, delaying their differentiation into myelinating oligodendrocytes and thus remyelination. These studies have identified CEMIP as a target for hyaluronidase inhibitors to accelerate functional remyelination during inflammatory demyelination.

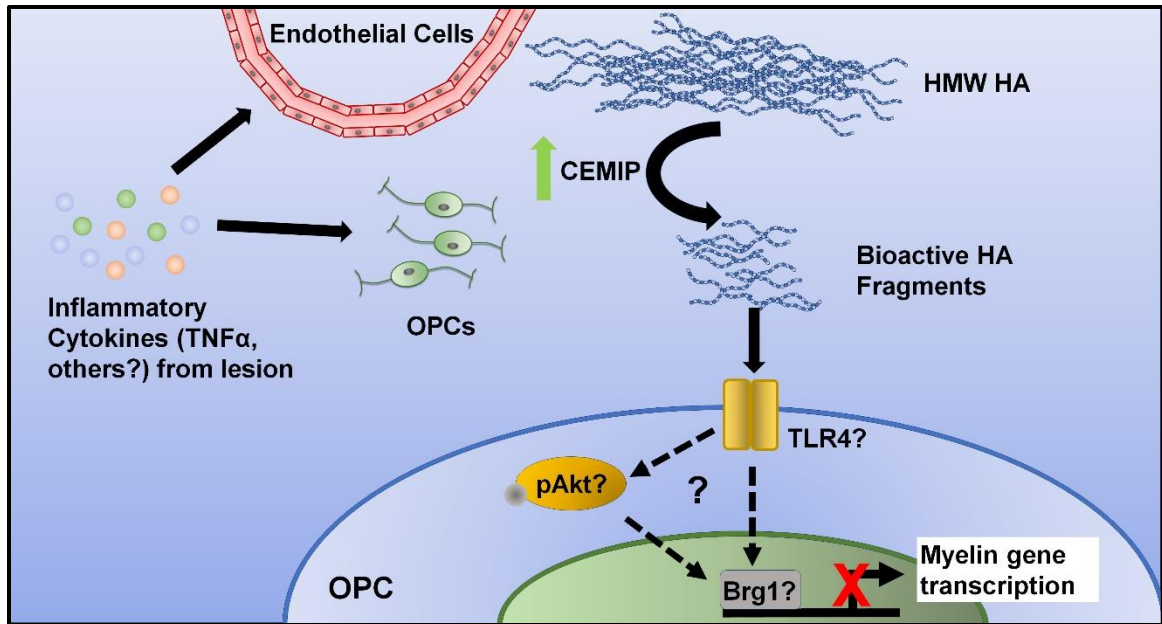


Figure 16: Summary of findings. Inflammatory cytokines released in a demyelinating lesion microenvironment increases *Cemip* expression in OPCs and endothelial cells, producing bioactive HA fragments that inhibit remyelination. Potential mechanisms for HA-fragment induced remyelination delay are included as well (dotted lines, question marks).

Naturally and synthetically derived small molecules inhibit CEMIP hyaluronidase activity

My studies have also determined that S3, which accelerates *in vivo* functional remyelination¹³⁵, also inhibits CEMIP hyaluronidase activity. I further found that one naturally derived compound, sulfuretin, and two synthetically derived small molecules, BIC-1A and BIC-4A, all inhibit CEMIP hyaluronidase activity in 293T cells and OPCs. Sulfuretin has some structural similarities to S3 and the flavonoid apigenin, which also has hyaluronidase inhibitory activity²²². BIC-1A and BIC-4A are better tolerated by 293T cells and can be used at higher

concentrations to block CEMIP activity when compared to S3, while sulfuretin is more potent at inhibiting CEMIP than S3 in both cell types.

The two cell types used, primary OPCs and the HEK 293T cell line, had different sensitivities to the compounds. S3 seems to be more toxic to 293T cells than OPCs, while the opposite seems to be true for sulfuretin. Furthermore, BIC-1A and BIC-4A only significantly inhibited CEMIP activity in 293T cells and not cultured OPCs overexpressing *Cemip*. This could be due to differences in *Cemip* expression after transient transfection between cell types, leading to lower expression of *Cemip* in OPCs, as well as the challenge of determining changes in HMW HA levels via gel electrophoresis. Analyzing the HA fragments with a solid state nanopore assay would more accurately determine if these compounds inhibit CEMIP activity, and by how much. It is also possible that the small molecule inhibitors have different exposure levels to CEMIP between the cell types, possibly due to CEMIP interacting with different partners between the cell types. The true reason for the cell type differences remains unclear.

Naturally and synthetically derived CEMIP inhibitors accelerate OPC differentiation in the presence of HMW HA

All three inhibitors, BIC-1A, BIC-4A, and sulfuretin accelerated functional remyelination in the presence of HMW HA. BIC-1A and BIC-4A can be used at higher concentrations than S3 to rescue OPC maturation, as they are better tolerated by OPCs. On the other hand, sulfuretin was more potent than S3 at

accelerating OPC maturation. These promising results show that small molecules related to flavonoids, or synthetically derived small molecules, can possibly be used to accelerate functional remyelination by inhibiting CEMIP activity during inflammatory demyelination. The biological effects of inhibiting CEMIP activity and accelerating OPC differentiation do not seem to be unique to a small number of compounds, leading to the possibility of large libraries of compounds being screened to develop a potent CEMIP inhibitor that is well tolerated by cells and can accelerate OPC differentiation and functional remyelination.

Currently, BIC-1A, BIC-4A, and sulfuretin may all be tested for their abilities to accelerate functional remyelination after focal demyelination, much like S3¹³⁵. If the results of these studies are promising, some of these compounds could possibly be used in trials to increase remyelination rates in Japanese macaque encephalomyelitis a model of neuroinflammatory demyelination that closely mimics MS²⁴²⁻²⁴⁴, to test their potential safety and efficacy. BIC-1A and BIC-4A were designed to cross the blood brain barrier more readily than S3, leading to the possibility of developing an intravenous or even oral treatment to accelerate functional remyelination in humans.

Other potential uses for bioactive flavonoids and related compounds

CEMIP expression is correlated with increased metastasis and poor prognosis in multiple cancer types^{192, 193}. It is possible that elevated CEMIP hyaluronidase activity in tumors can increase their ability to metastasize and

colonize other organs in the body. In fact, the presence of CEMIP in tumor exosomes increases the ability of tumors to colonize the CNS²¹⁷. More studies remain to be completed to determine if CEMIP hyaluronidase activity plays a role in tumor cell progression, metastasis, or colonization of other tissues. If so, there is a potential to use small molecule flavonoid-like compounds as a treatment option to reduce tumor cell metastasis and colonization.

Sulfuretin is toxic to OPCs at levels that are tolerated by tumorigenic 293T cells, and OPCs are more tolerant to S3 than 293T cells. BIC-1A and BIC-4A do not alter cell viabilities at the tested concentrations. These findings suggest developing small molecules that are toxic to specific cell types, namely tumor cells. The same viability and proliferation assays used here can be applied to tumor cell lines and primary tumor cultures to screen for compounds that have selective toxicity to tumor cells. This approach would potentially lead to more treatments to combat cancers.

Final Conclusions

My studies have provided evidence that the hyaluronidase CEMIP is elevated during inflammatory demyelination in the CNS, and that this activity produces bioactive hyaluronic acid fragments that inhibit OPC differentiation and functional remyelination more potently than high molecular weight HA alone. Furthermore, multiple small molecules were found that inhibit CEMIP activity and accelerate OPC differentiation in the presence of high molecular weight HA.

These studies have identified CEMIP as a promising therapeutic target for remyelination therapies in MS, and reveal potential small molecule CEMIP inhibitors that fit this therapeutic role.

APPENDIX: ADDITIONAL STUDIES PERFORMED

Adapted from Su W, Matsumoto S, Banine F, Srivastava T, Dean J, Foster S, Pham P, Hammond B, Peters A, Girish KS, Rangappa KS, Basappa, Jose J, Hennebold JD, Murphy MJ, Bennett-Toomey J, Back SA, Sherman LS. A modified flavonoid accelerates oligodendrocyte maturation and functional remyelination. Glia. 2020 Feb;68(2):263-279. doi: 10.1002/glia.23715. Epub 2019 Sep 6. PMID: 31490574; PMCID: PMC8693768.

I performed inhibitor studies to determine if the Cell Migration Inducing and Hyaluronan binding Protein (CEMIP) hyaluronidase activity is inhibited by the modified flavonoid S3. A *Cemip* expression vector and empty vector were purchased from Origene. 293T cell cultures were transfected with empty vectors or *Cemip* expression vector, then the cell growth medium was replaced with serum-free and phenol red-free DMEM containing 50 µg/ml high molecular weight hyaluronic acid, 4.5g/L D-glucose and glutamine, and 110mg/L sodium pyruvate, and different concentrations of S3. Twenty-four hours later, cell medium was collected, centrifuged at 12k rpm for 10 minutes, and supernatant collected.

100 microliters of cell supernatant was mixed with 2 µl of 0.02% Bromophenol Blue loading buffer (Bio-Rad Laboratories) and analyzed by gel electrophoresis using a 0.5% agarose (high-gelling-temperature, Fisher) in Tris–acetate–EDTA

buffer (40 mM Tris, 5 mM acetate [CH₃COONa], and 0.9 mM EDTA, pH 7.9). Gels were stained using the cationic dye Stains-All (Bio-Rad Laboratories) as previously described²³² and then photographed. The distribution and intensity of HA in each lane was determined using ImageJ.

I found that S3 inhibited CEMIP hyaluronidase activity in a dose-dependent manner. Other findings demonstrated that S3 accelerated functional remyelination in a mouse model of focal demyelination. These findings together indicate that S3 may be inhibiting CEMIP activity to accelerate *in vivo* functional remyelination.

Results not included in manuscript preparations

Previous studies have demonstrated that hyaluronic acid (HA) accumulates in the central nervous system (CNS) with aging⁹³⁻⁹⁵. However, there has been no analysis of how *CEMIP* changes with aging. I sought to begin to determine if *Cemip* transcription changes in the CNS with normative aging in mice.

I collected brains of mice at 3, 6, and 12 months of age (4 mice for each age) and extracted the cerebral cortex, hippocampus, cerebellum, and brainstem. RNA was extracted. These four parts, as well as the remaining brain tissue, using an Macherey-Nagel Nucleospin RNA Plus kit. cDNA was prepared from extracted

RNA using an Applied Biosciences high capacity cDNA reverse transcription kit, and qPCR performed with a SybrGreen master mix from Fisher.

I assessed transcript changes of *Cemip*, as well as hyaluronic acid synthases 1-3. I found that in all brain regions except the cortex, where *Cemip* transcription first increases then decreases again with age, *Cemip* transcripts levels decrease with time (Fig 17A). Hyaluronic acid synthase transcript levels did not change, except for *Has2* which decreases with age in the cortex and hippocampus (Fig 17B-D).

These results indicate that *Cemip* expression may decrease in the mouse CNS with age, which could possible explain why hyaluronan levels increase with age. This is further supported by the results indicating that *Has* expression does not change with age.

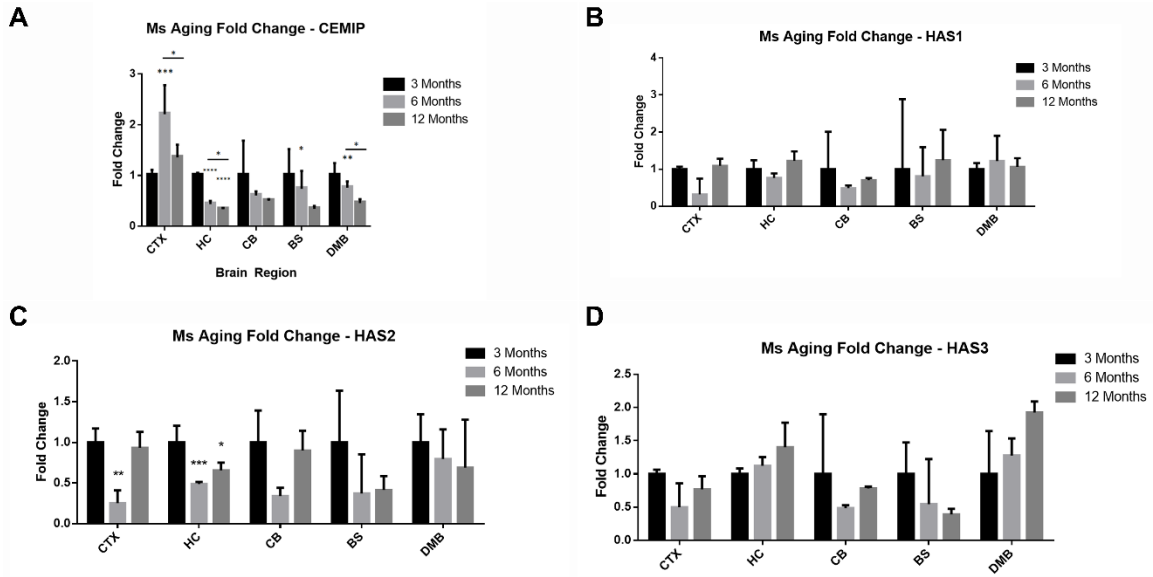


Figure 17: *Cemip* and hyaluronic acid synthase transcript changes with age in the mouse CNS. Changes in A) *Cemip*, B) *Has1*, C) *Has2*, and D) *Has3* transcript levels with age in the mouse cortex (CTX), hippocampus (HC), cerebellum (CB), brainstem (BS), and remaining brain tissue (DMB). *Cemip* transcription generally decreases with age, except in the cortex and cerebellum. *Has1* and *Has3* transcript levels were not found to change with age, while *Has2* transcription decreased in the cortex at 6 months of age, and in the hippocampus with age. Statistically significant differences were detected using a one-way ANOVA with Tukey's multiple comparisons test. * - $p < 0.05$, ** - $p < 0.01$, *** - $p < 0.001$, **** - $p < 0.0001$.

REFERENCES

1. Weissmann B, Meyer K. The Structure of Hyalobiuronic Acid and of Hyaluronic Acid from Umbilical Cord. *Journal of the American Chemical Society*. 1954;76(7):1753-7.
2. Fallacara A, Baldini E, Manfredini S, Vertuani S. Hyaluronic Acid in the Third Millennium. *Polymers (Basel)*. 2018;10(7). Epub 2019/04/10. doi: 10.3390/polym10070701. PubMed PMID: 30960626; PMCID: PMC6403654.
3. Fraser JRE, Laurent TC, Laurent UBG. Hyaluronan: its nature, distribution, functions and turnover. *Journal of Internal Medicine*. 1997;242:27-33.
4. Decker B, McGuckin WF, McKenzie B, Slocumb CH. Concentration of Hyaluronic Acid in Synovial Fluid. *Clinical Chemistry*. 1959;5:465-9.
5. Salwowska NM, Bebenek KA, Źądło DA, Wcisło-Dziadecka DL. Physiochemical properties and application of hyaluronic acid: a systematic review. *Journal of Cosmetic Dermatology*. 2016;15(4):520-6.
6. Litwiniuk M, Krejner A, Speyrer MS, Gauto AR, Grzela T. Hyaluronic Acid in Inflammation and Tissue Regeneration. *Wounds*. 2016;28(3):78-88.
7. Entwistle J, Hall CL, Turley EA. HA Receptors: Regulators of Signalling to the Cytoskeleton. *Journal of Cellular Biochemistry*. 1996;61:569-77.
8. Chistyakov DV, Astakhova AA, Azbukina NV, Goriainov SV, Chistyakov VV, Sergeeva MG. High and Low Molecular Weight Hyaluronic Acid Differentially

Influences Oxylipins Synthesis in Course of Neuroinflammation. *Int J Mol Sci.* 2019;20(16). Epub 2019/08/14. doi: 10.3390/ijms20163894. PubMed PMID: 31405034; PMCID: PMC6719050.

9. Struve J, Maher PC, Li YQ, Kinney S, Fehlings MG, Kuntz Ct, Sherman LS. Disruption of the hyaluronan-based extracellular matrix in spinal cord promotes astrocyte proliferation. *Glia.* 2005;52(1):16-24. Epub 2005/05/14. doi: 10.1002/glia.20215. PubMed PMID: 15892130.

10. Khaing ZZ, Milman BD, Vanscoy JE, Seidlits SK, Grill RJ, Schmidt CE. High molecular weight hyaluronic acid limits astrocyte activation and scar formation after spinal cord injury. *Journal of Neural Engineering.* 2011;8(4):046033. Epub 2011/07/15. doi: 10.1088/1741-2560/8/4/046033. PubMed PMID: 21753237.

11. Marret S, Delpech B, Delpech A, Asou H, Girard N, Courel MN, Chauzy C, Maingonnat C, Fessard C. Expression and Effects of Hyaluronan and of the Hyaluronan-Binding Protein Hyaluronectin in Newborn Rat Brain Glial Cell Cultures. *Journal of Neurochemistry.* 1994;62:1285-95.

12. Su W, Foster SC, Xing R, Feistel K, Olsen RH, Acevedo SF, Raber J, Sherman LS. CD44 Transmembrane Receptor and Hyaluronan Regulate Adult Hippocampal Neural Stem Cell Quiescence and Differentiation. *J Biol Chem.* 2017;292(11):4434-45. Epub 2017/02/06. doi: 10.1074/jbc.M116.774109. PubMed PMID: 28154169; PMCID: PMC5377763.

13. Meszar Z, Felszeghy S, Veress G, Matesz K, Szekely G, Modis L. Hyaluronan accumulates around differentiating neurons in spinal cord of chicken embryos. *Brain Research Bulletin*. 2008;75(2-4):414-8. Epub 2008/03/12. doi: 10.1016/j.brainresbull.2007.10.052. PubMed PMID: 18331908.
14. Simpson RM, Hong X, Wong MM, Karamariti E, Bhaloo SI, Warren D, Kong W, Hu Y, Xu Q. Hyaluronan Is Crucial for Stem Cell Differentiation into Smooth Muscle Lineage. *Stem Cells*. 2016;34(5):1225-38. Epub 2016/02/13. doi: 10.1002/stem.2328. PubMed PMID: 26867148; PMCID: PMC4864761.
15. Sloane JA, Batt C, Ma Y, Harris ZM, Trapp B, Vartanian T. Hyaluronan blocks oligodendrocyte progenitor maturation and remyelination through TLR2. *Proc Natl Acad Sci U S A*. 2010;107(25):11555-60. Epub 2010/06/11. doi: 10.1073/pnas.1006496107. PubMed PMID: 20534434; PMCID: PMC2895128.
16. Milev P, Maurel P, Chiba A, Mevissen M, Popp S, Yamaguchi Y, Margolis RK, Margolis RU. Differential Regulation of Expression of Hyaluronan-Binding Proteoglycans in Developing Brain Aggrecan, Versican, Neurocan, and Brevican. *Biochemical and Biophysical Research Communications*. 1998;247(2):207-12.
17. Galtrey CM, Kwok JC, Carulli D, Rhodes KE, Fawcett JW. Distribution and synthesis of extracellular matrix proteoglycans, hyaluronan, link proteins and tenascin-R in the rat spinal cord. *Eur J Neurosci*. 2008;27(6):1373-90. Epub 2008/03/28. doi: 10.1111/j.1460-9568.2008.06108.x. PubMed PMID: 18364019.

18. Costa C, Tortosa R, Domenech A, Vidal E, Pumarola M, Bassols A. Mapping of aggrecan, hyaluronic acid, heparan sulphate proteoglycans and aquaporin 4 in the central nervous system of the mouse. *J Chem Neuroanat.* 2007;33(3):111-23. Epub 2007/03/14. doi: 10.1016/j.jchemneu.2007.01.006. PubMed PMID: 17349777.
19. Perris R, Danuta K, Lallier T, Domingo C, Sorrell JM, Bronner-Fraser M. Spatial and temporal changes in the distribution of proteoglycans during avian neural crest development. *Development.* 1991;111:583-99.
20. Jin J, Tilve S, Huang Z, Zhou L, Geller HM, Yu P. Effect of chondroitin sulfate proteoglycans on neuronal cell adhesion, spreading and neurite growth in culture. *Neural Regeneration Research.* 2018;13(2):289-97. Epub 2018/03/21. doi: 10.4103/1673-5374.226398. PubMed PMID: 29557379; PMCID: PMC5879901.
21. Inatani M, Honjo M, Otori Y, Oobira A, Kido N, Tano Y, Honda Y, Tanibara H. Inhibitory Effects of Neurocan and Phosphacan on Neurite Outgrowth from Retinal Ganglion Cells in Culture. *Investigative Ophthalmology & Visual Science.* 2001;42(8):1930-8.
22. Friedlander DR, Milev P, Karthikeyan L, Margolis RK, Margolis RU, Grumet M. The Neuronal Chondroitin Sulfate Proteoglycan Neurocan Binds to the Neural Cell Adhesion Molecules Ng-CAM1NILE and N-CAM, and Inhibits Neuronal Adhesion and Neurite Outgrowth. *Journal of Cell Biology.* 1994;125(3):669-80.

23. Rowlands D, Lensjo KK, Dinh T, Yang S, Andrews MR, Hafting T, Fyhn M, Fawcett JW, Dick G. Aggrecan Directs Extracellular Matrix-Mediated Neuronal Plasticity. *J Neurosci*. 2018;38(47):10102-13. Epub 2018/10/05. doi: 10.1523/JNEUROSCI.1122-18.2018. PubMed PMID: 30282728; PMCID: PMC6596198.
24. Hering TM, Beller JA, Calulot CM, Snow DM. Contributions of Chondroitin Sulfate, Keratan Sulfate and N-linked Oligosaccharides to Inhibition of Neurite Outgrowth by Aggrecan. *Biology (Basel)*. 2020;9(2). Epub 2020/02/16. doi: 10.3390/biology9020029. PubMed PMID: 32059349.
25. Johnson WE, Caterson B, Eisenstein SM, Hynds DL, Snow DM, Roberts S. Human intervertebral disc aggrecan inhibits nerve growth in vitro. *Arthritis & Rheumatism*. 2002;46(10):2658-64. Epub 2002/10/18. doi: 10.1002/art.10585. PubMed PMID: 12384924.
26. Schmalfeldt M, Bandtlow CE, Dours-Zimmermann MT, Winterhalter KH, Zimmermann DR. Brain derived versican V2 is a potent inhibitor of axonal growth. *Journal of Cell Science*. 2000;113:807-16. Epub February 14, 2000.
27. Braunwell KH, Pesheva P, McCarthy JB, Furcht LT, Schmitz B, Schachner M. Functional Involvement of Sciatic Nerve-derived Versican- and Decorin-like Molecules and other Chondroitin Sulphate Proteoglycans in ECM-mediated Cell Adhesion and Neurite Outgrowth. *European Journal of Neuroscience*. 1995;7(4):805-14.

28. Dutt S, Kleber M, Matasci M, Sommer L, Zimmermann DR. Versican V0 and V1 guide migratory neural crest cells. *J Biol Chem*. 2006;281(17):12123-31. Epub 2006/03/03. doi: 10.1074/jbc.M510834200. PubMed PMID: 16510447.
29. Wu Y, Sheng W, Chen L, Dong H, Lee V, Lu F, Wong CS, Lu WY, Yang BB. Versican V1 isoform induces neuronal differentiation and promotes neurite outgrowth. *Mol Biol Cell*. 2004;15(5):2093-104. Epub 2004/02/24. doi: 10.1091/mbc.e03-09-0667. PubMed PMID: 14978219; PMCID: PMC404007.
30. Suwan K, Choocheep K, Hatano S, Kongtawelert P, Kimata K, Watanabe H. Versican/PG-M Assembles Hyaluronan into Extracellular Matrix and Inhibits CD44-mediated Signaling toward Premature Senescence in Embryonic Fibroblasts. *J Biol Chem*. 2009;284(13):8596-604. Epub 2009/01/24. doi: 10.1074/jbc.M806927200. PubMed PMID: 19164294; PMCID: PMC2659218.
31. Baranova NS, Nileback E, Haller FM, Briggs DC, Svedhem S, Day AJ, Richter RP. The inflammation-associated protein TSG-6 cross-links hyaluronan via hyaluronan-induced TSG-6 oligomers. *J Biol Chem*. 2011;286(29):25675-86. Epub 2011/05/21. doi: 10.1074/jbc.M111.247395. PubMed PMID: 21596748; PMCID: PMC3138277.
32. Lesley J, Gal I, Mahoney DJ, Cordell MR, Rugg MS, Hyman R, Day AJ, Mikecz K. TSG-6 modulates the interaction between hyaluronan and cell surface CD44. *J Biol Chem*. 2004;279(24):25745-54. Epub 2004/04/03. doi: 10.1074/jbc.M313319200. PubMed PMID: 15060082.

33. Sanggaard KW, Scavenius C, Rasmussen AJ, Wisniewski HG, Thogersen IB, Enghild JJ. The TSG-6/HC2-mediated transfer is a dynamic process shuffling heavy chains between glycosaminoglycans. *J Biol Chem*. 2010;285(29):21988-93. Epub 2010/05/14. doi: 10.1074/jbc.M109.041046. PubMed PMID: 20463016; PMCID: PMC2903360.
34. Bertling F, Bendix I, Drommelschmidt K, Wisniewski HG, Felderhoff-Mueser U, Keller M, Prager S. Tumor necrosis factor-inducible gene 6 protein: A novel neuroprotective factor against inflammation-induced developmental brain injury. *Exp Neurol*. 2016;279:283-9. Epub 2016/03/10. doi: 10.1016/j.expneurol.2016.03.005. PubMed PMID: 26953231.
35. Coulson-Thomas VJ, Lauer ME, Soleman S, Zhao C, Hascall VC, Day AJ, Fawcett JW. Tumor Necrosis Factor-stimulated Gene-6 (TSG-6) Is Constitutively Expressed in Adult Central Nervous System (CNS) and Associated with Astrocyte-mediated Glial Scar Formation following Spinal Cord Injury. *J Biol Chem*. 2016;291(38):19939-52. Epub 2016/07/21. doi: 10.1074/jbc.M115.710673. PubMed PMID: 27435674; PMCID: PMC5025681.
36. Hu Y, Li G, Zhang Y, Liu N, Zhang P, Pan C, Nie H, Li Q, Tang Z. Upregulated TSG-6 Expression in ADSCs Inhibits the BV2 Microglia-Mediated Inflammatory Response. *BioMed Research International*. 2018;2018:7239181. Epub 2018/12/26. doi: 10.1155/2018/7239181. PubMed PMID: 30584538; PMCID: PMC6280241.

37. Margolis RU, Margolis RK, Chang LB, Preti C. Glycosaminoglycans of brain during development. *Biochemistry*. 1975;14(1):85-8.
38. Polansky J, Toole BP, Gross J. Brain Hyaluronidase Changes in Activity during Chick Development. *Science*. 1971;183(4127):862-4.
39. Morriss-Kay GM, Tuckett F, Solursh M. The effects of *Streptomyces* hyaluronidase on tissue organization and cell cycle time in rat embryos. *Journal of Embryology and Experimental Morphology*. 1986;98:59-70.
40. Casini P, Nardi I, Ori M. RHAMM mRNA expression in proliferating and migrating cells of the developing central nervous system. *Gene Expression Patterns*. 2010;10(2-3):93-7. Epub 2010/01/02. doi: 10.1016/j.gep.2009.12.003. PubMed PMID: 20044037.
41. Naruse M, Shibasaki K, Yokoyama S, Kurachi M, Ishizaki Y. Dynamic changes of CD44 expression from progenitors to subpopulations of astrocytes and neurons in developing cerebellum. *PLoS One*. 2013;8(1):e53109. Epub 2013/01/12. doi: 10.1371/journal.pone.0053109. PubMed PMID: 23308146; PMCID: PMC3537769.
42. Fietz SA, Lachmann R, Brandl H, Kircher M, Samusik N, Schroder R, Lakshmanaperumal N, Henry I, Vogt J, Riehn A, Distler W, Nitsch R, Enard W, Paabo S, Huttner WB. Transcriptomes of germinal zones of human and mouse fetal neocortex suggest a role of extracellular matrix in progenitor self-renewal.

- Proc Natl Acad Sci U S A. 2012;109(29):11836-41. Epub 2012/07/04. doi: 10.1073/pnas.1209647109. PubMed PMID: 22753484; PMCID: PMC3406833.
43. Long KR, Newland B, Florio M, Kalebic N, Langen B, Kolterer A, Wimberger P, Huttner WB. Extracellular Matrix Components HAPLN1, Lumican, and Collagen I Cause Hyaluronic Acid-Dependent Folding of the Developing Human Neocortex. *Neuron*. 2018;99(4):702-19 e6. Epub 2018/08/07. doi: 10.1016/j.neuron.2018.07.013. PubMed PMID: 30078576.
44. Lin L, Wang J, Chan CK, Chan SO. Localization of hyaluronan in the optic pathway of mouse embryos. *Developmental Neuroscience*. 2007;18(4):355-8.
45. Chan CK, Wang J, Lin L, Hao Y, Chan SO. Enzymatic removal of hyaluronan affects routing of axons in the mouse optic chiasm. *NeuroReport*. 2007;18(15):1533-8.
46. Lin L, Chan SO. Perturbation of CD44 function affects chiasmatic routing of retinal axons in brain slice preparations of the mouse retinofugal pathway. *European Journal of Neuroscience*. 2003;17(11):2299-312. Epub 2003/06/20. doi: 10.1046/j.1460-9568.2003.02686.x. PubMed PMID: 12814363.
47. Baier C, Baader SL, Jankowski J, Gieselmann V, Schilling K, Rauch U, Kappler J. Hyaluronan is organized into fiber-like structures along migratory pathways in the developing mouse cerebellum. *Matrix Biol*. 2007;26(5):348-58. Epub 2007/03/27. doi: 10.1016/j.matbio.2007.02.002. PubMed PMID: 17383168.

48. Epperlein HH, Radomski N, Wonka F, Walther P, Wilsch M, Muller M, Schwarz H. Immunohistochemical demonstration of hyaluronan and its possible involvement in axolotl neural crest cell migration. *Journal of Structural Biology*. 2000;132(1):19-32. Epub 2000/12/21. doi: 10.1006/jsbi.2000.4298. PubMed PMID: 11121304.
49. Ripellino JA, Klinger MM, Margolis RU, Margolis RK. The hyaluronic acid binding region as a specific probe for the localization of hyaluronic acid in tissue sections. Application to chick embryo and rat brain. *Journal of Histochemistry and Cytochemistry*. 1985;33(10):1060-6.
50. Nardini M, Ori M, Vigetti D, Gornati R, Nardi I, Perris R. Regulated gene expression of hyaluronan synthases during *Xenopus laevis* development. *Gene Expression Patterns*. 2004;4(3):303-8. Epub 2004/04/01. doi: 10.1016/j.modgep.2003.10.006. PubMed PMID: 15053979.
51. Casini P, Nardi I, Ori M. Hyaluronan is required for cranial neural crest cells migration and craniofacial development. *Developmental Dynamics*. 2012;241(2):294-302. Epub 2011/12/21. doi: 10.1002/dvdy.23715. PubMed PMID: 22184056.
52. Tien JY, Spicer AP. Three vertebrate hyaluronan synthases are expressed during mouse development in distinct spatial and temporal patterns. *Developmental Dynamics*. 2005;233(1):130-41. Epub 2005/03/15. doi: 10.1002/dvdy.20328. PubMed PMID: 15765504.

53. Ori M, Nardini M, Casini P, Perris R, Nardi I. XHas2 activity is required during somitogenesis and precursor cell migration in *Xenopus* development. *Development*. 2006;133(4):631-40. Epub 2006/01/20. doi: 10.1242/dev.02225. PubMed PMID: 16421194.
54. Bignami A, Asher R, Perides G. The extracellular matrix of rat spinal cord: A comparative study on the localization of hyaluronic acid, glial hyaluronate-binding protein, and chondroitin sulfate proteoglycan. *Experimental Neurology*. 1992;117:90-3.
55. Bignami A, Asher R. Some observations on the localization of hyaluronic acid in adult, newborn and embryonal rat brain. *International Journal of Developmental Neuroscience*. 1992;10(1):45-57.
56. Ueno H, Suemitsu S, Murakami S, Kitamura N, Wani K, Matsumoto Y, Okamoto M, Ishihara T. Layer-specific expression of extracellular matrix molecules in the mouse somatosensory and piriform cortices. *IBRO Reports*. 2019;6:1-17. Epub 2018/12/26. doi: 10.1016/j.ibror.2018.11.006. PubMed PMID: 30582064; PMCID: PMC6293036.
57. Ripellino JA, Bailo M, Margolis RU, Margolis RK. Light and Electron Microscopic Studies on the Localization of Hyaluronic Acid in Developing Rat Cerebellum. *Journal of Cell Biology*. 1988;106:845-55.
58. Miyata S, Nishimura Y, Hayashi N, Oohira A. Construction of perineuronal net-like structure by cortical neurons in culture. *Neuroscience*. 2005;136(1):95-

104. Epub 2005/09/27. doi: 10.1016/j.neuroscience.2005.07.031. PubMed PMID: 16182457.

59. Eggli PS, Lucocq J, Ott P, Graber W, Van der Zypen E. Ultrastructural localization of hyaluronan in myelin sheaths of the rat central and rat and human peripheral nervous systems using hyaluronan-binding protein-gold and link protein-gold. *Neuroscience*. 1992;48(3):737-44.

60. Sherpa AD, Guilfoyle DN, Naik AA, Isakovic J, Irie F, Yamaguchi Y, Hrabe J, Aoki C, Hrabetova S. Integrity of White Matter is Compromised in Mice with Hyaluronan Deficiency. *Neurochem Res*. 2020;45(1):53-67. Epub 2019/06/09. doi: 10.1007/s11064-019-02819-z. PubMed PMID: 31175541; PMCID: PMC6898766.

61. Lindwall C, Olsson M, Osman AM, Kuhn HG, Curtis MA. Selective expression of hyaluronan and receptor for hyaluronan mediated motility (Rhamm) in the adult mouse subventricular zone and rostral migratory stream and in ischemic cortex. *Brain Research* 2013;1503:62-77. Epub 2013/02/09. doi: 10.1016/j.brainres.2013.01.045. PubMed PMID: 23391595.

62. Ma W, Suh WH. Cost-Effective Cosmetic-Grade Hyaluronan Hydrogels for ReNcell VM Human Neural Stem Cell Culture. *Biomolecules & Therapeutics*. 2019;9(10). Epub 2019/09/25. doi: 10.3390/biom9100515. PubMed PMID: 31547190; PMCID: PMC6843608.

63. Okun E, Griffioen KJ, Son TG, Lee JH, Roberts NJ, Mughal MR, Hutchison E, Cheng A, Arumugam TV, Lathia JD, van Praag H, Mattson MP. TLR2 activation inhibits embryonic neural progenitor cell proliferation. *J Neurochem.* 2010;114(2):462-74. Epub 2010/05/12. doi: 10.1111/j.1471-4159.2010.06778.x. PubMed PMID: 20456021; PMCID: PMC2910143.
64. Raber J, Olsen RH, Su W, Foster S, Xing R, Acevedo SF, Sherman LS. CD44 is required for spatial memory retention and sensorimotor functions. *Behavioural Brain Research.* 2014;275:146-9. Epub 2014/09/16. doi: 10.1016/j.bbr.2014.09.010. PubMed PMID: 25219362; PMCID: PMC4253558.
65. Seidlits SK, Khaing ZZ, Petersen RR, Nickels JD, Vanscoy JE, Shear JB, Schmidt CE. The effects of hyaluronic acid hydrogels with tunable mechanical properties on neural progenitor cell differentiation. *Biomaterials.* 2010;31(14):3930-40. Epub 2010/02/23. doi: 10.1016/j.biomaterials.2010.01.125. PubMed PMID: 20171731.
66. Georges PC, Miller WJ, Meaney DF, Sawyer ES, Janmey PA. Matrices with compliance comparable to that of brain tissue select neuronal over glial growth in mixed cortical cultures. *Biophysical Journal.* 2006;90(8):3012-8. Epub 2006/02/08. doi: 10.1529/biophysj.105.073114. PubMed PMID: 16461391; PMCID: PMC1414567.
67. Engler AJ, Sen S, Sweeney HL, Discher DE. Matrix elasticity directs stem cell lineage specification. *Cell.* 2006;126(4):677-89. Epub 2006/08/23. doi: 10.1016/j.cell.2006.06.044. PubMed PMID: 16923388.

68. Kim MC, Silberberg YR, Abeyaratne R, Kamm RD, Asada HH. Computational modeling of three-dimensional ECM-rigidity sensing to guide directed cell migration. *Proc Natl Acad Sci U S A*. 2018;115(3):E390-E9. Epub 2018/01/04. doi: 10.1073/pnas.1717230115. PubMed PMID: 29295934; PMCID: PMC5776995.
69. Ambrosio L, Borzacchiello A, Netti PA, Nicolais L. Rheological Study on Hyaluronic Acid and Its Derivative Solutions. *Journal of Macromolecular Science, Part A*. 1999;36(7-8):991-1000. doi: 10.1080/10601329908951195.
70. Caires R, Luis E, Taberner FJ, Fernandez-Ballester G, Ferrer-Montiel A, Balazs EA, Gomis A, Belmonte C, de la Pena E. Hyaluronan modulates TRPV1 channel opening, reducing peripheral nociceptor activity and pain. *Nature Communications*. 2015;6:8095. Epub 2015/08/28. doi: 10.1038/ncomms9095. PubMed PMID: 26311398; PMCID: PMC4560824.
71. Ferrari LF, Araldi D, Bogen O, Levine JD. Extracellular matrix hyaluronan signals via its CD44 receptor in the increased responsiveness to mechanical stimulation. *Neuroscience*. 2016;324:390-8. Epub 2016/03/22. doi: 10.1016/j.neuroscience.2016.03.032. PubMed PMID: 26996509; PMCID: PMC5365238.
72. Kochlamazashvili G, Henneberger C, Bukalo O, Dvoretzkova E, Senkov O, Lievens PM, Westenbroek R, Engel AK, Catterall WA, Rusakov DA, Schachner M, Dityatev A. The extracellular matrix molecule hyaluronic acid regulates hippocampal synaptic plasticity by modulating postsynaptic L-type

Ca²⁺ channels. *Neuron*. 2010;67(1):116-28. Epub 2010/07/14. doi: 10.1016/j.neuron.2010.05.030. PubMed PMID: 20624596; PMCID: PMC3378029.

73. Frischknecht R, Heine M, Perrais D, Seidenbecher CI, Choquet D, Gundelfinger ED. Brain extracellular matrix affects AMPA receptor lateral mobility and short-term synaptic plasticity. *Nat Neurosci*. 2009;12(7):897-904. Epub 2009/06/02. doi: 10.1038/nn.2338. PubMed PMID: 19483686.

74. Su W, Matsumoto S, Sorg B, Sherman LS. Distinct roles for hyaluronan in neural stem cell niches and perineuronal nets. *Matrix Biol*. 2019;78-79:272-83. Epub 2018/02/07. doi: 10.1016/j.matbio.2018.01.022. PubMed PMID: 29408010; PMCID: PMC6068007.

75. Kwok JC, Carulli D, Fawcett JW. In vitro modeling of perineuronal nets: hyaluronan synthase and link protein are necessary for their formation and integrity. *J Neurochem*. 2010;114(5):1447-59. Epub 2010/06/30. doi: 10.1111/j.1471-4159.2010.06878.x. PubMed PMID: 20584105.

76. Maleski M, Hockfield S. Glial cells assemble hyaluronan-based pericellular matrices in vitro. *Glia*. 1997;20(3):193-202. doi: 10.1002/(sici)1098-1136(199707)20:3<193::Aid-glia3>3.0.Co;2-9.

77. Fowke TM, Karunasinghe RN, Bai JZ, Jordan S, Gunn AJ, Dean JM. Hyaluronan synthesis by developing cortical neurons in vitro. *Sci Rep*.

2017;7:44135. Epub 2017/03/14. doi: 10.1038/srep44135. PubMed PMID: 28287145; PMCID: PMC5347017.

78. Giamanco KA, Matthews RT. Deconstructing the perineuronal net: cellular contributions and molecular composition of the neuronal extracellular matrix. *Neuroscience*. 2012;218:367-84. Epub 2012/06/05. doi: 10.1016/j.neuroscience.2012.05.055. PubMed PMID: 22659016; PMCID: PMC3400135.

79. Koppe G, Bruckner G, Brauer K, Hartig W, Bigl V. Developmental patterns of proteoglycan-containing extracellular matrix in perineuronal nets and neuropil of the postnatal rat brain. *Cell and Tissue Research*. 1997;288:33-41.

80. Ueno H, Suemitsu S, Okamoto M, Matsumoto Y, Ishihara T. Sensory experience-dependent formation of perineuronal nets and expression of Cat-315 immunoreactive components in the mouse somatosensory cortex. *Neuroscience*. 2017;355:161-74. Epub 2017/05/13. doi: 10.1016/j.neuroscience.2017.04.041. PubMed PMID: 28495333.

81. Lensjo KK, Lepperød ME, Dick G, Hafting T, Fyhn M. Removal of Perineuronal Nets Unlocks Juvenile Plasticity Through Network Mechanisms of Decreased Inhibition and Increased Gamma Activity. *J Neurosci*. 2017;37(5):1269-83. Epub 2017/01/01. doi: 10.1523/JNEUROSCI.2504-16.2016. PubMed PMID: 28039374; PMCID: PMC6596863.

82. Yasuhara O, Akiyama H, McGeer EG, McGeer PL. Immunohistochemical localization of hyaluronic acid in rat and human brain. *Brain Research*. 1994;635:269-82.
83. Schweitzer B, Singh J, Fejtova A, Groc L, Heine M, Frischknecht R. Hyaluronic acid based extracellular matrix regulates surface expression of GluN2B containing NMDA receptors. *Sci Rep*. 2017;7(1):10991. Epub 2017/09/10. doi: 10.1038/s41598-017-07003-3. PubMed PMID: 28887453; PMCID: PMC5591221.
84. Vedunova M, Sakharnova T, Mitroshina E, Perminova M, Pimashkin A, Zakharov Y, Dityatev A, Mukhina I. Seizure-like activity in hyaluronidase-treated dissociated hippocampal cultures. *Front Cell Neurosci*. 2013;7:149. Epub 2013/09/26. doi: 10.3389/fncel.2013.00149. PubMed PMID: 24062641; PMCID: PMC3770920.
85. Balashova A, Pershin V, Zaborskaya O, Tkachenko N, Mironov A, Guryev E, Kurbatov L, Gainullin M, Mukhina I. Enzymatic Digestion of Hyaluronan-Based Brain Extracellular Matrix in vivo Can Induce Seizures in Neonatal Mice. *Front Neurosci*. 2019;13:1033. Epub 2019/10/22. doi: 10.3389/fnins.2019.01033. PubMed PMID: 31632233; PMCID: PMC6779145.
86. Mauney SA, Athanas KM, Pantazopoulos H, Shaskan N, Passeri E, Berretta S, Woo TU. Developmental pattern of perineuronal nets in the human prefrontal cortex and their deficit in schizophrenia. *Biol Psychiatry*.

2013;74(6):427-35. Epub 2013/06/25. doi: 10.1016/j.biopsych.2013.05.007.
PubMed PMID: 23790226; PMCID: PMC3752333.

87. Asher R, Bignami A. Localization of hyaluronate in primary glial cell cultures derived from newborn rat brain. *Experimental Cell Research*. 1991;195:401-11.

88. Bourguignon LY, Gilad E, Peyrollier K, Brightman A, Swanson RA. Hyaluronan-CD44 interaction stimulates Rac1 signaling and PKN gamma kinase activation leading to cytoskeleton function and cell migration in astrocytes. *J Neurochem*. 2007;101(4):1002-17. Epub 2007/04/04. doi: 10.1111/j.1471-4159.2007.04485.x. PubMed PMID: 17403031.

89. Konopka A, Zeug A, Skupien A, Kaza B, Mueller F, Chwedorowicz A, Ponimaskin E, Wilczynski GM, Dzwonek J. Cleavage of Hyaluronan and CD44 Adhesion Molecule Regulate Astrocyte Morphology via Rac1 Signalling. *PLoS One*. 2016;11(5):e0155053. Epub 2016/05/11. doi: 10.1371/journal.pone.0155053. PubMed PMID: 27163367; PMCID: PMC4862642.

90. Turley EA, Hossain MZ, Sorokan T, Jordan LM, Nagy JI. Astrocyte and microglial motility in vitro is functionally dependent on the hyaluronan receptor RHAMM. *Glia*. 1994;12:68-80.

91. Hayashi MK, Nishioka T, Shimizu H, Takahashi K, Kakegawa W, Mikami T, Hirayama Y, Koizumi S, Yoshida S, Yuzaki M, Tammi M, Sekino Y, Kaibuchi K,

Shigemoto-Mogami Y, Yasui M, Sato K. Hyaluronan synthesis supports glutamate transporter activity. *J Neurochem*. 2019;150(3):249-63. Epub 2019/06/13. doi: 10.1111/jnc.14791. PubMed PMID: 31188471.

92. Jenkins HG, Bachelard HS. Developmental and Age-Related Changes in Rat Brain Glycosaminoglycans. *Journal of Neurochemistry*. 1988;51:1634-40.

93. Cargill R, Kohama SG, Struve J, Su W, Banine F, Witkowski E, Back SA, Sherman LS. Astrocytes in aged nonhuman primate brain gray matter synthesize excess hyaluronan. *Neurobiol Aging*. 2012;33(4):830 e13-24. Epub 2011/08/30. doi: 10.1016/j.neurobiolaging.2011.07.006. PubMed PMID: 21872361; PMCID: PMC3227765.

94. Reed MJ, Vernon RB, Damodarasamy M, Chan CK, Wight TN, Bentov I, Banks WA. Microvasculature of the Mouse Cerebral Cortex Exhibits Increased Accumulation and Synthesis of Hyaluronan With Aging. *J Gerontol A Biol Sci Med Sci*. 2017;72(6):740-6. Epub 2017/05/10. doi: 10.1093/gerona/glw213. PubMed PMID: 28482035; PMCID: PMC6075594.

95. Reed MJ, Damodarasamy M, Pathan JL, Erickson MA, Banks WA, Vernon RB. The Effects of Normal Aging on Regional Accumulation of Hyaluronan and Chondroitin Sulfate Proteoglycans in the Mouse Brain. *Journal of Histochemistry and Cytochemistry*. 2018;66(10):697-707. Epub 2018/05/22. doi: 10.1369/0022155418774779. PubMed PMID: 29782809; PMCID: PMC6158629.

96. Smith K, Semenov MV. The impact of age on number and distribution of proliferating cells in subgranular zone in adult mouse brain. *IBRO Reports*. 2019;6:18-30. Epub 2018/12/26. doi: 10.1016/j.ibror.2018.12.002. PubMed PMID: 30582065; PMCID: PMC6297242.
97. Sherman LS, Matsumoto S, Su W, Srivastava T, Back SA. Hyaluronan Synthesis, Catabolism, and Signaling in Neurodegenerative Diseases. *Int J Cell Biol*. 2015;2015:368584. Epub 2015/10/09. doi: 10.1155/2015/368584. PubMed PMID: 26448752; PMCID: PMC4581574.
98. Srivastava T, Sherman LS, Back SA. Dysregulation of Hyaluronan Homeostasis During White Matter Injury. *Neurochem Res*. 2020;45(3):672-83. Epub 2019/09/23. doi: 10.1007/s11064-019-02879-1. PubMed PMID: 31542857; PMCID: PMC7060835.
99. Al'Qteishat A, Gaffney J, Krupinski J, Rubio F, West D, Kumar S, Kumar P, Mitsios N, Slevin M. Changes in hyaluronan production and metabolism following ischaemic stroke in man. *Brain*. 2006;129(Pt 8):2158-76. Epub 2006/05/30. doi: 10.1093/brain/awl139. PubMed PMID: 16731541.
100. Lin CM, Lin JW, Chen YC, Shen HH, Wei L, Yeh YS, Chiang YH, Shih R, Chiu PL, Hung KS, Yang LY, Chiu WT. Hyaluronic acid inhibits the glial scar formation after brain damage with tissue loss in rats. *Surg Neurol*. 2009;72 Suppl 2:S50-4. Epub 2009/12/01. doi: 10.1016/j.wneu.2009.09.004. PubMed PMID: 19944826.

101. Austin JW, Gilchrist C, Fehlings MG. High molecular weight hyaluronan reduces lipopolysaccharide mediated microglial activation. *J Neurochem.* 2012;122(2):344-55. Epub 2012/05/17. doi: 10.1111/j.1471-4159.2012.07789.x. PubMed PMID: 22587438.
102. Al-Ahmad AJ, Patel R, Palecek SP, Shusta EV. Hyaluronan impairs the barrier integrity of brain microvascular endothelial cells through a CD44-dependent pathway. *J Cereb Blood Flow Metab.* 2019;39(9):1759-75. Epub 2018/03/29. doi: 10.1177/0271678X18767748. PubMed PMID: 29589805; PMCID: PMC6727144.
103. Winkler CW, Foster SC, Matsumoto SG, Preston MA, Xing R, Bebo BF, Banine F, Berny-Lang MA, Itakura A, McCarty OJ, Sherman LS. Hyaluronan anchored to activated CD44 on central nervous system vascular endothelial cells promotes lymphocyte extravasation in experimental autoimmune encephalomyelitis. *J Biol Chem.* 2012;287(40):33237-51. Epub 2012/08/07. doi: 10.1074/jbc.M112.356287. PubMed PMID: 22865853; PMCID: PMC3460429.
104. West DC, Hampson IN, Arnold F, Kumar S. Angiogenesis induced by degradation products of hyaluronic acid. *Science.* 1985;228(4705):1324-6.
105. Silva LP, Pirraco RP, Santos TC, Novoa-Carballal R, Cerqueira MT, Reis RL, Correlo VM, Marques AP. Neovascularization Induced by the Hyaluronic Acid-Based Spongy-Like Hydrogels Degradation Products. *ACS Applied Materials & Interfaces.* 2016;8(49):33464-74. Epub 2016/12/15. doi: 10.1021/acsami.6b11684. PubMed PMID: 27960396.

106. Srivastava T, Diba P, Dean JM, Banine F, Shaver D, Hagen M, Gong X, Su W, Emery B, Marks DL, Harris EN, Baggenstoss B, Weigel PH, Sherman LS, Back SA. A TLR/AKT/FoxO3 immune tolerance-like pathway disrupts the repair capacity of oligodendrocyte progenitors. *J Clin Invest*. 2018;128(5):2025-41. Epub 2018/04/18. doi: 10.1172/JCI94158. PubMed PMID: 29664021; PMCID: PMC5919806.

107. Preston M, Gong X, Su W, Matsumoto SG, Banine F, Winkler C, Foster S, Xing R, Struve J, Dean J, Baggenstoss B, Weigel PH, Montine TJ, Back SA, Sherman LS. Digestion products of the PH20 hyaluronidase inhibit remyelination. *Annals of Neurology*. 2013;73(2):266-80. Epub 2013/03/07. doi: 10.1002/ana.23788. PubMed PMID: 23463525; PMCID: PMC3608752.

108. Reed MJ, Damodarasamy M, Pathan JL, Chan CK, Spiekerman C, Wight TN, Banks WA, Day AJ, Vernon RB, Keene CD. Increased Hyaluronan and TSG-6 in Association with Neuropathologic Changes of Alzheimer's Disease. *J Alzheimers Dis*. 2019;67(1):91-102. Epub 2018/12/07. doi: 10.3233/JAD-180797. PubMed PMID: 30507579; PMCID: PMC6398602.

109. Baranova NS, Foulcer SJ, Briggs DC, Tilakaratna V, Enghild JJ, Milner CM, Day AJ, Richter RP. Inter-alpha-inhibitor impairs TSG-6-induced hyaluronan cross-linking. *J Biol Chem*. 2013;288(41):29642-53. Epub 2013/09/06. doi: 10.1074/jbc.M113.477422. PubMed PMID: 24005673; PMCID: PMC3795262.

110. Bugiani M, Postma N, Polder E, Dieleman N, Scheffer PG, Sim FJ, van der Knaap MS, Boor I. Hyaluronan accumulation and arrested oligodendrocyte

progenitor maturation in vanishing white matter disease. *Brain*. 2013;136(Pt 1):209-22. Epub 2013/02/01. doi: 10.1093/brain/aws320. PubMed PMID: 23365098.

111. Itano N, Sawai T, Yoshida M, Lenas P, Yamada Y, Imagawa M, Shinomura T, Hamaguchi M, Yoshida Y, Ohnuki Y, Miyauchi S, Spicer AP, McDonald JA, Kimita K. Three Isoforms of Mammalian Hyaluronan Synthases Have Distinct Enzymatic Properties. *Journal of Biological Chemistry*. 1999;274(35):25085-92.

112. Saito T, Kawana H, Azuma K, Toyoda A, Fujita H, Kitagawa M, Harigaya K. Fragmented hyaluronan is an autocrine chemokinetic motility factor supported by the HAS2-HYAL2/CD44 system on the plasma membrane. *Int J Oncol*. 2011;39(5):1311-20. Epub 2011/07/12. doi: 10.3892/ijo.2011.1114. PubMed PMID: 21743962.

113. Marei WF, Salavati M, Fouladi-Nashta AA. Critical role of hyaluronidase-2 during preimplantation embryo development. *Mol Hum Reprod*. 2013;19(9):590-9. Epub 2013/04/30. doi: 10.1093/molehr/gat032. PubMed PMID: 23625939.

114. Choudhary M, Zhang X, Stojkovic P, Hyslop L, Anyfantis G, Herbert M, Murdoch AP, Stojkovic M, Lako M. Putative role of hyaluronan and its related genes, HAS2 and RHAMM, in human early preimplantation embryogenesis and embryonic stem cell characterization. *Stem Cells*. 2007;25(12):3045-57. Epub 2007/09/18. doi: 10.1634/stemcells.2007-0296. PubMed PMID: 17872502.

115. Itano N, Atsumi F, Sawai T, Yamada Y, Miyaishi O, Senga T, Hamaguchi M, Kimata K. Abnormal accumulation of hyaluronan matrix diminishes contact inhibition of cell growth and promotes cell migration. *Proceedings of the National Academy of Sciences of the United States of America*. 2002;99(6):3609-14.
116. Toole BP. Hyaluronan in morphogenesis. *seminars in Cell & Developmental Biology*. 2001;12(2):79-87. Epub 2001/04/09. doi: 10.1006/scdb.2000.0244. PubMed PMID: 11292373.
117. Arranz AM, Perkins KL, Irie F, Lewis DP, Hrabe J, Xiao F, Itano N, Kimata K, Hrabetova S, Yamaguchi Y. Hyaluronan deficiency due to Has3 knock-out causes altered neuronal activity and seizures via reduction in brain extracellular space. *J Neurosci*. 2014;34(18):6164-76. Epub 2014/05/03. doi: 10.1523/JNEUROSCI.3458-13.2014. PubMed PMID: 24790187; PMCID: PMC4004806.
118. Mueller AM, Yoon BH, Sadiq SA. Inhibition of hyaluronan synthesis protects against central nervous system (CNS) autoimmunity and increases CXCL12 expression in the inflamed CNS. *J Biol Chem*. 2014;289(33):22888-99. Epub 2014/06/29. doi: 10.1074/jbc.M114.559583. PubMed PMID: 24973214; PMCID: PMC4132791.
119. Wang W, Wang J, Li F. Hyaluronidase and Chondroitinase. *Advances in Experimental Medicine and Biology*. 2017;1:75-87. Epub September 28 2016.

120. Kaneiwa T, Mizumoto S, Sugahara K, Yamada S. Identification of human hyaluronidase-4 as a novel chondroitin sulfate hydrolase that preferentially cleaves the galactosaminidic linkage in the trisulfated tetrasaccharide sequence. *Glycobiology*. 2010;20(3):300-9. Epub 2009/11/06. doi: 10.1093/glycob/cwp174. PubMed PMID: 19889881.

121. Triggs-Raine B, Salo TJ, Zhang H, Wicklow BA, Natowicz MR. Mutations in HYAL1, a member of a tandemly distributed multigene family encoding disparate hyaluronidase activities, cause a newly described lysosomal disorder, mucopolysaccharidosis IX. *Proceedings of the National Academy of Sciences of the United States of America*. 1999;96(11):6296-300.

122. Rai SK, Duh FM, Vigdorovich V, Danilkovitch-Miagkova A, Lerman MI, Miller AD. Candidate tumor suppressor HYAL2 is a glycosylphosphatidylinositol (GPI)-anchored cell-surface receptor for jaagsiekte sheep retrovirus, the envelope protein of which mediates oncogenic transformation. *Proceedings of the National Academy of Sciences of the United States of America*. 2001;98(8):4443-8.

123. Yoshida H, Nagaoka A, Kusaka-Kikushima A, Tobiishi M, Kawabata K, Sayo T, Sakai S, Sugiyama Y, Enomoto H, Okada Y, Inoue S. KIAA1199, a deafness gene of unknown function, is a new hyaluronan binding protein involved in hyaluronan depolymerization. *Proc Natl Acad Sci U S A*. 2013;110(14):5612-7. Epub 2013/03/20. doi: 10.1073/pnas.1215432110. PubMed PMID: 23509262; PMCID: PMC3619336.

124. Yamamoto H, Tobisawa Y, Inubushi T, Irie F, Ohyama C, Yamaguchi Y. A mammalian homolog of the zebrafish transmembrane protein 2 (TMEM2) is the long-sought-after cell-surface hyaluronidase. *J Biol Chem.* 2017;292(18):7304-13. Epub 2017/03/02. doi: 10.1074/jbc.M116.770149. PubMed PMID: 28246172; PMCID: PMC5418033.

125. Yoshino Y, Goto M, Hara H, Inoue S. The role and regulation of TMEM2 (transmembrane protein 2) in HYBID (hyaluronan (HA)-binding protein involved in HA depolymerization/ KIAA1199/CEMIP)-mediated HA depolymerization in human skin fibroblasts. *Biochemical and Biophysical Research Communications.* 2018;505(1):74-80. Epub 2018/09/23. doi: 10.1016/j.bbrc.2018.09.097. PubMed PMID: 30241936.

126. Harada H, Takahashi M. CD44-dependent intracellular and extracellular catabolism of hyaluronic acid by hyaluronidase-1 and -2. *J Biol Chem.* 2007;282(8):5597-607. Epub 2006/12/16. doi: 10.1074/jbc.M608358200. PubMed PMID: 17170110.

127. Bourguignon LY, Singleton PA, Diedrich F, Stern R, Gilad E. CD44 interaction with Na⁺-H⁺ exchanger (NHE1) creates acidic microenvironments leading to hyaluronidase-2 and cathepsin B activation and breast tumor cell invasion. *J Biol Chem.* 2004;279(26):26991-7007. Epub 2004/04/20. doi: 10.1074/jbc.M311838200. PubMed PMID: 15090545.

128. Martin DC, Atmuri V, Hemming RJ, Farley J, Mort JS, Byers S, Hombach-Klonisch S, Csoka AB, Stern R, Triggs-Raine BL. A mouse model of human

mucopolysaccharidosis IX exhibits osteoarthritis. *Hum Mol Genet.* 2008;17(13):1904-15. Epub 2008/03/18. doi: 10.1093/hmg/ddn088. PubMed PMID: 18344557.

129. Atmuri V, Martin DC, Hemming R, Gutsol A, Byers S, Sahebjam S, Thliveris JA, Mort JS, Carmona E, Anderson JE, Dakshinamurti S, Triggs-Raine B. Hyaluronidase 3 (HYAL3) knockout mice do not display evidence of hyaluronan accumulation. *Matrix Biol.* 2008;27(8):653-60. Epub 2008/09/03. doi: 10.1016/j.matbio.2008.07.006. PubMed PMID: 18762256.

130. Chowdhury B, Hemming R, Hombach-Klonisch S, Flamion B, Triggs-Raine B. Murine hyaluronidase 2 deficiency results in extracellular hyaluronan accumulation and severe cardiopulmonary dysfunction. *J Biol Chem.* 2013;288(1):520-8. Epub 2012/11/23. doi: 10.1074/jbc.M112.393629. PubMed PMID: 23172227; PMCID: PMC3537049.

131. Chowdhury B, Hemming R, Faiyaz S, Triggs-Raine B. Hyaluronidase 2 (HYAL2) is expressed in endothelial cells, as well as some specialized epithelial cells, and is required for normal hyaluronan catabolism. *Histochemistry and Cell Biology.* 2016;145:53-66. Epub October 29, 2015.

132. Yoshino Y, Shimazawa M, Nakamura S, Inoue S, Yoshida H, Shimoda M, Okada Y, Hara H. Targeted deletion of HYBID (hyaluronan binding protein involved in hyaluronan depolymerization/ KIAA1199/CEMIP) decreases dendritic spine density in the dentate gyrus through hyaluronan accumulation. *Biochemical*

and Biophysical Research Communications. 2018;503(3):1934-40. Epub 2018/08/01. doi: 10.1016/j.bbrc.2018.07.138. PubMed PMID: 30060951.

133. Yoshino Y, Ishisaka M, Tsuruma K, Shimazawa M, Yoshida H, Inoue S, Shimoda M, Okada Y, Hara H. Distribution and function of hyaluronan binding protein involved in hyaluronan depolymerization (HYBID, KIAA1199) in the mouse central nervous system. *Neuroscience*. 2017;347:1-10. Epub 2017/02/13. doi: 10.1016/j.neuroscience.2017.01.049. PubMed PMID: 28189611.

134. Marella M, Ouyang J, Zombeck J, Zhao C, Huang L, Connor RJ, Phan KB, Jorge MC, Printz MA, Paladini RD, Gelb AB, Huang Z, Frost GI, Sugarman BJ, Steinman L, Wei G, Shepard HM, Maneval DC, Lapinskas PJ. PH20 is not expressed in murine CNS and oligodendrocyte precursor cells. *Annals of Clinical and Translational Neurology*. 2017;4(3):191-211. Epub 2017/03/10. doi: 10.1002/acn3.393. PubMed PMID: 28275653; PMCID: PMC5338182.

135. Su W, Matsumoto S, Banine F, Srivastava T, Dean J, Foster S, Pham P, Hammond B, Peters A, Girish KS, Rangappa KS, Basappa, Jose J, Hennebold JD, Murphy MJ, Bennett-Toomey J, Back SA, Sherman LS. A modified flavonoid accelerates oligodendrocyte maturation and functional remyelination. *Glia*. 2020;68(2):263-79. Epub 2019/09/07. doi: 10.1002/glia.23715. PubMed PMID: 31490574.

136. Goodison S, Urquidi V, Tarin D. CD44 cell adhesion molecules. *Journal of Clinical Pathology*. 1999;52:189-96.

137. Kaaijk P, Pals ST, Morsink F, A. BD, Troost D. Differential expression of CD44 splice variants in the normal human central nervous system. *Journal of Neuroimmunology*. 1997;73(1-2):70-6.
138. English NM, Lesley JF, Hyman R. Site-specific De-N-glycosylation of CD44 Can Activate Hyaluronan Binding, and CD44 Activation States Show Distinct Threshold Densities for Hyaluronan Binding. *Cancer Research*. 1998;58:3736-42.
139. Banerji S, Wright AJ, Noble M, Mahoney DJ, Campbell ID, Day AJ, Jackson DG. Structures of the Cd44-hyaluronan complex provide insight into a fundamental carbohydrate-protein interaction. *Nat Struct Mol Biol*. 2007;14(3):234-9. Epub 2007/02/13. doi: 10.1038/nsmb1201. PubMed PMID: 17293874.
140. Yang C, Cao M, Liu H, He Y, Xu J, Du Y, Liu Y, Wang W, Cui L, Hu J, Gao F. The high and low molecular weight forms of hyaluronan have distinct effects on CD44 clustering. *J Biol Chem*. 2012;287(51):43094-107. Epub 2012/11/03. doi: 10.1074/jbc.M112.349209. PubMed PMID: 23118219; PMCID: PMC3522304.
141. Jiang J, Mohan P, Maxwell CA. The cytoskeletal protein RHAMM and ERK1/2 activity maintain the pluripotency of murine embryonic stem cells. *PLoS One*. 2013;8(9):e73548. Epub 2013/09/11. doi: 10.1371/journal.pone.0073548. PubMed PMID: 24019927; PMCID: PMC3760809.

142. Lynn BD, Turley EA, Nagy JI. Subcellular distribution, calmodulin interaction, and mitochondrial association of the hyaluronan-binding protein RHAMM in rat brain. *Journal of Neuroscience Research*. 2001;65:6-16.
143. Jiang D, Liang J, Fan J, Yu S, Chen S, Luo Y, Prestwich GD, Mascarenhas MM, Garg HG, Quinn DA, Homer RJ, Goldstein DR, Bucala R, Lee PJ, Medzhitov R, Noble PW. Regulation of lung injury and repair by Toll-like receptors and hyaluronan. *Nat Med*. 2005;11(11):1173-9. Epub 2005/10/26. doi: 10.1038/nm1315. PubMed PMID: 16244651.
144. Liu Y, Han SS, Wu Y, Tuohy TM, Xue H, Cai J, Back SA, Sherman LS, Fischer I, Rao MS. CD44 expression identifies astrocyte-restricted precursor cells. *Developmental Biology*. 2004;276(1):31-46. Epub 2004/11/09. doi: 10.1016/j.ydbio.2004.08.018. PubMed PMID: 15531362.
145. Skupien A, Konopka A, Trzaskoma P, Labus J, Gorlewicz A, Swiech L, Babraj M, Dolezyczek H, Figiel I, Ponimaskin E, Wlodarczyk J, Jaworski J, Wilczynski GM, Dzwonek J. CD44 regulates dendrite morphogenesis through Src tyrosine kinase-dependent positioning of the Golgi. *J Cell Sci*. 2014;127(Pt 23):5038-51. Epub 2014/10/11. doi: 10.1242/jcs.154542. PubMed PMID: 25300795.
146. Roszkowska M, Skupien A, Wojtowicz T, Konopka A, Gorlewicz A, Kisiel M, Bekisz M, Ruszczycki B, Dolezyczek H, Rejmak E, Knapska E, Mozrzymas JW, Wlodarczyk J, Wilczynski GM, Dzwonek J. CD44: a novel synaptic cell adhesion molecule regulating structural and functional plasticity of dendritic

- spines. *Mol Biol Cell*. 2016;27(25):4055-66. Epub 2016/11/01. doi: 10.1091/mbc.E16-06-0423. PubMed PMID: 27798233; PMCID: PMC5156546.
147. Girgrah N, Letarte M, Becker LE, Cruz TF, Theriault E, Moscarello MA. Localization of the CD44 Glycoprotein to Fibrous Astrocytes in Normal White Matter and to Reactive Astrocytes in Active Lesions in Multiple Sclerosis. *Journal of Neuropathology and Experimental Neurology*. 1991;50(6):779-92.
148. Hasebe T, Fujimoto K, Kajita M, Ishizuya-Oka A. Essential Roles of Thyroid Hormone-Regulated Hyaluronan/CD44 Signaling in Adult Stem Cell Development During *Xenopus laevis* Intestinal Remodeling. *Stem Cells*. 2017;35(10):2175-83. Epub 2017/08/02. doi: 10.1002/stem.2671. PubMed PMID: 28758360.
149. Nairn AV, Kinoshita-Toyoda A, Toyoda H, Xie J, Harris K, Dalton S, Kulik M, Pierce JM, Toida T, Moremen KW, Linhardt RJ. Glycomics of Proteoglycan Biosynthesis in Murine Embryonic Stem Cell Differentiation. *Journal of Proteome Research*. 2007;6:4374-87.
150. Barzilay R, Ventorp F, Segal-Gavish H, Aharony I, Bieber A, Dar S, Vescan M, Globus R, Weizman A, Naor D, Lipton J, Janelidze S, Brundin L, Offen D. CD44 Deficiency Is Associated with Increased Susceptibility to Stress-Induced Anxiety-like Behavior in Mice. *J Mol Neurosci*. 2016;60(4):548-58. Epub 2016/09/14. doi: 10.1007/s12031-016-0835-3. PubMed PMID: 27619521.

151. Oliferenko S, Kaverina I, Small JV, Huber LA. Hyaluronic Acid (Ha) Binding to Cd44 Activates Rac1 and Induces Lamellipodia Outgrowth. *Journal of Cell Biology*. 2000;148(6):1159-64.
152. Zoltan-Jones A, Huang L, Ghatak S, Toole BP. Elevated hyaluronan production induces mesenchymal and transformed properties in epithelial cells. *Journal of Biological Chemistry*. 2003;278(46):45801-10. Epub 2003/09/05. doi: 10.1074/jbc.M308168200. PubMed PMID: 12954618.
153. Kim Y, Lee YS, Choe J, Lee H, Kim YM, Jeoung D. CD44-Epidermal Growth Factor Receptor Interaction Mediates Hyaluronic Acid-promoted Cell Motility by Activating Protein Kinase C Signaling Involving Akt, Rac1, Phox, Reactive Oxygen Species, Focal Adhesion Kinase, and MMP-2. *Journal of Biological Chemistry*. 2008;283(33):22513-28. doi: 10.1074/jbc.
154. Piao JH, Wang Y, Duncan ID. CD44 is required for the migration of transplanted oligodendrocyte progenitor cells to focal inflammatory demyelinating lesions in the spinal cord. *Glia*. 2013;61(3):361-7. Epub 2013/01/03. doi: 10.1002/glia.22438. PubMed PMID: 23280959.
155. Razinia Z, Castagnino P, Xu T, Vazquez-Salgado A, Pure E, Assoian RK. Stiffness-dependent motility and proliferation uncoupled by deletion of CD44. *Sci Rep*. 2017;7(1):16499. Epub 2017/12/01. doi: 10.1038/s41598-017-16486-z. PubMed PMID: 29184125; PMCID: PMC5705666.

156. Stojkovic M, Krebs O, Kolle S, Prella K, Assmann V, Zakhartchenko V, Sinowatz F, Wolf E. Developmental regulation of hyaluronan-binding protein (RHAMM/IHABP) expression in early bovine embryos. *Biology of Reproduction*. 2003;68(1):60-6. Epub 2002/12/21. doi: 10.1095/biolreprod.102.007716. PubMed PMID: 12493696.
157. Prager A, Hagenlocher C, Ott T, Schambony A, Feistel K. HMMR mediates anterior neural tube closure and morphogenesis in the frog *Xenopus*. *Developmental Biology*. 2017;430(1):188-201. Epub 2017/08/06. doi: 10.1016/j.ydbio.2017.07.020. PubMed PMID: 28778799.
158. Lynn BD, Li X, Cattini PA, Turley EA, Nagy JI. Identification of sequence, protein isoforms, and distribution of the hyaluronan-binding protein RHAMM in adult and developing rat brain. *Journal of Comparative Neurology*. 2001;439:315-30.
159. Nagy JI, Hacking J, Frankenstein UN, Turley EA. Requirement of the hyaluronan receptor RHAMM in neurite extension and motility as demonstrated in primary neurons and neuronal cell lines. *Journal of Neuroscience*. 1995;15(1):241-52.
160. Shechter R, Ronen A, Rolls A, London A, Bakalash S, Young MJ, Schwartz M. Toll-like receptor 4 restricts retinal progenitor cell proliferation. *J Cell Biol*. 2008;183(3):393-400. Epub 2008/11/05. doi: 10.1083/jcb.200804010. PubMed PMID: 18981228; PMCID: PMC2575781.

161. Grasselli C, Ferrari D, Zalfa C, Soncini M, Mazzoccoli G, Facchini FA, Marongiu L, Granucci F, Copetti M, Vescovi AL, Peri F, De Filippis L. Toll-like receptor 4 modulation influences human neural stem cell proliferation and differentiation. *Cell Death & Disease*. 2018;9(3):280. Epub 2018/02/17. doi: 10.1038/s41419-017-0139-8. PubMed PMID: 29449625; PMCID: PMC5833460.
162. Rolls A, Shechter R, London A, Ziv Y, Ronen A, Levy R, Schwartz M. Toll-like receptors modulate adult hippocampal neurogenesis. *Nat Cell Biol*. 2007;9(9):1081-8. Epub 2007/08/21. doi: 10.1038/ncb1629. PubMed PMID: 17704767.
163. Vinukonda G, Dohare P, Arshad A, Zia MT, Panda S, Korumilli R, Kayton R, Hascall VC, Lauer ME, Ballabh P. Hyaluronidase and Hyaluronan Oligosaccharides Promote Neurological Recovery after Intraventricular Hemorrhage. *J Neurosci*. 2016;36(3):872-89. Epub 2016/01/23. doi: 10.1523/JNEUROSCI.3297-15.2016. PubMed PMID: 26791217; PMCID: PMC4719021.
164. Xing G, Ren M, Verma A. Divergent Temporal Expression of Hyaluronan Metabolizing Enzymes and Receptors with Craniotomy vs. Controlled-Cortical Impact Injury in Rat Brain: A Pilot Study. *Front Neurol*. 2014;5:173. Epub 2014/10/14. doi: 10.3389/fneur.2014.00173. PubMed PMID: 25309501; PMCID: PMC4161003.
165. Lipponen A, Paananen J, Puhakka N, Pitkanen A. Analysis of Post-Traumatic Brain Injury Gene Expression Signature Reveals Tubulins, Nfe2l2,

Nfkb, Cd44, and S100a4 as Treatment Targets. *Sci Rep.* 2016;6:31570. Epub 2016/08/18. doi: 10.1038/srep31570. PubMed PMID: 27530814; PMCID: PMC4987651.

166. Pinner E, Gruper Y, Ben Zimra M, Kristt D, Laudon M, Naor D, Zisapel N. CD44 Splice Variants as Potential Players in Alzheimer's Disease Pathology. *J Alzheimers Dis.* 2017;58(4):1137-49. Epub 2017/05/28. doi: 10.3233/JAD-161245. PubMed PMID: 28550248.

167. Neal ML, Boyle AM, Budge KM, Safadi FF, Richardson JR. The glycoprotein GPNMB attenuates astrocyte inflammatory responses through the CD44 receptor. *J Neuroinflammation.* 2018;15(1):73. Epub 2018/03/10. doi: 10.1186/s12974-018-1100-1. PubMed PMID: 29519253; PMCID: PMC5842560.

168. Reinbach C, Stadler MS, Probstl N, Chrzanowski U, Schmitz C, Kipp M, Hochstrasser T. CD44 expression in the cuprizone model. *Brain Research.* 2020;1745:146950. Epub 2020/06/12. doi: 10.1016/j.brainres.2020.146950. PubMed PMID: 32524994.

169. Flynn KM, Michaud M, Madri JA. CD44 deficiency contributes to enhanced experimental autoimmune encephalomyelitis: a role in immune cells and vascular cells of the blood-brain barrier. *American Journal of Pathology.* 2013;182(4):1322-36. Epub 2013/02/19. doi: 10.1016/j.ajpath.2013.01.003. PubMed PMID: 23416161; PMCID: PMC3620422.

170. Guan H, Nagarkatti PS, Nagarkatti M. CD44 Reciprocally regulates the differentiation of encephalitogenic Th1/Th17 and Th2/regulatory T cells through epigenetic modulation involving DNA methylation of cytokine gene promoters, thereby controlling the development of experimental autoimmune encephalomyelitis. *J Immunol*. 2011;186(12):6955-64. Epub 2011/05/10. doi: 10.4049/jimmunol.1004043. PubMed PMID: 21551360; PMCID: PMC3650091.
171. Chitrala KN, Guan H, Singh NP, Busbee B, Gandy A, Mehrpouya-Bahrami P, Ganewatta MS, Tang C, Chatterjee S, Nagarkatti P, Nagarkatti M. CD44 deletion leading to attenuation of experimental autoimmune encephalomyelitis results from alterations in gut microbiome in mice. *Eur J Immunol*. 2017;47(7):1188-99. Epub 2017/05/26. doi: 10.1002/eji.201646792. PubMed PMID: 28543188; PMCID: PMC5704912.
172. Sun Z, Nyanzu M, Yang S, Zhu X, Wang K, Ru J, Yu E, Zhang H, Wang Z, Shen J, Zhuge Q, Huang L. VX765 Attenuates Pyroptosis and HMGB1/TLR4/NF-kappaB Pathways to Improve Functional Outcomes in TBI Mice. *Oxid Med Cell Longev*. 2020;2020:7879629. Epub 2020/05/08. doi: 10.1155/2020/7879629. PubMed PMID: 32377306; PMCID: PMC7181015.
173. Zhou Y, Wang S, Zhao J, Fang P. Asiaticoside attenuates neonatal hypoxic-ischemic brain damage through inhibiting TLR4/NF-kappaB/STAT3 pathway. *Annals of Translational Medicine*. 2020;8(10):641. Epub 2020/06/23. doi: 10.21037/atm-20-3323. PubMed PMID: 32566578; PMCID: PMC7290617.

174. Wang J, Wang X, Wei J, Wang M. Hyaluronan tetrasaccharide exerts neuroprotective effect and promotes functional recovery after acute spinal cord injury in rats. *Neurochem Res.* 2015;40(1):98-108. Epub 2014/11/07. doi: 10.1007/s11064-014-1470-4. PubMed PMID: 25373446.
175. Sunabori T, Koike M, Asari A, Oonuki Y, Uchiyama Y. Suppression of Ischemia-Induced Hippocampal Pyramidal Neuron Death by Hyaluronan Tetrasaccharide through Inhibition of Toll-Like Receptor 2 Signaling Pathway. *American Journal of Pathology.* 2016;186(8):2143-51. Epub 2016/06/16. doi: 10.1016/j.ajpath.2016.03.016. PubMed PMID: 27301359.
176. Hauser SL, Cree BAC. Treatment of Multiple Sclerosis: A Review. *Am J Med.* 2020;133(12):1380-90 e2. Epub 20200717. doi: 10.1016/j.amjmed.2020.05.049. PubMed PMID: 32682869; PMCID: PMC7704606.
177. Dobson R, Giovannoni G. Multiple sclerosis - a review. *Eur J Neurol.* 2019;26(1):27-40. Epub 2018/10/10. doi: 10.1111/ene.13819. PubMed PMID: 30300457.
178. Kuhlmann T, Miron V, Cui Q, Wegner C, Antel J, Bruck W. Differentiation block of oligodendroglial progenitor cells as a cause for remyelination failure in chronic multiple sclerosis. *Brain.* 2008;131(Pt 7):1749-58. Epub 20080530. doi: 10.1093/brain/awn096. PubMed PMID: 18515322.

179. Patani R, Balaratnam M, Vora A, Reynolds R. Remyelination can be extensive in multiple sclerosis despite a long disease course. *Neuropathol Appl Neurobiol.* 2007;33(3):277-87. Epub 20070418. doi: 10.1111/j.1365-2990.2007.00805.x. PubMed PMID: 17442065.
180. Patrikios P, Stadelmann C, Kutzelnigg A, Rauschka H, Schmidbauer M, Laursen H, Sorensen PS, Bruck W, Lucchinetti C, Lassmann H. Remyelination is extensive in a subset of multiple sclerosis patients. *Brain.* 2006;129(Pt 12):3165-72. Epub 20060818. doi: 10.1093/brain/awl217. PubMed PMID: 16921173.
181. Prineas JW, Connell F. Remyelination in multiple sclerosis. *Ann Neurol.* 1979;5(1):22-31. doi: 10.1002/ana.410050105. PubMed PMID: 426466.
182. Back SA, Tuohy TM, Chen H, Wallingford N, Craig A, Struve J, Luo NL, Banine F, Liu Y, Chang A, Trapp BD, Bebo BF, Jr., Rao MS, Sherman LS. Hyaluronan accumulates in demyelinated lesions and inhibits oligodendrocyte progenitor maturation. *Nat Med.* 2005;11(9):966-72. Epub 2005/08/09. doi: 10.1038/nm1279. PubMed PMID: 16086023.
183. Dias MC, Pinto D, Silva AMS. Plant Flavonoids: Chemical Characteristics and Biological Activity. *Molecules.* 2021;26(17). Epub 20210904. doi: 10.3390/molecules26175377. PubMed PMID: 34500810; PMCID: PMC8434187.
184. Maleki SJ, Crespo JF, Cabanillas B. Anti-inflammatory effects of flavonoids. *Food Chem.* 2019;299:125124. Epub 20190703. doi: 10.1016/j.foodchem.2019.125124. PubMed PMID: 31288163.

185. Bishop M, Rumrill PD. Multiple sclerosis: Etiology, symptoms, incidence and prevalence, and implications for community living and employment. *Work*. 2015;52(4):725-34. Epub 2015/12/08. doi: 10.3233/WOR-152200. PubMed PMID: 26639011.
186. Freedman MS, Selchen D, Prat A, Giacomini PS. Managing Multiple Sclerosis: Treatment Initiation, Modification, and Sequencing. *Can J Neurol Sci*. 2018;45(5):489-503. Epub 2018/06/13. doi: 10.1017/cjn.2018.17. PubMed PMID: 29893652.
187. Neil Scolding RF, Sarah Stevens, Carl-Henrik Heldin, Alastair Compston, Jia Newcombe. Oligodendrocyte progenitors are present in the normal adult human CNS and in the lesions of multiple sclerosis. *Brain*. 1998;121:7.
188. Wolswijk G. Chronic Stage Multiple Sclerosis Lesions Contain a Relatively Quiescent Population of Oligodendrocyte Precursor Cells. *The Journal of Neuroscience*. 1998;18(2):8.
189. Yasuhiro Maeda MS, Joseph Menonna, John Chapin, Weiping Li, Peter Dowling. Platelet-derived growth factor- α receptor-positive oligodendroglia are frequent in multiple sclerosis lesions. *Annals of Neurology*. 2001;49:9.
190. Ansi Chang WMT, Richard Rudick, Bruce Trapp. Premyelinating oligodendrocytes in chronic lesions of multiple sclerosis. *New England Journal of Medicine*. 2002;346(3):8.

191. Peters A, Sherman LS. Diverse Roles for Hyaluronan and Hyaluronan Receptors in the Developing and Adult Nervous System. *Int J Mol Sci*. 2020;21(17). Epub 2020/08/23. doi: 10.3390/ijms21175988. PubMed PMID: 32825309; PMCID: PMC7504301.
192. Domanegg K, Sleeman JP, Schmaus A. CEMIP, a Promising Biomarker That Promotes the Progression and Metastasis of Colorectal and Other Types of Cancer. *Cancers (Basel)*. 2022;14(20). Epub 20221018. doi: 10.3390/cancers14205093. PubMed PMID: 36291875; PMCID: PMC9600181.
193. Li L, Yan LH, Manoj S, Li Y, Lu L. Central Role of CEMIP in Tumorigenesis and Its Potential as Therapeutic Target. *J Cancer*. 2017;8(12):2238-46. Epub 2017/08/19. doi: 10.7150/jca.19295. PubMed PMID: 28819426; PMCID: PMC5560141.
194. Marella M, Jadin L, Keller GA, Sugarman BJ, Frost GI, Shepard HM. KIAA1199 expression and hyaluronan degradation colocalize in multiple sclerosis lesions. *Glycobiology*. 2018;28(12):958-67. Epub 2018/07/15. doi: 10.1093/glycob/cwy064. PubMed PMID: 30007349; PMCID: PMC6243203.
195. Downing AE. *Laboratory Methods in Histotechnology*. Prophet EB, editor. Washington, D. C.: Armed Forces Institute of Pathology; 1992 1/1/1992. 279 p.
196. Zhang Y, Chen K, Sloan SA, Bennett ML, Scholze AR, O'Keeffe S, Phatnani HP, Guarnieri P, Caneda C, Ruderisch N, Deng S, Liddelow SA, Zhang C, Daneman R, Maniatis T, Barres BA, Wu JQ. An RNA-sequencing

transcriptome and splicing database of glia, neurons, and vascular cells of the cerebral cortex. *J Neurosci*. 2014;34(36):11929-47. Epub 2014/09/05. doi: 10.1523/JNEUROSCI.1860-14.2014. PubMed PMID: 25186741; PMCID: PMC4152602.

197. Zilkha-Falb R, Kaushansky N, Ben-Nun A. The Median Eminence, A New Oligodendrogenic Niche in the Adult Mouse Brain. *Stem Cell Reports*. 2020;14(6):1076-92. Epub 20200514. doi: 10.1016/j.stemcr.2020.04.005. PubMed PMID: 32413277; PMCID: PMC7355143.

198. Rivas F, Zahid OK, Reesink HL, Peal BT, Nixon AJ, DeAngelis PL, Skardal A, Rahbar E, Hall AR. Label-free analysis of physiological hyaluronan size distribution with a solid-state nanopore sensor. *Nat Commun*. 2018;9(1):1037. Epub 20180312. doi: 10.1038/s41467-018-03439-x. PubMed PMID: 29531292; PMCID: PMC5847568.

199. Andre B, Duterme C, Van Moer K, Mertens-Strijthagen J, Jadot M, Flamion B. Hyal2 is a glycosylphosphatidylinositol-anchored, lipid raft-associated hyaluronidase. *Biochem Biophys Res Commun*. 2011;411(1):175-9. Epub 20110625. doi: 10.1016/j.bbrc.2011.06.125. PubMed PMID: 21740893.

200. Girish KS, Kemparaju K. The magic glue hyaluronan and its eraser hyaluronidase: a biological overview. *Life Sci*. 2007;80(21):1921-43. Epub 20070306. doi: 10.1016/j.lfs.2007.02.037. PubMed PMID: 17408700.

201. Sato T, Shirai R, Isogai M, Yamamoto M, Miyamoto Y, Yamauchi J. Hyaluronic acid and its receptor CD44, acting through TMEM2, inhibit morphological differentiation in oligodendroglial cells. *Biochem Biophys Res Commun.* 2022;624:102-11. Epub 20220731. doi: 10.1016/j.bbrc.2022.07.092. PubMed PMID: 35940122.
202. Longhi L, Perego C, Ortolano F, Aresi S, Fumagalli S, Zanier ER, Stocchetti N, De Simoni MG. Tumor necrosis factor in traumatic brain injury: effects of genetic deletion of p55 or p75 receptor. *J Cereb Blood Flow Metab.* 2013;33(8):1182-9. Epub 20130424. doi: 10.1038/jcbfm.2013.65. PubMed PMID: 23611870; PMCID: PMC3734767.
203. Michev A, Orsini A, Santi V, Bassanese F, Veraldi D, Brambilla I, Marseglia GL, Savasta S, Foadelli T. An Overview of The Role of Tumor Necrosis Factor-Alpha in Epileptogenesis and Its Therapeutic Implications. *Acta Biomed.* 2022;92(S4):e2021418. Epub 20220321. doi: 10.23750/abm.v92iS4.12667. PubMed PMID: 35441606; PMCID: PMC9179056.
204. Xue Y, Zeng X, Tu WJ, Zhao J. Tumor Necrosis Factor-alpha: The Next Marker of Stroke. *Dis Markers.* 2022;2022:2395269. Epub 20220227. doi: 10.1155/2022/2395269. PubMed PMID: 35265224; PMCID: PMC8898850.
205. Kenta HT Cho NH, Evelyn McClendon, Art Riddle, Basappa, Simerdeep K Dhillon, Laura Bennet, Stephen Back, Larry S Sherman, Alistair J Gunn, Justin Mark Dean. Postischemic infusion of apigenin reduces seizure burden in preterm sheep. *International Journal of Molecular Sciences.* 2023;In Press.

206. Lapato AS, Szu JI, Hasselmann JPC, Khalaj AJ, Binder DK, Tiwari-Woodruff SK. Chronic demyelination-induced seizures. *Neuroscience*. 2017;346:409-22. Epub 20170130. doi: 10.1016/j.neuroscience.2017.01.035. PubMed PMID: 28153692; PMCID: PMC5394933.
207. Walker C, Mojares E, Del Rio Hernandez A. Role of Extracellular Matrix in Development and Cancer Progression. *Int J Mol Sci*. 2018;19(10). Epub 20181004. doi: 10.3390/ijms19103028. PubMed PMID: 30287763; PMCID: PMC6213383.
208. De Luca C, Papa M. Matrix Metalloproteinases, Neural Extracellular Matrix, and Central Nervous System Pathology. *Prog Mol Biol Transl Sci*. 2017;148:167-202. Epub 20170504. doi: 10.1016/bs.pmbts.2017.04.002. PubMed PMID: 28662822.
209. Fawcett JW. The extracellular matrix in plasticity and regeneration after CNS injury and neurodegenerative disease. *Prog Brain Res*. 2015;218:213-26. Epub 20150329. doi: 10.1016/bs.pbr.2015.02.001. PubMed PMID: 25890139.
210. McAtee CO, Barycki JJ, Simpson MA. Emerging roles for hyaluronidase in cancer metastasis and therapy. *Adv Cancer Res*. 2014;123:1-34. doi: 10.1016/B978-0-12-800092-2.00001-0. PubMed PMID: 25081524; PMCID: PMC4445717.
211. Xu J, Liu Y, Wang X, Huang J, Zhu H, Hu Z, Wang D. Association between KIAA1199 overexpression and tumor invasion, TNM stage, and poor prognosis in

colorectal cancer. *Int J Clin Exp Pathol.* 2015;8(3):9. Epub 20150301; PMID: PMC4440108.

212. Hua Q, Zhang B, Xu G, Wang L, Wang H, Lin Z, Yu D, Ren J, Zhang D, Zhao L, Zhang T. CEMIP, a novel adaptor protein of OGT, promotes colorectal cancer metastasis through glutamine metabolic reprogramming via reciprocal regulation of beta-catenin. *Oncogene.* 2021;40(46):6443-55. Epub 20211004. doi: 10.1038/s41388-021-02023-w. PubMed PMID: 34608265.

213. Jiao X, Ye J, Wang X, Yin X, Zhang G, Cheng X. KIAA1199, a Target of MicoRNA-486-5p, Promotes Papillary Thyroid Cancer Invasion by Influencing Epithelial-Mesenchymal Transition (EMT). *Med Sci Monit.* 2019;25:6788-96. Epub 20190910. doi: 10.12659/MSM.918682. PubMed PMID: 31501407; PMID: PMC6752488.

214. Jia S, Qu T, Wang X, Feng M, Yang Y, Feng X, Ma R, Li W, Hu Y, Feng Y, Ji K, Li Z, Jiang W, Ji J. KIAA1199 promotes migration and invasion by Wnt/beta-catenin pathway and MMPs mediated EMT progression and serves as a poor prognosis marker in gastric cancer. *PLoS One.* 2017;12(4):e0175058. Epub 2017/04/20. doi: 10.1371/journal.pone.0175058. PubMed PMID: 28422983; PMID: PMC5397282.

215. Zhai X, Wang W, Ma Y, Zeng Y, Dou D, Fan H, Song J, Yu X, Xin D, Du G, Jiang Z, Zhang H, Zhang X, Jin B. Serum KIAA1199 is an advanced-stage prognostic biomarker and metastatic oncogene in cholangiocarcinoma. *Aging.* 2015;12(23):16. Epub 20201010. doi: 10.18632/aging.103964.

216. Liu J, Han P, Gong J, Wang Y, Chen B, Liao J, Tian D. Knockdown of KIAA1199 attenuates growth and metastasis of hepatocellular carcinoma. *Cell Death Discov.* 2018;4:102. Epub 20181112. doi: 10.1038/s41420-018-0099-5. PubMed PMID: 30455988; PMCID: PMC6232158.
217. Rodrigues G, Hoshino A, Kenific CM, Matei IR, Steiner L, Freitas D, Kim HS, Oxley PR, Scandariato I, Casanova-Salas I, Dai J, Badwe CR, Gril B, Tesic Mark M, Dill BD, Molina H, Zhang H, Benito-Martin A, Bojmar L, Ararso Y, Offer K, LaPlant Q, Buehring W, Wang H, Jiang X, Lu TM, Liu Y, Sabari JK, Shin SJ, Narula N, Ginter PS, Rajasekhar VK, Healey JH, Meylan E, Costa-Silva B, Wang SE, Rafii S, Altorki NK, Rudin CM, Jones DR, Steeg PS, Peinado H, Ghajar CM, Bromberg J, de Sousa M, Pisapia D, Lyden D. Tumour exosomal CEMIP protein promotes cancer cell colonization in brain metastasis. *Nat Cell Biol.* 2019;21(11):1403-12. Epub 20191104. doi: 10.1038/s41556-019-0404-4. PubMed PMID: 31685984; PMCID: PMC7354005.
218. Love S. Demyelinating diseases. *J Clin Pathol.* 2006;59(11):1151-9. Epub 2006/10/31. doi: 10.1136/jcp.2005.031195. PubMed PMID: 17071802; PMCID: PMC1860500.
219. Gebalski J, Graczyk F, Zaluski D. Paving the way towards effective plant-based inhibitors of hyaluronidase and tyrosinase: a critical review on a structure-activity relationship. *J Enzyme Inhib Med Chem.* 2022;37(1):1120-95. doi: 10.1080/14756366.2022.2061966. PubMed PMID: 35470749; PMCID: PMC9045780.

220. UR K, HE K, NP D. Structure-activity studies of flavonoids as inhibitors of hyaluronidase. *Biochemical Pharmacology*. 1990;40(2):4. doi: 10.1016/0006-2952(90)90709-t PMID: 2375774.
221. MW L, AI Y, CA V, K S, P P, JW O. Inhibition of monkey sperm hyaluronidase activity and heterologous cumulus penetration by flavonoids. *Biology of Reproduction*. 1997;56(6):6. doi: 10.1095/biolreprod56.6.1383 PMID: 9166689.
222. Tatemoto H, Tokeshi I, Nakamura S, Muto N, Nakada T. Inhibition of boar sperm hyaluronidase activity by tannic acid reduces polyspermy during in vitro fertilization of porcine oocytes. *Zygote*. 2006;14(4):275-85. doi: 10.1017/S0967199406003819. PubMed PMID: 17266786.
223. Alsaif G, Almosnid N, Hawkins I, Taylor Z, Knott DLT, Handy S, Altman E, Gao Y. Evaluation of Fourteen Aurone Derivatives as Potential Anti-Cancer Agents. *Curr Pharm Biotechnol*. 2017;18(5):384-90. doi: 10.2174/1389201018666170502112303. PubMed PMID: 28464771.
224. Rudrapal M, Khan J, Dukhyil AAB, Alarousy R, Attah EI, Sharma T, Khairnar SJ, Bendale AR. Chalcone Scaffolds, Bioprecursors of Flavonoids: Chemistry, Bioactivities, and Pharmacokinetics. *Molecules*. 2021;26(23). Epub 20211126. doi: 10.3390/molecules26237177. PubMed PMID: 34885754; PMID: PMC8659147.

225. Srinivasa V, Sundaram MS, Anusha S, Hemshekhar M, Chandra Nayaka S, Kemparaju K, Basappa, Girish KS, Rangappa KS. Novel apigenin based small molecule that targets snake venom metalloproteases. PLoS One. 2014;9(9):e106364. Epub 20140903. doi: 10.1371/journal.pone.0106364. PubMed PMID: 25184206; PMCID: PMC4153592.
226. Feoktistova M, Geserick P, Leverkus M. Crystal Violet Assay for Determining Viability of Cultured Cells. Cold Spring Harb Protoc. 2016;2016(4):pdb prot087379. Epub 20160401. doi: 10.1101/pdb.prot087379. PubMed PMID: 27037069.
227. Mario Stefanini CDM, Luciano Zamboni. Fixation of Ejaculated Spermatozoa for Electron Microscopy. Nature. 1967;216:2.
228. Vicario-Abejon C. Long-term culture of hippocampal neurons. Curr Protoc Neurosci. 2004;Chapter 3:Unit 3 2. doi: 10.1002/0471142301.ns0302s26. PubMed PMID: 18428599.
229. Morin G, Lalancette C, Sullivan R, Leclerc P. Identification of the bull sperm p80 protein as a PH-20 ortholog and its modification during the epididymal transit. Mol Reprod Dev. 2005;71(4):523-34. doi: 10.1002/mrd.20308. PubMed PMID: 15892045.
230. Chowpongpan SS, Haw-Sook; Kim, Eun-Ki. Cloning and characterization of the bovine testicular PH-20 hyaluronidase core domain. Biotechnology Letters.

2004;26(15):6. doi: <https://doi.org/10.1023/B:BILE.0000036606.07433.5b>;
PMCID: 15289682.

231. Hofinger ES, Hoechstetter J, Oettl M, Bernhardt G, Buschauer A. Isoenzyme-specific differences in the degradation of hyaluronic acid by mammalian-type hyaluronidases. *Glycoconj J*. 2008;25(2):101-9. Epub 20070710. doi: 10.1007/s10719-007-9058-8. PubMed PMID: 17620008.

232. Lee HG, Cowman, M. K. An agarose gel electrophoretic method for analysis of hyaluronan molecular weight distribution. *Analytical Biochemistry*. 1994;219(2):9. doi: 10.1006/abio.1994.1267 PMCID: 8080084.

233. Poudel S, Song J, Jin EJ, Song K. Sulfuretin-induced miR-30C selectively downregulates cyclin D1 and D2 and triggers cell death in human cancer cell lines. *Biochem Biophys Res Commun*. 2013;431(3):572-8. Epub 20130111. doi: 10.1016/j.bbrc.2013.01.012. PubMed PMID: 23318178.

234. Lee YR, Hwang JK, Koh HW, Jang KY, Lee JH, Park JW, Park BH. Sulfuretin, a major flavonoid isolated from *Rhus verniciflua*, ameliorates experimental arthritis in mice. *Life Sci*. 2012;90(19-20):799-807. Epub 20120412. doi: 10.1016/j.lfs.2012.04.015. PubMed PMID: 22521292.

235. Choi SJL, M. Y.; Jo, H.; Lim, S. S.; Jung, S. H. Preparative isolation and purification of neuroprotective compounds from *Rhus verniciflua* by high speed counter-current chromatography. *Biological & Pharmacological Bulletin*. 2012;35(4):9. doi: 10.1248/bpb.35.559; PMCID: 22466561.

236. Cho N, Choi JH, Yang H, Jeong EJ, Lee KY, Kim YC, Sung SH. Neuroprotective and anti-inflammatory effects of flavonoids isolated from *Rhus verniciflua* in neuronal HT22 and microglial BV2 cell lines. *Food Chem Toxicol.* 2012;50(6):1940-5. Epub 20120320. doi: 10.1016/j.fct.2012.03.052. PubMed PMID: 22465834.
237. Song MY, Jeong GS, Lee HS, Kwon KS, Lee SM, Park JW, Kim YC, Park BH. Sulfuretin attenuates allergic airway inflammation in mice. *Biochem Biophys Res Commun.* 2010;400(1):83-8. Epub 20100807. doi: 10.1016/j.bbrc.2010.08.014. PubMed PMID: 20696133.
238. Stern R, Jedrzejewski MJ. Hyaluronidases: their genomics, structures, and mechanisms of action. *Chem Rev.* 2006;106(3):818-39. doi: 10.1021/cr050247k. PubMed PMID: 16522010; PMCID: PMC2547145.
239. Mohamed EM, Hetta MH, Rateb ME, Selim MA, AboulMagd AM, Badria FA, Abdelmohsen UR, Alhadrami HA, Hassan HM. Bioassay-Guided Isolation, Metabolic Profiling, and Docking Studies of Hyaluronidase Inhibitors from *Ravenala madagascariensis*. *Molecules.* 2020;25(7). Epub 20200408. doi: 10.3390/molecules25071714. PubMed PMID: 32276509; PMCID: PMC7180949.
240. Li X, Xu R, Cheng Z, Song Z, Wang Z, Duan H, Wu X, Ni T. Comparative study on the interaction between flavonoids with different core structures and hyaluronidase. *Spectrochim Acta A Mol Biomol Spectrosc.* 2021;262:120079. Epub 20210611. doi: 10.1016/j.saa.2021.120079. PubMed PMID: 34175762.

241. Parnigoni A, Moretto P, Viola M, Karousou E, Passi A, Vigetti D. Effects of Hyaluronan on Breast Cancer Aggressiveness. *Cancers (Basel)*. 2023;15(15). Epub 20230727. doi: 10.3390/cancers15153813. PubMed PMID: 37568628; PMCID: PMC10417239.
242. Tagge IJ, Kohama SG, Sherman LS, Bourdette DN, Woltjer R, Wang P, Wong SW, Rooney WD. MRI characteristics of Japanese macaque encephalomyelitis: Comparison to human diseases. *J Neuroimaging*. 2021;31(3):480-92. Epub 20210430. doi: 10.1111/jon.12868. PubMed PMID: 33930224; PMCID: PMC8722403.
243. Blair TC, Manoharan M, Rawlings-Rhea SD, Tagge I, Kohama SG, Hollister-Smith J, Ferguson B, Woltjer RL, Frederick MC, Pollaro J, Rooney WD, Sherman LS, Bourdette DN, Wong SW. Immunopathology of Japanese macaque encephalomyelitis is similar to multiple sclerosis. *J Neuroimmunol*. 2016;291:1-10. Epub 20151202. doi: 10.1016/j.jneuroim.2015.11.026. PubMed PMID: 26857488; PMCID: PMC4748211.
244. Axthelm MK, Bourdette DN, Marracci GH, Su W, Mullaney ET, Manoharan M, Kohama SG, Pollaro J, Witkowski E, Wang P, Rooney WD, Sherman LS, Wong SW. Japanese macaque encephalomyelitis: a spontaneous multiple sclerosis-like disease in a nonhuman primate. *Ann Neurol*. 2011;70(3):362-73. Epub 20110614. doi: 10.1002/ana.22449. PubMed PMID: 21674589; PMCID: PMC3170450.